RCA REVIEW

GEORGE M. K. BAKER
Manager

CHAS. C. FOSTER, JR.
Editorial Manager

THOMAS R. ROGERS
Business Manager

SUBSCRIPTIONS:

United States, Canada, and Postal Union: One Year $2.00, Two Years $3.50, Three Years $4.50
Other Countries: One Year $2.40, Two Years $4.30, Three Years $5.70

SINGLE COPIES:

United States: $.75 each. Other Countries: $.85 each

Published quarterly in March, June, September, and December by RCA Laboratories Division, Radio Corporation of America, Princeton, New Jersey

Entered as second class matter July 3, 1950, at the Post Office at Princeton, New Jersey, under the act of March 3, 1879

PRINTED IN U.S.A.

RCA REVIEW

a technical journal

RADIO AND ELECTRONICS
RESEARCH • ENGINEERING

Published quarterly by
RADIO CORPORATION OF AMERICA
RCA LABORATORIES DIVISION
in cooperation with

RCA VICTOR DIVISION
RADIOMARINE CORPORATION OF AMERICA
RCA INTERNATIONAL DIVISION
RCA COMMUNICATIONS, INC.
NATIONAL BROADCASTING COMPANY, INC.
RCA INSTITUTES, INC.

VOLUME XI DECEMBER 1950 NUMBER 4

CONTENTS

RCA Review is regularly abstracted and indexed by ***Industrial Arts Index Science Abstracts*** (I.E.E.-Brit.), ***Engineering Index, Electronic Engineering Master Index, Abstracts and References*** (***Wireless Engineer***-Brit. and ***Proc. I.R.E.***) and ***Digest-Index Bulletin.***

RCA REVIEW

BOARD OF EDITORS

DISTORTION IN MULTICHANNEL FREQUENCY-MODULATION RELAY SYSTEMS*†

By

LELAND E. THOMPSON

Engineering Products Department, RCA Victor Division, Camden, N. J.

Summary—Formulas for distortion and intermodulation, which are useful in the design of economical multichannel radio relay systems, are presented. Experimental results and an example of the application are shown.

INTRODUCTION

THE several sources of distortion in a frequency- or phase-modulation system are well known. The distortion produced by the modulator and discriminator due to nonlinear transfer characteristics is usually independent of the modulation frequency. The distortion caused by phase nonlinearity in tuned circuits varies with the modulating frequency. It is proposed to show the relation between these harmonic distortions and cross talk in multichannel communication systems.

MODULATOR AND DISCRIMINATOR

Single-sideband frequency division multiplex systems will be considered first. In a later section other types of multiplex will be discussed. The signal in each of the multiplex channels is assumed to be speech or other complex signalling waves.

The following formula was derived, as shown in the appendix, from the work of Brockbank and Wass:[1]

$$S/N_3 = \frac{163}{\sqrt{y}\, d_3} \sqrt{k}, \tag{1}$$

* Decimal Classification: R400×R630.3.

† Most of the work described in this paper was done under contract W-36-039-sc-32075 for the U. S. Army Signal Corps.

[1] R. A. Brockbank and C. A. A. Wass, "Non-Linear Distortion in Transmission Systems", *Jour. Inst. Elec. Eng.*, Part III, Vol. 92, pp. 45-46, March 1945.

where

S = signal voltage in one channel (root-mean-square),

N_3 = cross-talk voltage in one channel (root-mean-square) due to 3rd harmonic distortion,

y = distribution factor (see Figure 1),

d_3 = 3rd harmonic distortion, in per cent, of sine wave signal modulating carrier at the peak deviation of the system,

k = the ratio of the frequency separation between the center of one channel and the next one and the channel width. (Usually this factor is 1.33).

Formula (1) shows the relation between 3rd order distortion and signal to cross-talk ratio. The formula is valid only under certain conditions. First, the distortion must be independent of the modulating frequency. It therefore applies to the distortion in modulators and discriminators but not to tuned-circuit distortion. Second, it is assumed that the input-output characteristic of the nonlinear circuit can be expressed by the following power series:

$$V = a\,v + b\,v^2 + c\,v^3 + \cdots, \tag{2}$$

where V is the output, v the input and a, b, c are constants. The characteristics of typical modulators and discriminators are in this classification. Measurements showed that, below the overload point of the circuit, the 2nd harmonic distortion increased directly with the frequency deviation and the 3rd harmonic distortion increased as the square of the frequency deviation.

The third condition is that the number of channels be 10 or larger and all be active. It is of interest to note that in this case the signal to cross-talk ratio is independent of the number of channels in the system. The actual cross talk will be less than Formula (1) by several decibels if the number of channels in the system is as low as 3.

The fourth condition is that each channel have the same frequency deviation. In practice, it is found desirable to allow a higher deviation to the higher frequency channels so the tube and circuit noise will be more uniform in the various channels. Straight phase modulation is not desirable, however, because the lower frequency channels would have a considerably higher cross-talk level than the higher frequency channels. A satisfactory compromise between the noise and cross-talk distributions in the different channels is usually found by having uniform deviation per channel on the lowest one-quarter of the modulation-frequency range with the deviation per channel increasing on the

higher frequency channels to a value of perhaps 6 decibels on the highest frequency channel compared to one of the lower frequency channels.

With this modification of a straight frequency-modulation system, Formula (1) can be used with only a slight error. Brockbank and Wass[1] show that the total cross-talk power depends only on the total power of the multiplex signal and not on the relative power of the different channels. Therefore if the root-mean-square frequency modulation of the total multiplex signal is the same as it would be with straight frequency modulation, the total cross-talk power will be the same. Since the frequency deviation is different in the various chan-

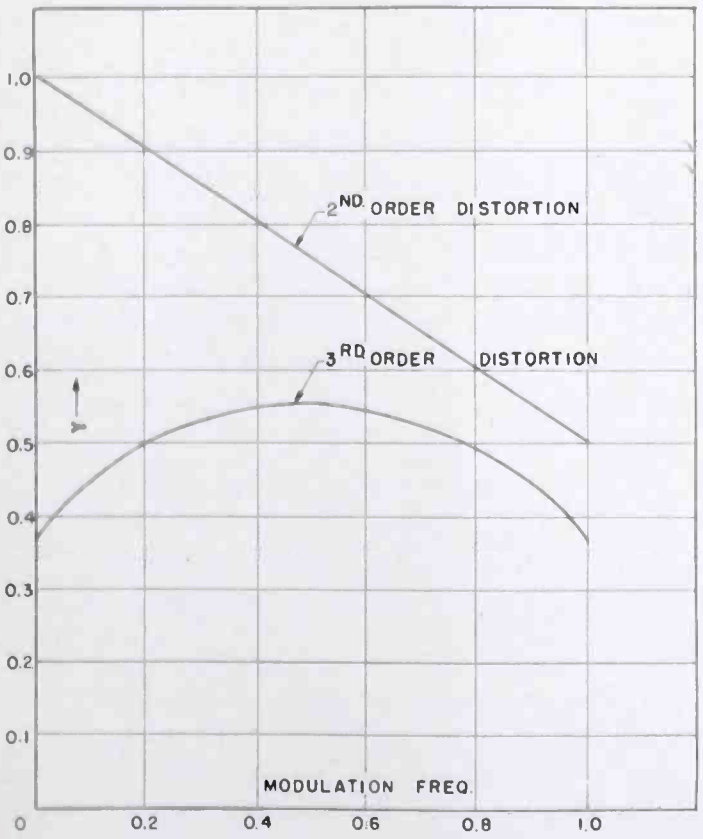

Fig. 1—Distribution of cross talk over the modulation frequency band.

nels, however, the results of calculation based on Formula (1) must be modified for each particular channel. For example, suppose in a particular system, each channel could have a root-mean-square deviation of 100 kilocycles in a straight frequency-modulation system. With a modified frequency-modulation characteristic, the lowest channel may have a root-mean-square deviation of 70 kilocycles and would then have 3 decibels lower signal to cross-talk ratio than the result of Formula (1). The highest channel may have a root-mean-square

deviation of 140 kilocycles and would have 3 decibels higher signal to cross-talk ratio than the value calculated from Formula (1).

Figure 1 shows the value of the intermodulation distribution factor (y) over the modulation range of frequencies and is taken from the reference paper.[1] The data shown for 2nd harmonic distortion is valid only for cases where the ratio of the highest to lowest modulation frequency is high.

The following formula shows the relation between 2nd harmonic distortion and signal to cross-talk ratio:

$$S/N_2 = \frac{141}{\sqrt{y}\, d_2} \sqrt{k}, \tag{3}$$

where

d_2 = 2nd harmonic distortion, in per cent, of sine wave signal modulating carrier at the peak deviation of the system.

In carefully designed modulators and discriminators, the 2nd order distortion is minimized by circuit adjustment so the distortion contributing the most to intermodulation is likely to be of the 3rd order. The 3rd order intermodulation may be larger than the 2nd, particularly where there are several non-linear circuits in a system, because that produced by each of the non-linear circuits adds on a voltage basis while the addition of the 2nd order distortion components is usually on a power basis. The total intermodulation in a channel is the sum of the powers of both the 2nd order and 3rd order components. Harmonic distortions higher than the 3rd do not ordinarily contribute much to the total intermodulation.

Tuned-Circuit Distortion

Several papers[2-4] have been published on the distortion produced on a frequency-modulated wave by tuned circuits or transformers. None of the references developed a formula suitable for the design of multichannel relay systems.

---

[2] H. Roder, "Effects of Tuned Circuits Upon a Frequency Modulated Signal", *Proc. I.R.E.*, Vol. 25, pp. 1617-1647, December 1937.

[3] D. L. Jaffee, "A Theoretical and Experimental Investigation of Tuned Circuit Distortion in Frequency-Modulation Systems", *Proc. I.R.E.*, Vol. 33, pp. 318-334, May 1945.

[4] A. S. Gladwin, "The Distortion of Frequency-Modulated Waves by Transmission Networks", *Proc. I.R.E.*, Vol. 35, pp. 1436-1445, December 1947.

The interstage-coupling circuits in intermediate-frequency amplifiers are usually the principal source of tuned-circuit distortion. The distortion produced by a single critically-coupled interstage transformer can be calculated from the following formulas developed by D. R. Crosby:[5]

$$d_3' = \frac{f_b D^2}{\sqrt{2}\,(BW)^3} \times 100 \text{ (frequency modulation)}, \tag{4}$$

$$d_3' = \frac{f_b D^2}{3\sqrt{2}\,(BW)^3} \times 100 \text{ (phase modulation)}, \tag{5}$$

where

d_3' = 3rd harmonic distortion in per cent,

f_b = modulation frequency in cycles per second,

D = peak-to-peak frequency deviation in cycles per second,

(BW) = 3-decibel bandwidth of transformer in cycles per second.

These formulas may be used for peak-to-peak frequency deviations up to one half the 3-decibel bandwidth with only a slight error. Frequency deviations greater than this are not usually of interest where there are a large number of such transformers in a system.

In order to determine the relation between this type of distortion and cross talk, the first thing of interest is the amplitude distribution of the various intermodulation components. Measurements were made on a frequency-modulation system in which the modulator and demodulator characteristics were sufficiently linear to be neglected and, therefore, the measured intermodulation components depended only on the phase characteristic of the tuned circuits in the system. The result of applying two equal-amplitude tones, A and B, to the system is shown in Figure 2. The intermodulation spectrum is triangular, the same as the noise spectrum in a frequency-modulation system. Further tests show the amplitude of the intermodulation components always falls on the dotted line regardless of the frequency of the tones A and B.

Furthermore, except for the triangular spectrum of the intermodulation components, the amplitude of the components has the same relation to the amplitude of the 3rd harmonic as in circuits in which the distortion is independent of frequency.

In a frequency modulation system, therefore, the cross talk due to

---

[5] Engineering Products Department, RCA Victor Division, Camden, N.J.

tuned-circuit distortion is highest in the top channel. The signal to cross-talk voltage ratio is

$$S/N_3 = \frac{163}{\sqrt{y}\, d_3'} \sqrt{k}, \tag{6}$$

where

d_3' = 3rd harmonic distortion, in per cent, of sine wave signal, in the *channel under consideration*, modulating carrier at the peak deviation of the system.

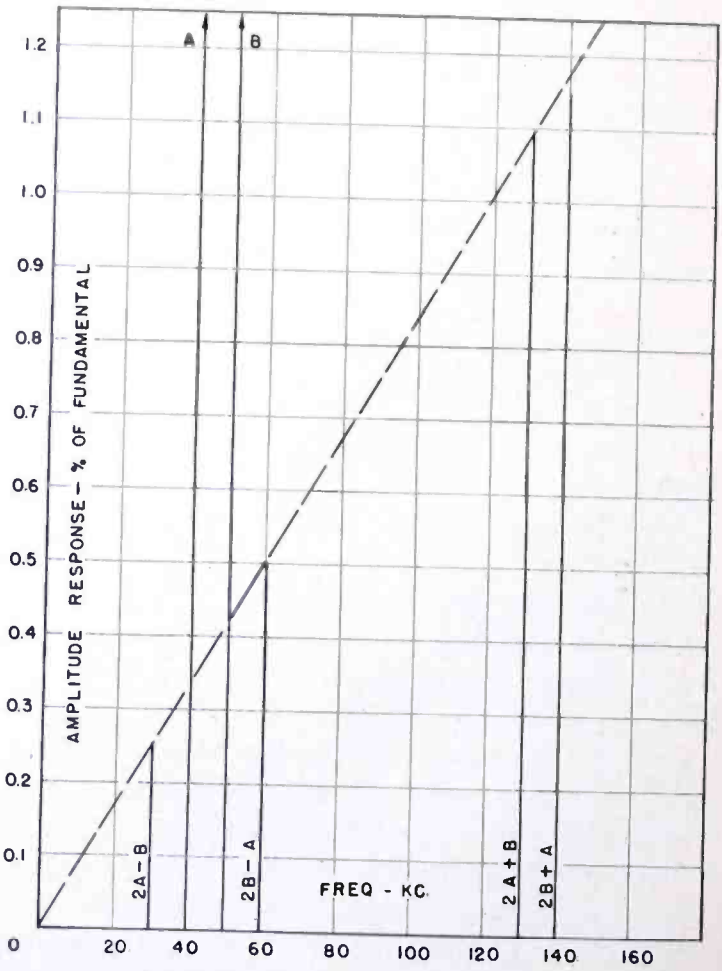

Fig. 2 — Amplitude of intermodulation components in a frequency - modulation system caused by non-linear phase characteristics of tuned circuits.

The distortion (d_3') should be calculated from Formula (5) instead of (4) because the cross talk of interest in Formula (6) is that at the frequency which d_3' is calculated and not at the 3rd harmonic frequency. The result of the calculation from Formula (5) should be multiplied by the number of such transformers in the system.

Since the 3rd order distortion adds on a voltage basis, it is assumed that it will be greater than any 2nd order distortion caused by mis-

tuning of the circuits in the system. Sufficient experience in systems has not yet been obtained to prove this assumption.

If the modified frequency-modulation characteristic suggested earlier is used, the signal to cross-talk ratio will be a little higher in the higher frequency channels than Formula (6) indicates, and will be slightly lower in the lower frequency channels.

In the case of straight phase modulation, the signal to cross-talk ratio is

$$S/N_3 = \frac{282}{\sqrt{y}\, d_3''} \sqrt{k}, \tag{7}$$

where

d_3'' = 3rd harmonic distortion, in per cent, of sine wave signal in the *highest frequency channel,* modulating carrier at the peak deviation of the system.

Formula (7) is based on the assumption that the intermodulation components will have a uniform distribution after de-emphasis in the receiver, except for the factor y. There is some error in this assumption according to the work of Fast[6] but it appears to be sufficiently small to neglect in practical systems design.

Experimental Confirmation

Signal to cross-talk measurements were made on a phase modulation system having a much greater bandwidth than the interstage circuit to be tested. The multiplex equipment consisted of 10 channels between 18 and 77 kilocycles. The principal source of distortion was the phase nonlinearity of the circuit under test. The results of the measurements and the calculations from Formula (7) are shown in Figure 3.

Other tests, where the principal sources of distortion were the modulator and discriminator, showed agreement with Formulas (1) and (3) within several decibels.

Other Systems of Multiplex

If frequency-modulated subcarrier channels are used instead of single-sideband channel signals, the result can be predicted from Formulas (1) and (6). Formula (1) nows shows the subcarrier to cross-talk ratio instead of the channel signal to cross-talk ratio. If narrow-band frequency modulation is used on the subcarriers, a loss

[6] S. Fast, "Cross Talk in Frequency and Phase Modulated Radio Relays Used in Conjunction with Multichannel Telephony Equipment", paper presented at I.R.E. National Convention, March 7, 1950.

of about 7 decibels occurs in the root-mean-square signal to cross-talk ratio in the demodulation process, providing the signal modulation is a complex wave and not a sine wave. An additional loss of 6 decibels occurs from Formula (6) because the modulation band of frequencies is doubled. Furthermore, this loss cannot be made up by a wide frequency deviation on the subcarriers, so far as phase distortion is concerned (Formula (6)), because d_3' increases in proportion to the increase in deviation of the subcarriers.

Although time-division multiplex systems are not in the scope of this paper, a general comparison in view of Formulas (1), (5) and (6) is of interest. Landon[7] has shown that time-division systems

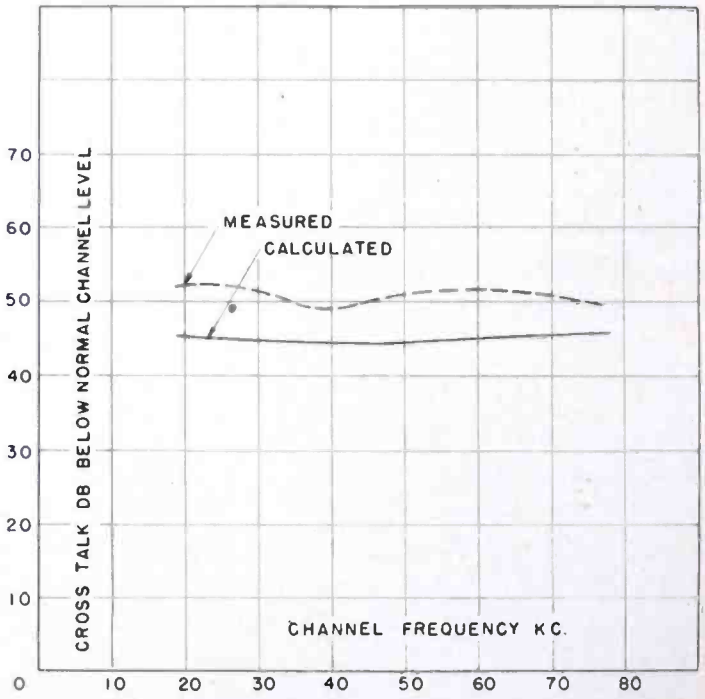

Fig. 3—Comparison of measured and calculated cross talk in a phase-modulation system caused by non-linear phase characteristics of tuned circuits.

frequency modulating a carrier do not have as good a signal to circuit-noise level for the same transmitter power and bandwidth as single-sideband multiplex. If the deviation of the single-sideband multiplex signal was reduced 6 to 10 decibels to equal the signal to circuit-noise of a particular time-division system, the cross talk would be reduced 12 to 20 decibels. As can be seen from the following example, cross talk can be held to sufficiently low limits in a frequency division multiplex system, and can in fact compare favorably with time-division systems in this respect.

---

[7] V. D. Landon, "Theoretical Analysis of Various Systems of Multiplex Transmission", *RCA Review*, Vol. IX, pp. 287-351, June 1948, and pp. 433-482, September 1948.

Example of Application

As an example of the application of the formulas, a frequency modulation system will be assumed having the following characteristics:

10 channels (all active), each with a band of 3000 cycles.
4 kilocycles separation between midchannel frequencies.
Highest modulation frequency = 40 kilocycles.
Bandwidth of each receiver = 3.0 megacycles.
3-decibel bandwidth of each of 6 critically-coupled interstage transformers = 5 megacycles.
Number of repeaters = 20.
Peak frequency deviation = 1.5 megacycles.
Total number of interstage transformers = 120.

From Formula (5) the value of d_3' is 8.16 per cent for the highest frequency channel. Placing this value in Formula (6) gives a signal to cross-talk ratio of 37.3/1 or 31.5 decibels in the highest frequency channel.

A signal to circuit-noise calculation shows a value of 48 decibels in the highest channel over one link at receiver threshold and enough excess power is usually provided to make the average signal-to-noise ratio over one link 68 decibels and over 20 links this would be about 55 decibels. Therefore the deviation of each channel could be reduced 8 decibels giving a signal to cross-talk ratio of 47.5 decibels and a signal to circuit-noise ratio of 47 decibels. Since these values are for the ratio of the root-mean-square of a complex signal to the root-mean-square noise, and are not weighted, the results are quite adequate for most applications.

If the modified frequency modulation characteristic is used, the cross talk and noise will be about 2 decibels lower in the highest frequency channel. The lower frequency channels will all be better than the above figures.

If the radio frequency circuits in the system are 50 per cent or more wider than the intermediate-frequency circuits, they will not cause a measurable increase in the overall cross talk of the system.

To find the linearity requirements of the discriminator and modulator of this system, it will be assumed that a 50-decibel signal to cross-talk ratio, calculated on a straight frequency modulation basis, will be adequate. Solving Equation (1) for d_3, it is found to be 0.8 per cent for the reduced deviation or 5.0 per cent for the full 1500-kilocycle peak deviation of the system. These values are for the 3rd order distortion. It is assumed that the 2nd order distortion is lower than 0.8 per cent at the reduced peak deviation.

Conclusion

Although the experimental verification of the theory has been limited to laboratory measurements, it is believed the formulas are of great value in the design of long-distance multichannel radio relay systems.

Tuned circuit distortion was shown to be of great importance in long relay systems. This type of distortion may be reduced by increasing the bandwidth, reducing the frequency deviation, or making the phase characteristic of the circuits more linear by time delay equalizing circuits.[8] There may be other sources of distortion in particular systems which have not been considered here.

Acknowledgment

The author wishes to acknowledge the valuable help of D. R. Crosby in this work and the welcome suggestions of V. D. Landon.

Appendix

If a band of signal frequencies is passed through a nonlinear circuit, Brockbank and Wass[1] have shown that the total third order distortion power is quite closely given by the following formula:

$$D_3 = 24\, d_{3p}\, P^3, \tag{8}$$

where

D_3 = total distortion power caused by 3rd order distortion,

d_{3p} = the 3rd harmonic distortion power of a single sine-wave signal output of unit power,

P = total output power of the multiplex signal.

The distortion power in one channel is

$$D_{3b} = \frac{b}{B}\, 24\, d_{3p}\, P^3\, y, \tag{9}$$

where

D_{3b} = the distortion power in one channel,

B = total frequency band of multiplex signals,

b = bandwidth of one channel,

[8] H. T. Friis, "Microwave Repeater Research", *Bell Sys. Tech. Jour.*, Vol. XXVII, pp. 183-246, April 1948.

y = distribution factor (Figure 1).

The signal power in one channel is P/n, where n is the number of channels.

Then the signal to distortion power ratio in each channel is

$$S'/D_{3b} = \frac{P}{n}\,\frac{B}{b}\,\frac{1}{24\,d_{3p}\,P^3\,y}. \tag{10}$$

Substituting

$$\frac{B}{b} = n\,k$$

where

k = the ratio of the frequency separation between the channel centers and the channel width,

$$S'/D_{3b} = \frac{k}{24\,d_{3p}\,P^2\,y}. \tag{11}$$

Since it is more convenient to measure the distortion at the peak frequency deviation of the system than at the level of one of the channels, unit power will be defined as the power of a sine-wave signal deviating the carrier to the peak value of the system. Assuming that the peak to root-mean-square ratio of the multiplex signal is 12 decibels, or a power ratio of 16 to 1, the value of P will be

$$P = \frac{1}{8},$$

and

$$S'/D_{3b} = \frac{64\,k}{24\,d_{3p}\,y}. \tag{12}$$

Changing to a voltage ratio, by taking the square root and using

$$\left(\frac{d_3}{100}\right)^2 = d_{3p},$$

$$S/N_3 = \frac{163}{\sqrt{y}\, d_3} \sqrt{k.} \tag{1}$$

Similarly, for 2nd order distortion, the total distortion power was shown to be[1]

$$D_2 = 4\, d_{2p}\, P^2, \tag{13}$$

where

d_{2p} = the 2nd harmonic distortion power of a single sine wave signal output of unit power.

The root-mean-square signal to cross-talk voltage ratio is

$$S/N_2 = \frac{141}{\sqrt{y}\, d_2} \sqrt{k.} \tag{3}$$

NEW DEVELOPMENTS IN RADAR FOR MERCHANT MARINE SERVICE*

By

C. E. Moore

Engineering Department, Radiomarine Corporation of America, New York, N. Y.

Summary—This paper discusses a new 3-centimeter Merchant Marine radar designed especially for smaller vessels, such as tugs, ferries, and trawlers. Technical features and factors relating to the design are discussed. The apparatus is illustrated by various photographs.

Introduction

IMMEDIATELY after the war, there was great demand for a radar suitable for Merchant Marine use. Military radar emphasized detection of an object at the greatest possible range. Commercial applications require a radar for anticollision, navigation, and position finding, with emphasis on high discrimination and minimum range. Such services call for a great number of improvements because a narrow beam width, a short pulse length, and close-in seeing are of paramount importance.

To aid in guiding development of the newborn navigational aid, the U. S. Coast Guard issued, in the fall of 1945, an "Advisory Minimum Specification for Navigational Radars."[1] These recommendations included such items as a 30-mile maximum range, variable range marker, true bearing display, performance indicator, 60-cycle supply, and provision for future beacon use. The Great Lakes Radar Operational Research Project sponsored by the Great Lakes Carriers' Association resulted in further recommendations calling for six range scales of 1, 2, 4, 8, 20, and 40 miles each, and a 12-inch cathode-ray tube.

The basic factors involved in the design of such a radar were treated in an earlier paper,[2] and a later article[3] illustrated and de-

---

* Decimal Classification: R537.1.

[1] Office of Engineering, Electronics Division, U. S. Coast Guard, Treasury Department, Advisory Minimum Specifications for Navigational Radars, CG157-1 Supplement No. 1, 12 pages, August 1, 1946.

[2] I. F. Byrnes, "Merchant Marine Radar", *RCA Review*, Vol. VII, No. 1, pp. 54-66, March, 1946.

[3] F. E. Spaulding, Jr., "Radar for Merchant Marine Service", *RCA Review*, Vol. VIII, No. 2, pp. 312-330, June, 1947.

scribed the model CR-101 radar. Since that time several improvements have been made, such as longer tube life, reduction in the side lobes of the antenna pattern, and a new receiver with more stable automatic-frequency-control circuits. This model CR-101A radar has a 12-inch plan-position-indicator (PPI) tube, two-pulse-length operation at ¼ and 1 microsecond, a high repetition rate to give brighter pictures on the shorter ranges, true or relative bearing presentation, over 30-kilowatt peak radio frequency power, a 1.8-degree horizontal beam, an echo box for checking performance, and a variable range marker.

The longer ranges (up to 40 miles) of this model were of little use to vessels plying the inland waterways such as the Ohio and Mississippi Rivers where clear vision for five miles is seldom possible due to the numerous bends in the rivers. For this special application, a radar similar to the standard model was designed using ranges of 1, 2, 4, 8, and 20 miles. The personnel of tugs and towboats operating along the coasts and in the inland water routes along the Gulf, as well as in harbors, prefer the 12-inch PPI, the one-mile range for close navigation, and the 20-mile range for use after entering open water.

There are many vessels of lesser size, such as harbor tugs, fishing vessels, and small cargo ships which need radar facilities, but cannot accommodate a large unit. Also, even though space might be available, these smaller vessels cannot justify the expense of a larger, more elaborate installation. It was this need for a smaller, more compact, lower cost radar which led to the design of model CR-103 radar.

Design Considerations

There were two main problems to be solved: (1) reduction of the physical size and (2) lowering of cost by a substantial factor. High performance was to be maintained without compromising simple and reliable operation.

The size of any PPI indicator is largely determined by the size of the cathode-ray tube. To obtain a unit satisfactory for small, cramped pilot houses, it was decided to use a 7-inch cathode-ray tube, designed for this application. It uses the latest type gun construction; is flat faced; has magnetic focus and deflection; has improved spot size characteristics; and is small, rugged and compact.

A large reduction in overall size of the units has been achieved by using 400-cycle instead of 60-cycle components. Figure 1 shows, on the left, two transformers of approximately the same voltage and current ratings used to deliver 5,000 volts to the second anode of a cathode-ray tube; the extreme left unit is for 60 cycles and the smaller

one is for 400 cycles. The next unit is a 20-henry choke rated at 175 milliamperes. To the right is a 1-henry choke rated at 200 milliamperes. In place of the 10-microfarad capacitor used in CR-101A radar filter circuits, the 1-microfarad unit shown to the right is used in CR-103. Capacitor and inductor values can be reduced to about 15 per cent of those used for 60-cycle filtering.

For transformers of comparable current and voltage ratings, a 400-cycle design is approximately 30 to 35 per cent smaller in volume and may weigh 40 to 45 per cent less than a 60-cycle unit. Many factors contribute to the cost of a transformer. Smaller units are harder to handle and therefore require more labor. High voltage ratings require more space for increased insulation. It appears that the cost of low-voltage plate transformers, which supply 300 to 500

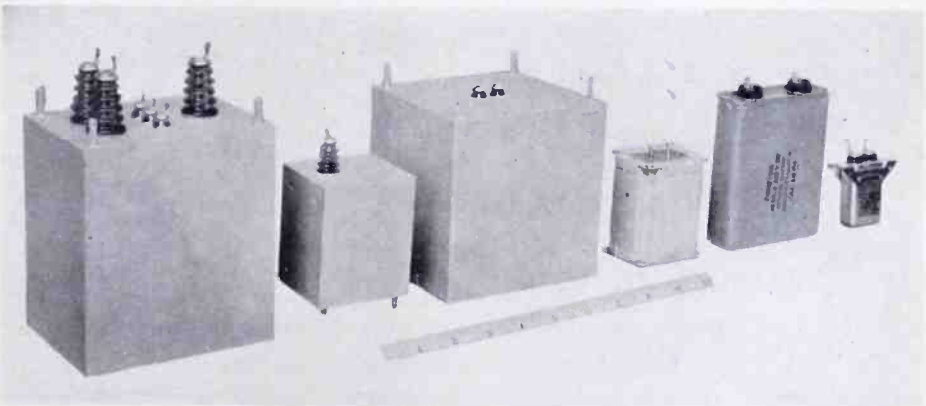

Fig. 1—Relative size of components.
Left to right: 60-cycle transformer, 400-cycle transformer, 20-henry choke, 1-henry choke, 10-microfarad 600-volt capacitor, 1-microfarad 600-volt capacitor.

volts direct current, is approximately the same for either a 60- or 400-cycle supply; 400-cycle filament transformers are small and cost about 15 per cent more; while for high-voltage units, which deliver 2,000 to 5,000 volts direct-current, the cost is approximately 50 per cent more for 400-cycle units.

When designing a small radar, it is tempting to consider reducing the radio frequency power output. However, the captain operating a vessel needs to see small buoys, as well as other objects, at as great a range as is practicable. Furthermore, there is little to be gained in either size or cost by choosing a lower-power magnetron. It was therefore decided that this radar should have the same peak-power output (30 kilowatts) and sensitivity as the larger CR-101A model. Reports from users indicate that this has been a wise choice.

The next step was to reduce the total number of tubes and to

minimize power-supply requirements. The CR-101A radar uses 61 tubes while CR-103 uses 45, a reduction of 26 per cent. This naturally reduces overall power drain, size, and cost. Instead of converting with the radar motor generator to operate blowers and the antenna drive motor, these devices are supplied directly from the line of the ship. As a result, ships with a limited primary source of 24, 32, 115, 230 volts direct current or 115/230 volts alternating current can use this radar.

The motor generator is also small in size, and is rated at 750 volt-amperes, 400-cycle output, although the actual load is only about 550 volt-amperes. The radar has sufficient regulation and compensation to operate satisfactorily for 400-cycle line fluctuations between 105 and 125 volts. A large voltmeter and field rheostat are provided so that proper adjustment may be made for low or high voltage on the ship. This unit is mounted near the indicator so that the operator may easily make the adjustment.

General Installation

The basic units which comprise a CR-103 radar installation are shown in Figure 2. The indicator unit is normally located in the wheelhouse where it may be easily operated by navigating personnel. The antenna is mounted on a small tower or other support at such a height that the radar beam is not shadowed by large structures, especially forward and off the bow. The transmitter-receiver unit may be installed in any convenient location so that the waveguide and cable lengths are reasonably short. The motor generator which converts the power from the ship to 115 volts, 400 cycles may be installed wherever desired, along with the line switch and motor starter.

Indicator

The indicator unit is of the rotating coil type, using a special 7-inch, high-definition, flat-face cathode-ray tube, type 7MP7. The trunnion type of indicator support permits mounting the unit from the ceiling, on a pedestal, on top of the transmitter-receiver unit, or on a table or other convenient place. The unit, shown in Figure 3, is rugged and light, measuring 10 inches high, 15 inches wide and 18 inches deep, and weighing 50 pounds. There are two aluminum protective covers, one for the top and one for the bottom. In Figure 4, the top cover has been removed, showing how tubes may easily be inspected and changed when required. The chassis is bent with a step on each side of the cabinet. Tubes mount in their sockets on top

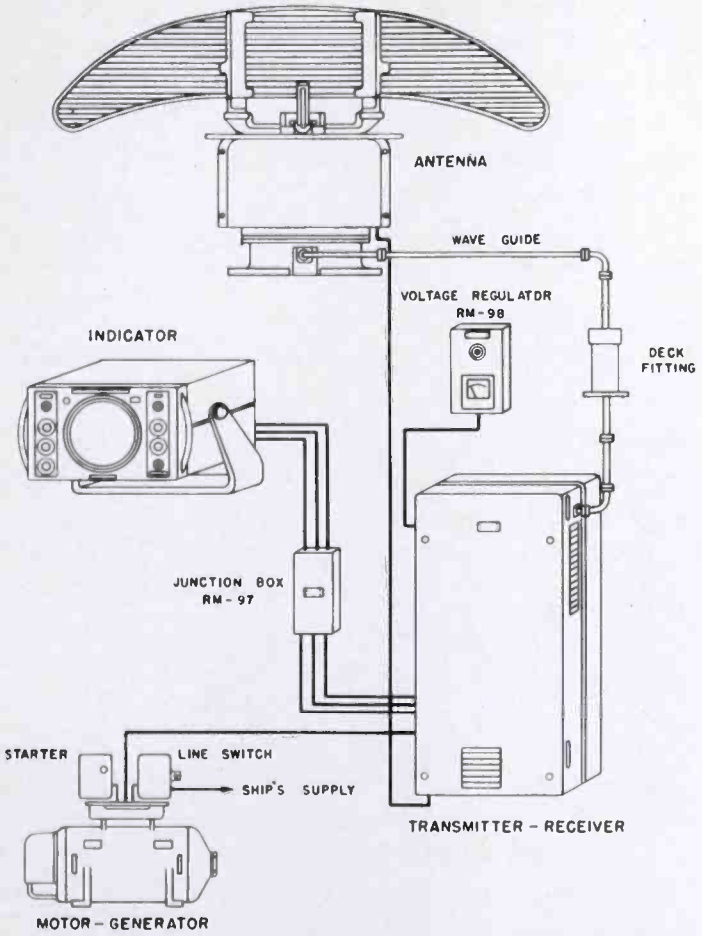

Fig. 2—Model CR-103 radar installation.

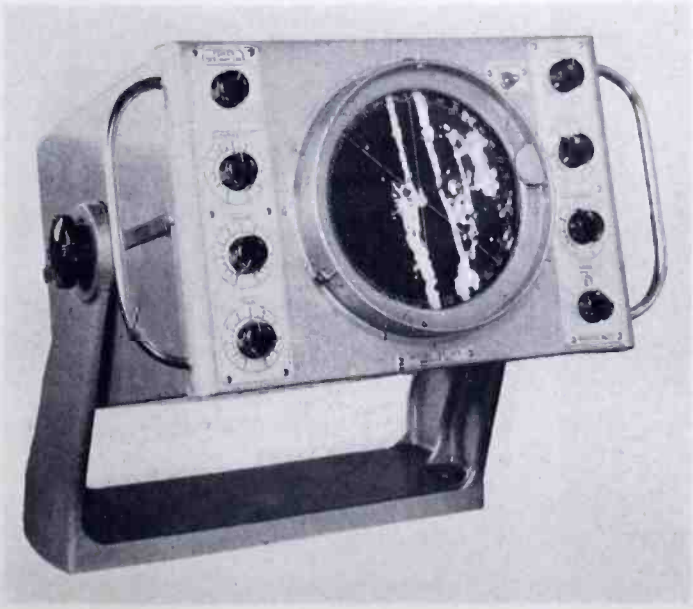

Fig. 3—Indicator.

of these steps. Beneath are the smaller parts and wiring as shown in Figure 5, in which the bottom cover has been removed.

Ranges provided are 1, 3, 8, and 20 miles, either statute or nautical, depending upon application. A block diagram of the indicator circuits is shown in Figure 6. The trigger is generated in the modulator. Thus the delay due to coaxial cables in trigger and video outputs are the same, both going to the indicator. Circuits in the indicator are conventional except for certain special features mentioned later.

Both heading and stern flashes are initiated by a cam operated switch in the antenna. The intensity may be varied by a potentiometer

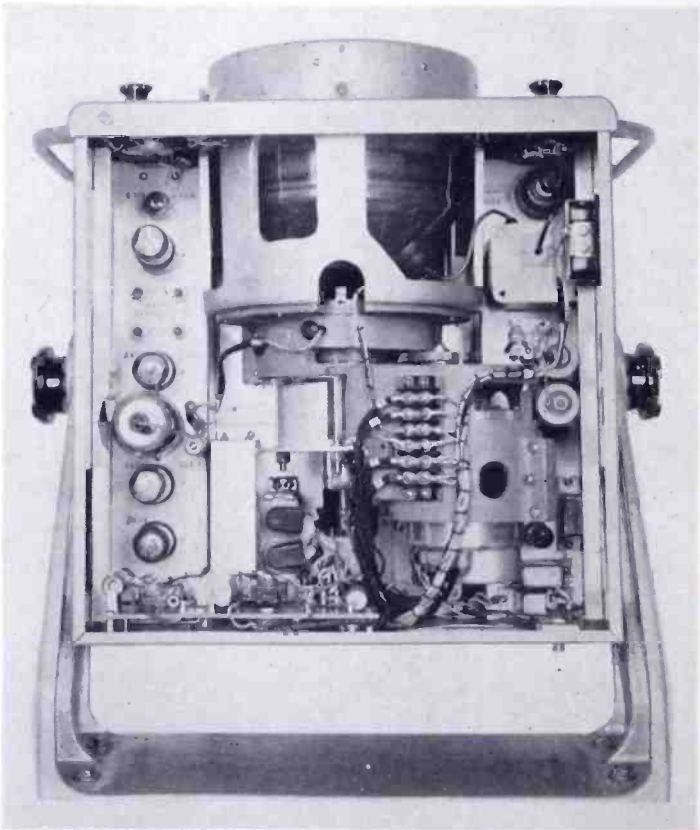

Fig. 4 — Indicator tipped up, cover removed.

on the front panel of the indicator. Usually these flashes are generated using vacuum tubes, but the charge and discharge of a capacitor has been found to be satisfactory. (See Figure 7.) When the cam closes the switch, the charging of capacitor C causes a negative pulse to appear across the cathode resistor of the cathode-ray tube. The positive pulse, which occurs when the switch is opened, is clipped by the diode across this resistor.

The second anode voltage for the cathode-ray tube is not regulated. If no corrective means were provided, the line voltage would vary the high voltage, and change the size of the picture. To prevent this, the

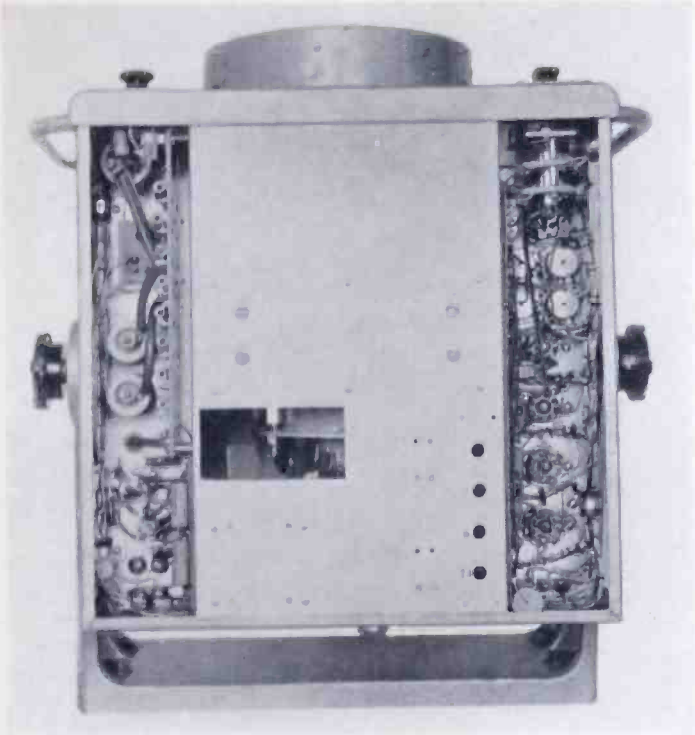

Fig. 5 — Indicator tipped up, bottom removed.

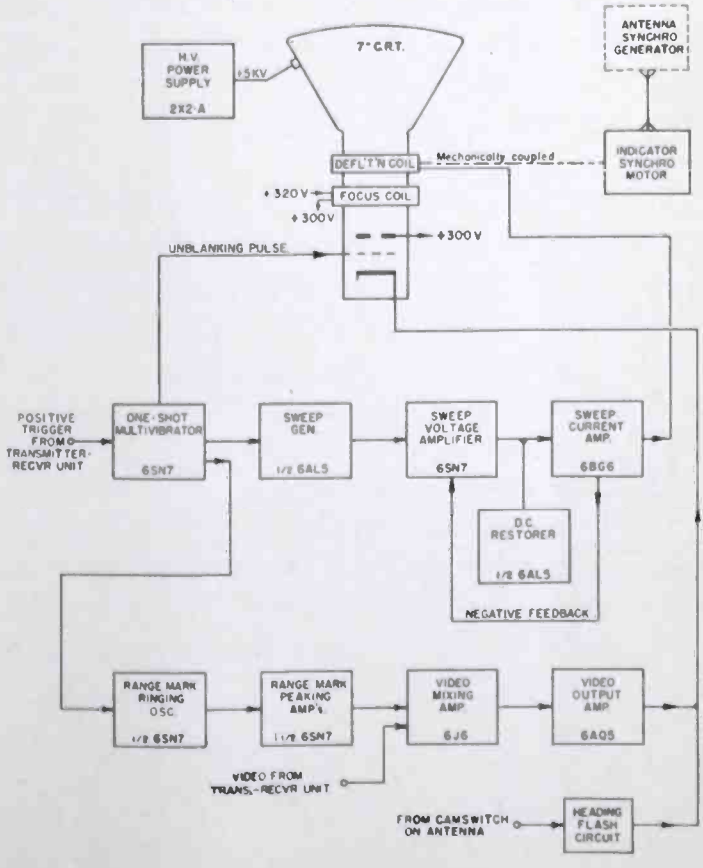

Fig. 6 — Indicator block diagram.

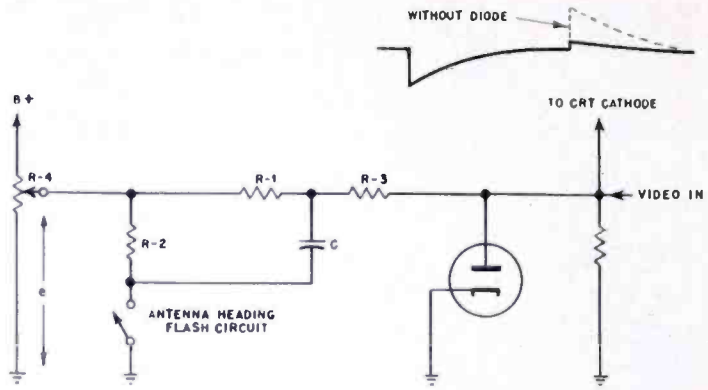

Fig. 7 — Heading-flash circuit.

drive for the 6BG6 tube is automatically changed by selecting the proper voltage between unregulated +600 volts and regulated +300 volts, using a bleeder, and feeding this voltage to the sweep charging capacitors. Thus as the line voltage increases, the drive increases to counteract the stiffer cathode-ray tube beam and maintains the same size picture.

As the second anode voltage on the cathode-ray tube changes due to line fluctuation, the cutoff of the cathode-ray tube changes, causing the intensity level (without video signals) to shift. The bleeder for the 5,000-volt second anode supply is returned to ground through a suitable resistor in the cathode circuit of the cathode-ray tube (See Figure 8). Thus, when the alternating-current line voltage fluctuates, the intensity is automatically stabilized by a change of cathode potential.

For a fixed repetition rate, the light, or intensity, decreases as the sweep speed is increased. Thus the picture tends to be dimmer on the one-mile than on the twenty-mile range. However, by partial dc restoration of the unblanking pulse on the grid of the cathode-ray

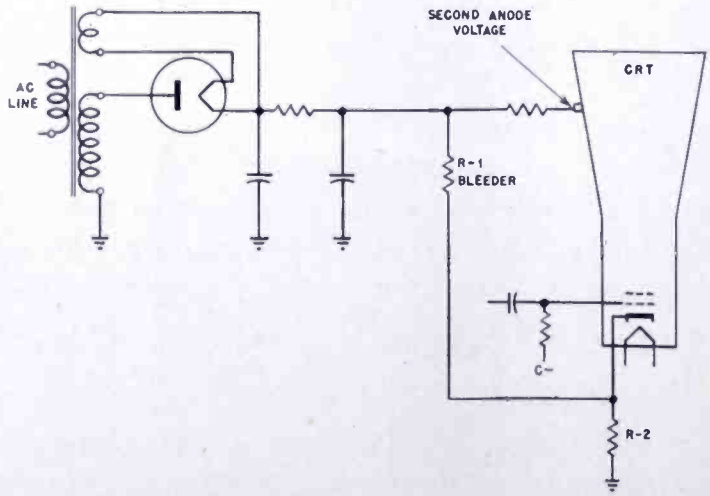

Fig. 8 — Intensity compensation for changes in cathode-ray-tube second anode voltage.

tube, the effective bias is made more negative for the longer ranges (See Figure 9). In practice, the intensity control is set so the sweep is just visible on the one-mile range. It becomes invisible for the longer ranges. However, this is in the right direction, because more receiver gain is needed for the longer ranges, and the general intensity is increased due to the noise background. Partial dc restoration is accomplished by shunting only part of the cathode-ray tube grid resistor with a germanium crystal.

Synchronization between antenna and sweep is obtained by synchros geared at a ratio of 10 to 1. The circuit shown in Figure 10 automatically removes the ambiguity of selecting the proper 36-degree sector. This arrangement has been used in other equipments made during the war and need not be described further.

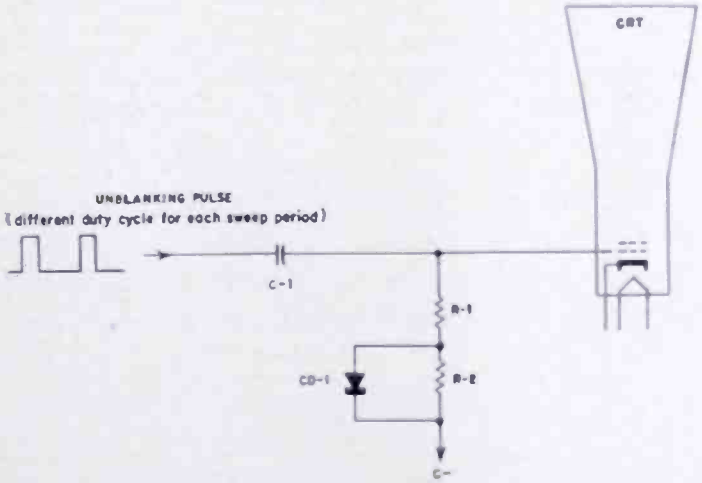

Fig. 9 — Intensity compensation for different ranges.

A glass magnifying lens is available as an accessory to increase the apparent size of picture to that of a 10-inch tube. A plastic, liquid-filled lens, although lighter in weight, was considered to be too fragile and too easily scratched. The lens fits on the front of the indicator in place of the normal viewing hood and a larger hood is supplied for use with it.

Distortion with this solid glass, ground and polished lens is negligible and the lens is designed so that a reasonable viewing angle can be used without impairing the picture. If too small a lens is used, the field of view is not sufficient to include the azimuth scale. If the picture is magnified much more, the angle of view is restricted by distortion.

ANTENNA

The antenna unit is shown in Figure 11. The reflector has a 50-inch aperture, is 11 inches high, and is made of aluminum cast in

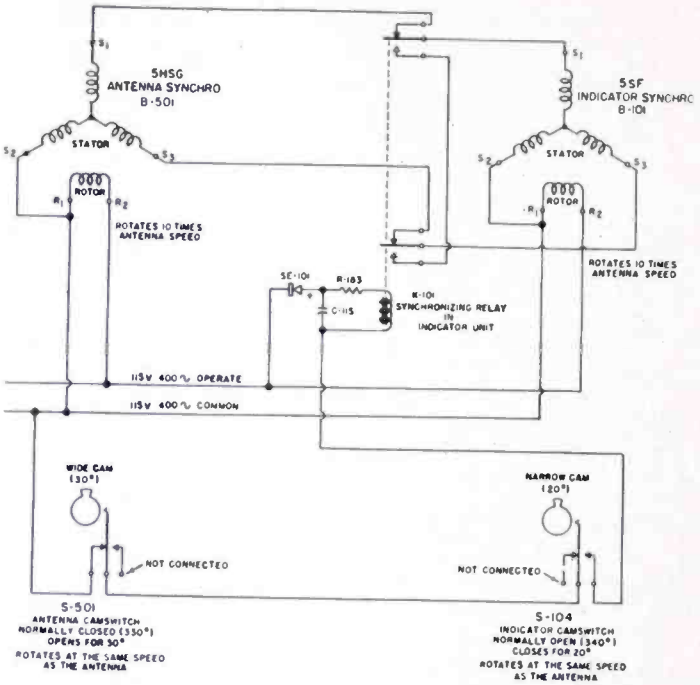

Fig. 10 — CR-103 synchro system schematic.

three pieces. Mating surfaces are machined, doweled, and bolted together after which the entire reflecting face is surfaced to a tolerance of ±1/64 inch (See Figure 12). The horizontal beam width at the half-power points is 1.9 degrees, while the vertical pattern is 20 degrees.

Lower side lobes are obtained when the perimeter of the reflector follows a given contour of the primary pattern. All energy from the horn at the edge of the reflector is down 20 decibels from that at the center of the reflector. The side lobes close to the main beam are 32

Fig. 11 — Antenna.

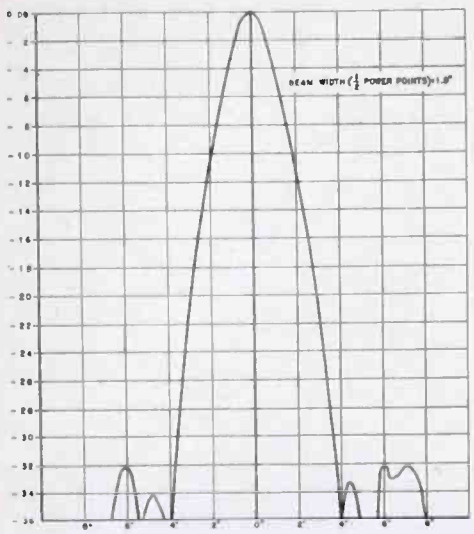

Fig. 12—CR-103 antenna horizontal pattern. Main beam width at half power points is 1.9 degrees.

decibels below the main beam, while the back radiation and energy overshooting the ends of the reflector are down more than 30 decibels. Experience has shown that if the leakage is greater than these limits, false targets clutter the scope when operating in narrow waters with large targets close by.

Inside the cast aluminum housing are the drive motor, the synchro, synchronizing and heading flash cams and switches, and power factor correcting capacitor (Figure 13). The cable gland and waveguide coupling are shown in Figure 14. All gears are immersed in oil, and all rotating shafts enter the top of the gear box to prevent oil leakage even if the oil seals should become worn. The waveguide rotating

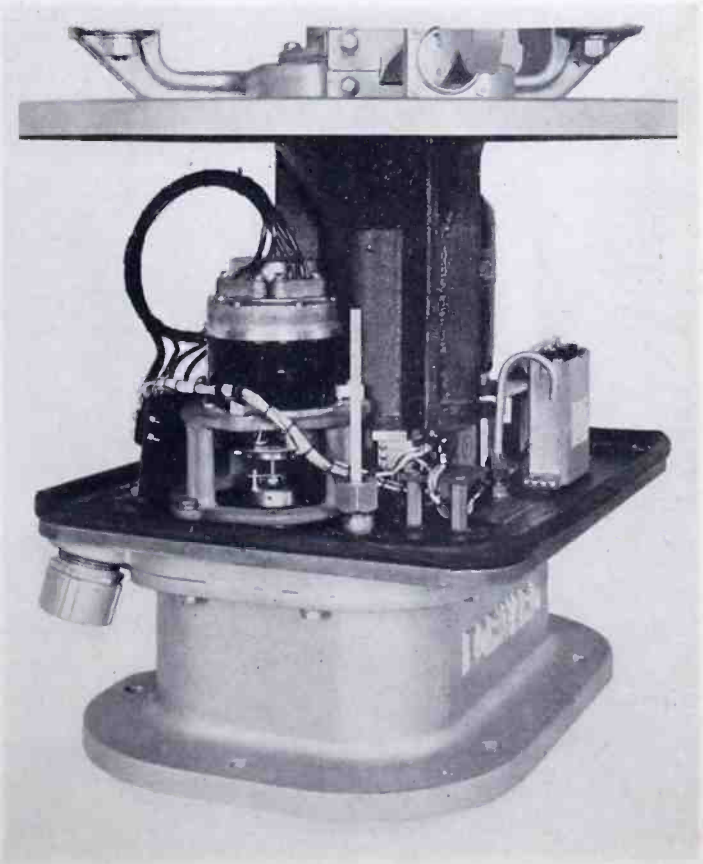

Fig. 13 — Antenna, housing removed.

joint and drive shaft for rotating the reflector are within the ribbed column.

Antenna heater strips controlled by a thermostat are available as an accessory. This allows the antenna to start easily in cold weather and inhibits icing.

Smaller vessels such as harbor craft turn faster than large ships. Therefore, it is necessary to increase the rate of the antenna rotation to minimize the jumping of the picture. CR-103 antenna rotates at 17 revolutions per minute, giving a "new picture" each 3½ seconds.

The antenna weighs 150 pounds. It can be mounted on a light tower as illustrated in Figure 15.

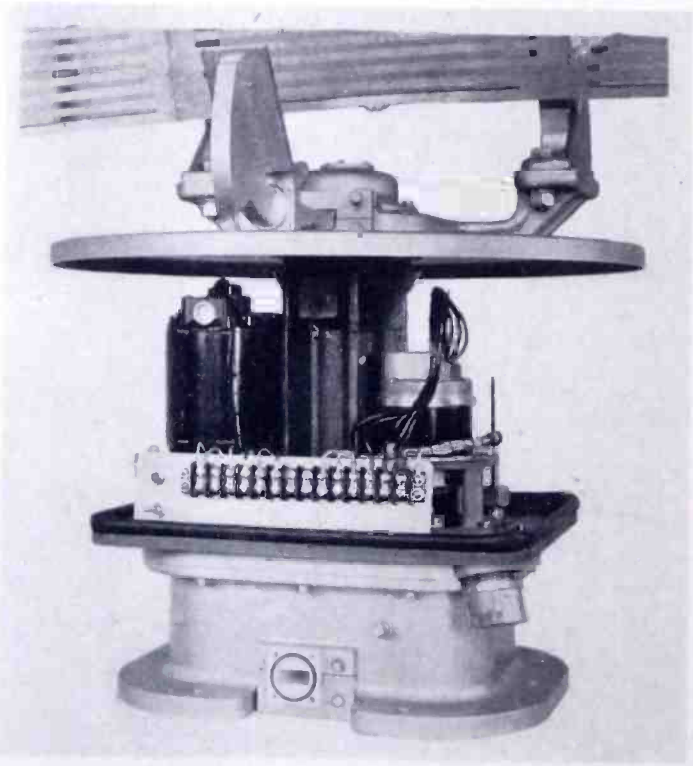

Fig. 14 — Antenna, housing removed.

TRANSMITTER-RECEIVER

This unit includes the magnetron, the modulator, the receiver, all low-voltage power supplies, and a ventilating system.

The entire unit is exceptionally easy to service. Four captive screws on the front of the cabinet allow the cover to be removed, exposing the magnetron; the receiver; the duplexer and mixer; the low voltage rectifiers, transformers, tubes, and filters; the blower intake air filter and distributing duct; as well as the test meter and self indicating fuses (See Figure 16).

Stray fields around the magnet are confined by a steel enclosure,

two sides of which are open. By loosening the three screws at the top and the three thumb screws at the bottom, one half of the box is removed to allow replacement of the magnetron. Only a screwdriver is required to make this change which is easily accomplished from the front of the unit.

Fig. 15—Experimental antenna installation.

A hinge on the left side of the panel allows this entire unit to swing out for servicing as shown in Figure 17. To do this, it is necessary to uncouple the waveguide by loosening the large clamping nut around the guide and to loosen two captive screws locking the panel. The modulator and high-voltage power supply are located in the compartment attached to the back of the panel. A partially per-

forated cover, not shown in this illustration, completes the shielding and protection. Removing this screen opens an interlock switch which shuts off the high voltage.

The modulator circuit is conventional, using a 4C35 hydrogen thyratron with dc resonant charging. The small receiving-type tubes mounted on the shelf as seen in Figure 17 are the three-minute time delay tube and the trigger generating and driving tubes for the 4C35.

This modulator drives a 725A magnetron to give a peak radio-frequency power output between 30 and 40 kilowatts at a repetition rate of 1,000 pulses per second and a pulse length of 0.4 microsecond.

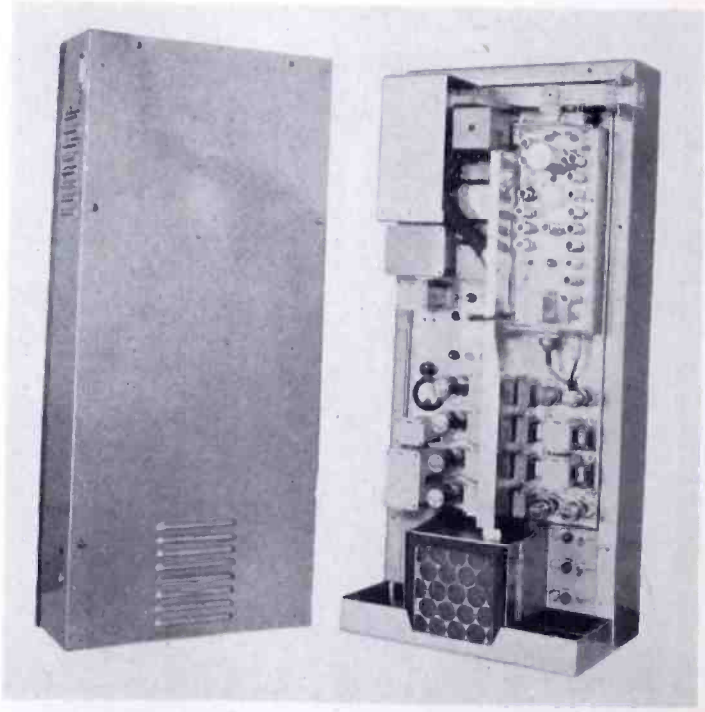

Fig. 16—Transmitter-receiver.

The keep-alive voltage for the transmit-receive switch tube is obtained by using two 1V2 tubes in a voltage-doubling circuit giving 900 volts output.

Since the output of the 725A magnetron is fed to a waveguide $1\frac{1}{4}'' \times \frac{5}{8}''$, and the same size guide is used between the transmitter-receiver unit and the antenna, it was decided to redesign the duplexer so that it uses the same size guide. A 1B35 anti-transmit-receive tube and a 1B24 transmit-receive tube are used in conjunction with this duplexer and the mixer.

The mixer is mounted directly on the receiver, so that no coaxial cables are necessary. The receiver itself uses a low-noise input circuit with conventional staggered tuned intermediate-frequency circuits, and provides automatic frequency control for the 723AB-2K25 local

oscillator. It also incorporates the sensitivity time control circuit for reducing sea clutter, adjusted by a knob on the indicator. The receiver, as a unit, can be easily removed and replaced by disconnecting the mixer from the duplexer, and removing the video and power cable plugs.

Behind the air filter is the blower which feeds the air distributing duct which can best be seen in Figure 16. This distributes air to the modulator, to the low-voltage power supplies, the receiver, and the magnetron. The output for the heated air is through louvres in the side and back of the cabinet.

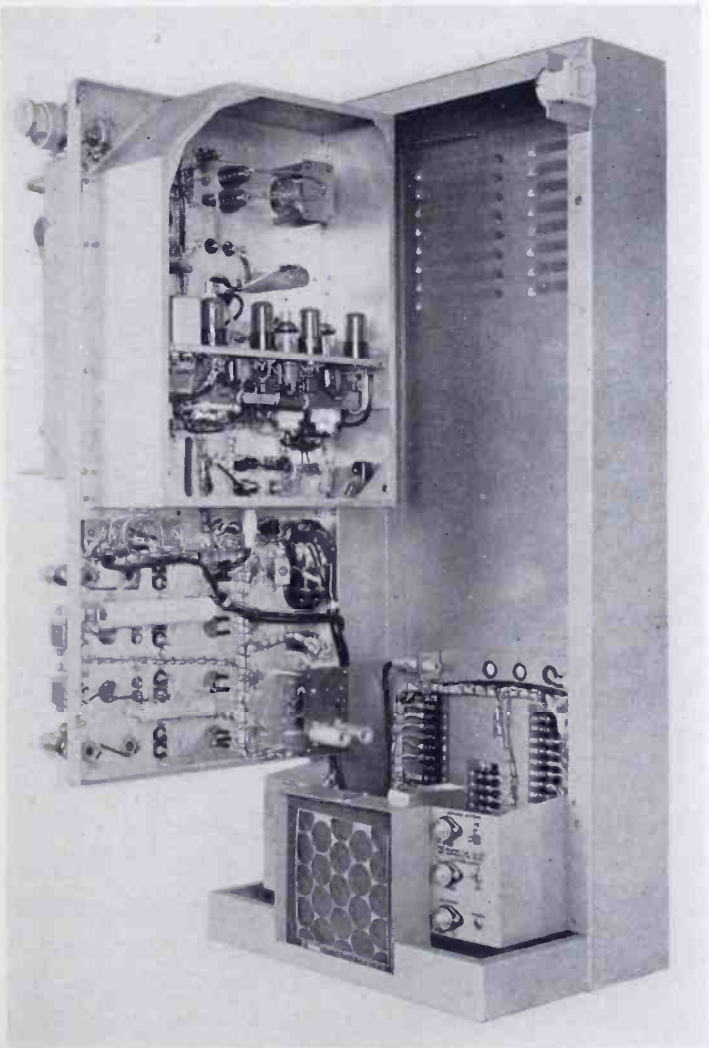

Fig. 17 — Transmitter-receiver unit, panel open for servicing.

The overall weight of the three major units, transmitter-receiver, indicator and antenna is approximately 400 pounds for the CR-103 model. This may be compared with the overall weight of 930 pounds for the CR-101-A and shows the reduction achieved in the design of the smaller model.

General Trends in Commercial Marine Radar

At the end of World War II there was no radar equipment available, designed specifically for merchant ships. Some vessels of United States registry and a few of foreign registry were equipped with military type radars. Beginning in 1946, and up to October 4, 1950, approximately 1,100 United States vessels have been fitted with commercial radars. The majority of these installations operate in the three-centimeter band, while about one-third of the total use the ten-centi-

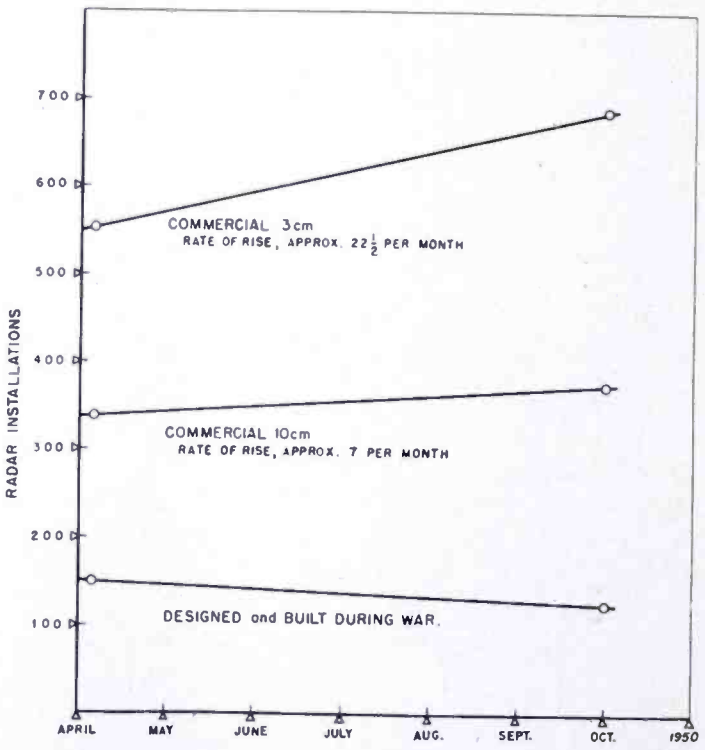

Fig. 18 — Commercial radar licensed by FCC as of September 29, 1950.

meter band. The rate of installations and the total number on United States ships is shown in Figure 18 for both frequency bands. Figure 18 also shows a gradual decrease in the number of installations of war-built radars which are being replaced by commercial designs.

Vessels of United Kingdom registry fitted with radar number approximately 600. All of these installations use the 3-centimeter band in accordance with the specifications of the British Ministry of Transport. Radar installations on other foreign vessels (Norway, Sweden, Denmark, Netherlands, etc.) total approximately 500. It is, therefore, evident that the merchant marine throughout the world has made good use of radar as a navigational and anti-collision aid.

Most of the time lost by shipping, due to weather conditions which hinder navigation, occurs when entering harbors or ports, or while traveling through rivers, channels, or other restricted waterways.

Under these adverse conditions it is obvious that the PPI presentation should have the maximum practicable bearing and range resolution, especially at short ranges. The average 3-centimeter installation, using an antenna with a four-foot aperture, provides a horizontal beam width of two degrees. Typical 10-centimeter radars with seven-foot aperture antennas have a 3.5-degree beam width. More recent developments have further reduced the beam width to one degree or less for 3-centimeter operation. This requires an antenna having an aperture of about nine feet. On the 10-centimeter band, beam widths of the order of two degrees are obtained with fourteen-foot apertures, although this results in a rather unwieldy structure which must withstand severe wind loading conditions at sea.

Close-in seeing is mainly a function of pulse length and receiver recovery time. Pulse lengths to the order of one-quarter to four-tenths microsecond are commonly used and provide minimum ranges of about 70 to 80 yards. While shorter pulse lengths will further reduce the minimum range, the designer must strike a suitable compromise in order to maintain long range performance where longer pulse lengths are preferred.

MAGNETO-OPTIC TRANSDUCERS*

By

ALBERT W. FRIEND

Research Department, RCA Laboratories Division,
Princeton, N. J.

Summary—The magneto-optic or Faraday effect, which was discovered and evaluated by Michael Faraday in 1845, has had few applications. An investigation was made to ascertain its applicability, in combination with more recently developed apparatus, in practical magnetic to optical and electrical transducers.

Some of the theoretical and experimental results, which have been obtained from evaluations of the magneto-optic effect as a means for producing an output voltage or current of instantaneous amplitude proportional to any applied magnetic potential, are described herein. The main objective was the development of a simple magneto-optic playback head for magnetic records. It is found that, with simple systems and presently available materials, the maximum signal-to-noise ratio is only about 30 decibels. This is considerably below the minimum desired value.

Various means for improving the signal-to-noise ratio are discussed. Other applications of the magneto-optic effect are suggested. A theoretical treatment of the system is developed so that the effect of proposed materials and variations of the system may be evaluated without difficulty.

INTRODUCTION

IT IS the customary practice to utilize or detect a magnetic field by causing its linkage with an inductor element (a coil of wire) to change in a prescribed manner and to utilize or to measure either the electrical potential induced across the terminals of the inductor or the electric current which that voltage may cause to flow in an external circuit. This practice has been followed in all of the well known magnetic record reproducer systems.

Such systems may utilize a source of magnetic potential which consists of a tape, coated with a uniform surface layer of finely divided particles, or a solid skin of a retentive magnetic material, which may be caused to traverse a very narrow gap in a magnetic circuit so that a portion of the magnetic potential of the tape is applied across the gap. This magnetic potential produces a field in the external magnetic circuit. It is customary to wind one or more inductor coils around the core of the external circuit. The variations of the strength of the magnetic field within the core change the amount of magnetic flux

* Decimal Classification: R535.3.

linking these coils and thus produce, between their terminals, an electric potential

$$E = -10^{-8} N \frac{d\phi}{dt}. \tag{1}$$

If the magnitude of the magnetic flux varies as a periodic function of time, its value at any instant may be represented as the summation of a series of terms of the form

$$\phi_n = \hat{\phi}_n \sin (\omega_n t + \gamma). \tag{2}$$

When the amplitudes of the applied magnetic potential signals are very small with respect to the magnetic saturation values of the core materials in the magnetic circuit, the various terms of the complete expression are essentially independent of one another. Hence, they may be considered separately. Substitution of (2) in (1) yields

$$E = -10^{-8} N \hat{\phi} \omega \cos \omega t, \tag{3}$$

when the phase angle, γ, is disregarded and a general term is assumed. This indicates that the output voltage is a function of the variational frequency,

$$f = \omega/2\pi. \tag{4}$$

Most recording and reproducing systems are, however, constructed to yield an amplitude response characteristic which is constant with frequency within the working spectrum. This requires that the frequency dependence of Equation (3) be compensated by amplitude corrective networks in the playback system.

The magneto-optical process does *not* involve a time derivative function, but produces an output current or voltage which is directly proportional to the instantaneous value of the applied magnetic flux density. It requires no compensation networks except those which may be used to correct for the decrease of the high frequency amplitudes, on account of the geometry and speed of the magnetic record, in relation to the magnetic properties of the tape and the gap between the pole pieces of the magnetic pickup device. When a magneto-optic transducer is used it may be preferable to perform this compensation in recording, so that no compensation is required in the playback system.

Description and Mathematical Analysis

In 1845, Michael Faraday[1] discovered that when optically isotropic substances are exposed to a magnetic field they cause the components of light passing in the direction of the magnetic field to be rotated in polarization. The angle of rotation (radians) was found to be

$$\theta = \mathcal{V} H d \cos \alpha = \mathcal{V} d \frac{B}{\mu_0} \cos \alpha, \qquad (5)$$

where

$\mathcal{V}$ = magneto-optic constant of the material (radians/cm. oersted),

H = intensity (Oersteds) of the magnetic field,

d = path length (centimeters) in the material which is common to the superimposed light and magnetic fields,

α = angle between the direction of propagation of the light and the applied magnetic field vector in the material,

β = flux density (Gauss) of the magnetic field,

μ_0 = relative magnetic permeability of the magneto-optic material.[2-10]

The magneto-optic constant of most ordinary transparent materials is quite small. A few such materials exhibit notably greater effects. A heavy leaded x-ray glass, manufactured by the Pittsburgh Plate Glass Company, appears, from these experiments, to produce the largest useful magneto-optic effect of all the solids which have been tested. It is somewhat better than the flint glass with which it was compared for obtaining its relative position in the tabulated list of magneto-optic substances. Table I has been prepared from published

---

[1] M. Faraday, EXPERIMENTAL RESEARCHES, Vol. III, p. 1, 1845.

[2] Rodger and Wilson, *Philos. Trans.*, Vol. 186, p. 621, 1895.

[3] Kundt and Roentgen, *Wied. Ann.*, Vol. 6, p. 332, 1879.

[4] M. Faraday, EXPERIMENTAL RESEARCHES, Vol. III, p. 453, 1845.

[5] E. Verdet, *Compt. Rend.*, Vol. 56, p. 630, 1863.

[6] E. Verdet, COLLECTED PAPERS, Vol. I, p. 112, 1872.

[7] J. E. H. Gordon, PHYSICAL TREATISE ON ELECTRICITY AND MAGNETISM, Vol. II, p. 218, Appleton and Company, New York, 1880.

[8] Lord Rayleigh, SCIENCE PAPERS, Vol. II, p. 360, Cambridge University Press, London, 1900.

[9] A. Winkelmann (Editor), HANDBUCH DER PHYSIK, Vol. V; F. Auerbach, ELEKTRIZITAT UND MAGNETISMUS, pp. 405-410, Verlag von J. A. Barth, Leipzig, 1908.

[10] E. V. Fleischl, *Wied. Ann.*, Vol. 25, p. 308, 1885.

Table I—Magneto-Optic Rotational Constants (Wavelength: $\lambda = 589.3$ millimicrons)

Substance	Verdet's Constant (radians/cm. oersted)	Temp. °C.	Remarks
Solids			
Glass, Heavy Lead X-Ray	3.10×10^{-5}	20	Measured by the Author.
Glass, Jena, S. 143	2.583×10^{-5}	18	
Glass, Flint (Medium)	1.22×10^{-5}	20	
Glass, Cobalt-Blue Plate (Crown)	1.22×10^{-5}	20	Measured by the Author.
Salt, NaCl	1.13×10^{-5}	16	
Glass, Jena, 0.451	9.221×10^{-6}	18	
Salt, KCl	8.314×10^{-6}	16	
Quartz ($\perp$ to optical axis)	5.003×10^{-6}	20	
Glass, Jena, S. 179	4.683×10^{-6}	18	
Amber	-2.79×10^{-6}	19	
Liquids and Solutions			
Ferric Chloride ($FeCl_3$)	-5.893×10^{-5}	20	Aqueous solution 1.4331g/cm^3
Carbon Disulfide (CS_2)	1.2508×10^{-5}	18	
Benzene (C_6H_6)	8.64×10^{-6}	20	
Sodium Carbonate (Na_2CO_3)	4.07×10^{-6}	20	Aqueous solution 1.1006g/cm^3
Water (H_2O)	3.80×10^{-6}	20	
Hydrogen Chloride (HCl)	3.374×10^{-6}	20	
Ethyl Alcohol (CH_3CH_2OH)	3.235×10^{-6}	25	
Ethyl Alcohol (CH_3CH_2OH)	3.11×10^{-6}	20	
Sulfuric Acid (H_2SO_4)	3.054×10^{-6}	16	
Nitric Acid (HNO_3)	2.548×10^{-6}	16	Aqueous solution 1.6933g/cm^3
Ferrous Chloride ($FeCl_2$)	7.27×10^{-7}	20	Aqueous solution 1.6933g/cm^3
Gases			
Air (under high pressure)	1.6028×10^{-7}	13	98.1 atmospheres pressure
Carbon Dioxide (CO_2)	3.78×10^{-9}	20	1.0 " "
Nitrogen	2.01×10^{-9}	20	" " "
Air (atmospheric pressure)	1.99×10^{-9}	20	" " "
Oxygen	1.83×10^{-9}	20	" " "

data,[11,12] with the addition of certain other data measured by comparison with available samples of flint glass, during the course of the present investigation.

A magneto-optic transducer system may be made by allowing a column of light to pass through a polarizer (Polaroid for instance), through a region containing a magneto-optic material and subject to the magnetic exciting field (H), through a polarity analyzer (a second Polaroid disc) and into a photoelectric cell, or photomultiplier tube. A system of this sort is sketched in Figure 1. It is essential that the light pass as nearly as possible in the same direction as the magnetic field in order to secure maximum reaction, as indicated by Equation (5)

It seems entirely logical to assume that one might find or produce more suitable materials than those in this list, by embarking upon a

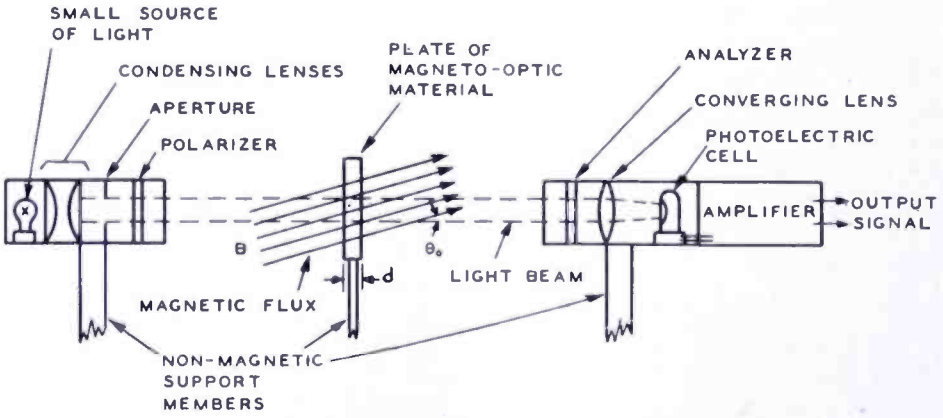

Fig. 1—Basic magneto-optic transducer system.

definite program of research directed toward the development of better magneto-optic materials. Several types of available materials were tested in an effort to find the best magneto-optic solids which were at hand. The heavy leaded x-ray glass, flint glass, and a cobalt-blue plate glass listed in Table I were by far the best materials tested. Ordinary clear plate glass, pyrex glass and fused quartz were inferior by at least one order of magnitude. It seems that the added "impurities" in the lead and cobalt glasses may provide an important clue to a possible avenue of attack upon the problem of increasing the magneto-optic constant.

All of the common types of transparent plastic resin sheets which were tried were found to produce excessive amounts of random polar-

[11] O. W. Eshbach, HANDBOOK OF ENGINEERING FUNDAMENTALS, Vol. I, Wiley Engineering Handbook Series, 1st Ed., John Wiley and Sons, New York, 1936.

[12] S. R. Williams, MAGNETIC PHENOMENA, 1st Ed., p. 217, Table VI, McGraw-Hill, New York, 1931.

ization dispersion, so no satisfactory test results were obtained with plastics.

In operation, the second polarizer or "analyzer" is so oriented with respect to the average angle of polarization of the incident light that only a small fraction of the total available light is transmitted. If the analyzer is adjusted to minimize the transmission of light, and if the magnetic field is varied at a frequency f, the light passing through the analyzer will vary in intensity chiefly at the double frequency $2f$. To avoid this effect, the analyzer may be rotated in either direction to transmit several times more than the minimum light intensity, or a constant supplementary magnetic bias field may be added. The former procedure is usually preferable.

The minimum transmission ratio is dependent upon the uniformity of polarization produced by the polarizer and analyzer elements and upon any random static polarization deviating properties of the magneto-optic material. Materials which possess very small random variations are found to be most satisfactory for these applications. When the better materials are used, the transmitted light *may* be reduced to a minimum of perhaps 10^{-4} to 10^{-6} of the light which is incident upon the first polarizer. As either the polarizer or the analyzer is rotated a slight amount in either direction, the transmitted light may increase by perhaps 50 to 300 times before the maximum sensitivity to magnetic excitation is achieved. The exact amount of rotation which is required to attain maximum sensitivity, and the consequent value of increase of the transmitted light energy, is dependent upon the degree of random polarization in the system. Near the orientation of minimum transmission some portions of the light beam increase in intensity with application of increasing magnetic field intensity, while in other portions the light intensity decreases. Sufficient rotation in one direction or the other causes the entire light beam to either decrease or increase with increase of magnetic field intensity. The relative sign is dependent upon the relative direction of rotation of the polarizers from the orientation of minimum transmission and upon the direction of the magnetic field. Figure 2 shows a typical plot which indicates the sensitivity to magnetic excitation versus the steady (dc) component of the transmitted light as indicated by the photomultiplier tube output current.

The intensity of the transmitted light (W_2) may be determined analytically, by the expression

$$W_2 = amb W_1 [\delta + \sin(\theta_0 + \theta)], \tag{6}$$

where

W_1 = intensity of the light incident upon the first polarizer,

a = fraction transmitted by that polarizer,

m = transmission coefficient of the magneto-optic material including obscuration by the magnetic structure,

b = average fraction of the light transmitted by the second polarizer (analyzer),

δ = remaining faction of light energy of random polarization which is transmitted by the system,

θ_0 = fixed angle of orientation between the polarizer and the analyzer,

θ = defined by Equation (5).

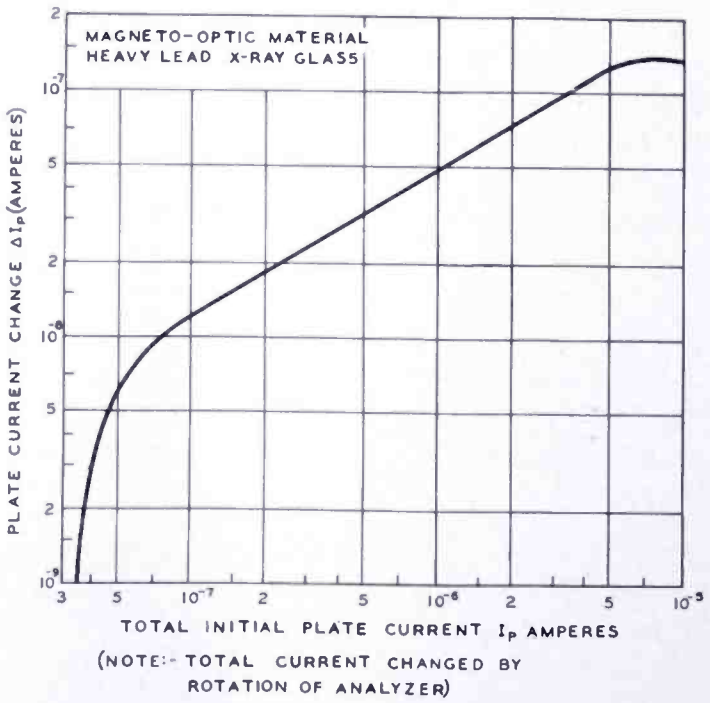

Fig. 2—Test of Faraday effect. (Output current change for a fixed increment of magnetic flux change as a function of initial dc current of photomultiplier tube.)

In general, the angle θ is so small that for practical application one may write

$$\sin\theta = \theta, \text{ and } \cos\theta = 1, \tag{7}$$

so, by the trigonometric relations and with reference to Equation (5), (6) becomes

$$W_2 = ambW_1\,(\delta + \sin\theta_0 + \mathcal{V}Hd\cos\alpha\cos\theta_0). \tag{8}$$

This equation indicates that the light intensity (power density), W_2,

transmitted by the second polarizer (analyzer) varies directly in accordance with the applied instantaneous magnetic field intensity (H).

It is well known that, for small signals, the plate current I_p of a photoelectric cell or photomultiplier tube is proportional to the variation of the total incident light energy W_2A_1, so

$$I_p = kS_pW_2A_1, \tag{9}$$

where

k = remaining fraction of the incident light energy (W_2) which actually reaches the sensitive area of the phototube,

S_p = sensitivity of the tube in amperes per lumen,

A_1 = area of the cross section of the beam of light.

If the magneto-optic transducer is to be utilized in operation in a magnetic field (of intensity H) in a space where there is no reason to consider any adjacent ferromagnetic or paramagnetic bodies which may modify the intensity of the field, Equations (8) and (9) may be combined to yield the complete equation for the transducer system, in the form

$$I_p = abkmA_1S_pW_1\ (\delta + \sin\theta_0 + \mathcal{V}Hd\cos\alpha\cos\theta_0). \tag{10}$$

When the application involves a definite magnetic circuit, such as that of a playback (reproducer) head for magnetic tape records, it is advantageous to design a magneto-optic transducer structure especially for the purpose. It is desirable that the configurations and dimensions of the magnetic and optical circuits be considered in combination to yield an optimum result. A block diagram of a possible arrangement of the magneto-optic transducer system for playing-back magnetic tape records is shown in Figure (3).

The magnetic potential ($\mathcal{F}$) and the reluctances ($\mathcal{R}$) of a magnetic circuit determine the value of total magnetic flux,

$$\phi_0 = B_0A_0 = \mu_0H_0A_0, \tag{11}$$

which passes through the magneto-optic material. The signal level is quite low, so that initial permeabilities of constant value may be assumed for all the magnetic materials which may be involved. An example of a typical simple magnetic circuit of a magneto-optic playback head is indicated in Figure 4. An approximately equivalent schematic magnetic circuit is sketched in Figure 5, where $\mathcal{R}_t$ is the internal

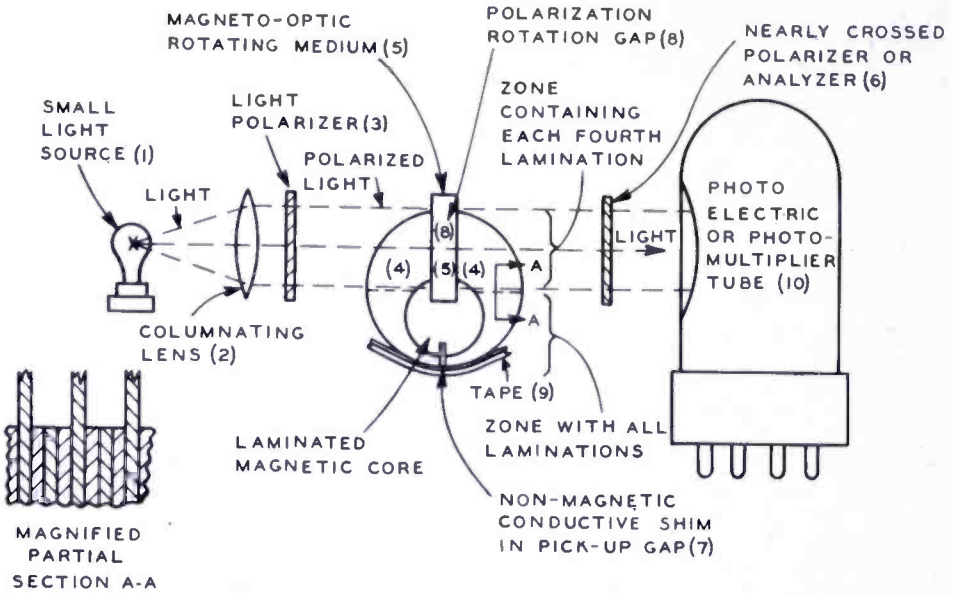

Fig. 3—Possible arrangement of a magneto-optic transducer system for playback of magnetic records.

magnetic reluctance of a short segment of the record tape, $\mathcal{R}_{s1}$ is the shunt reluctance of the space about the tape segment, $\mathcal{R}_{g1}$ and $\mathcal{R}_{g2}$ are the equivalent reluctances of the gaps between the tape and the tips of the core segments, $\mathcal{R}_{s2}$ is the leakage reluctance between the core tips, $\mathcal{R}_{c1}$ and $\mathcal{R}_{c2}$ are the reluctances of the opposite core segments, $\mathcal{R}_{s3}$ is the reluctance of the flux leakage (fringing flux) around the active magneto-optic material, and $\mathcal{R}_0$ is the magnetic reluctance of the *active* magneto-optic zone. The object is to produce

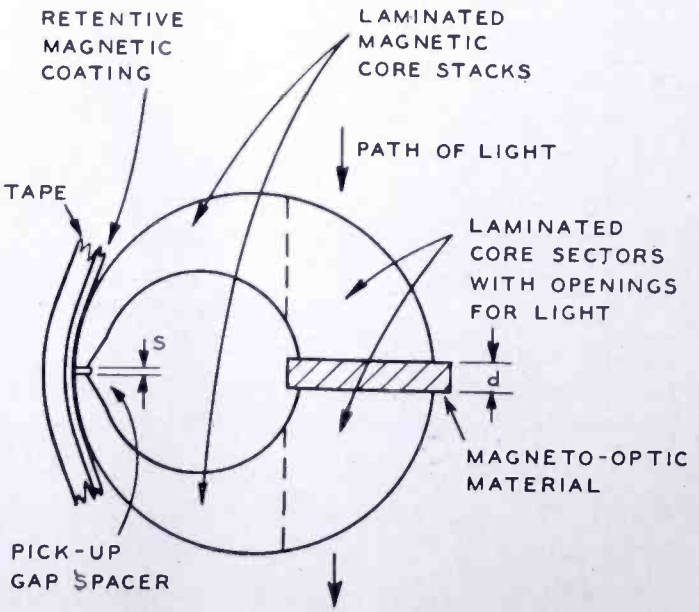

Fig. 4—Magnetic circuit of a typical magneto-optic playback head.

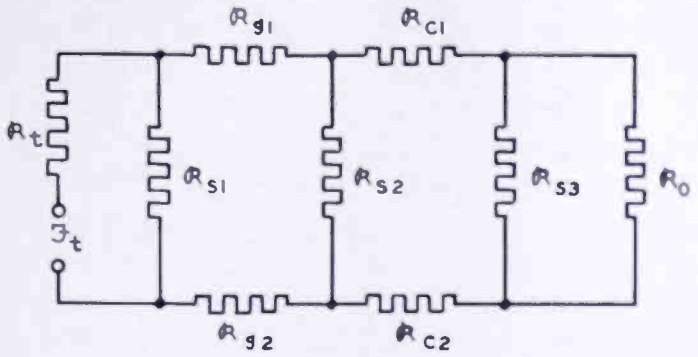

Fig. 5 — Approximate equivalent circuit of magnetic playback head of Figure 4.

a maximum of magnetic flux density within a maximum volume of magneto-optic material, or, in other words, to transfer a maximum amount of magnetic field energy into the space of utilization represented by the reluctance $\mathcal{R}_0$.

Experience indicates that in practical, well-designed systems of this sort, the reluctances $\mathcal{R}_{g1}$ and $\mathcal{R}_{g2}$ may be neglected by equating them to zero. Then $\mathcal{R}_{s1}$ and $\mathcal{R}_{s2}$ are combined in parallel, in terms

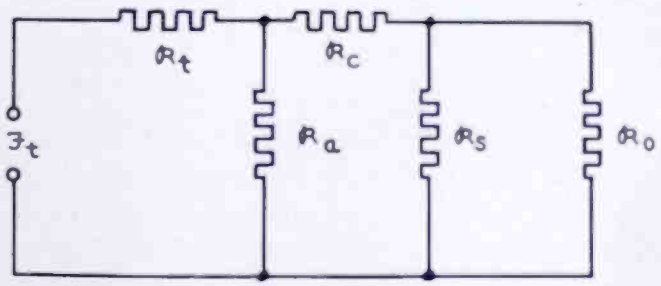

Fig. 6 — First simplification of equivalent circuit of magnetic playback head.

of reciprocal reluctances or values of permeance $\mathcal{P}_{s1}$ and $\mathcal{P}_{s2}$, to yield a single shunt arm of value

$$\mathcal{P}_a = \mathcal{P}_{s12} = \mathcal{P}_{s1} + \mathcal{P}_{s2} = 1/\mathcal{R}_a. \tag{12}$$

The core sectors are made identical, so that

$$\mathcal{R}_{c1} = \mathcal{R}_{c2}, \text{ and } \mathcal{R}_c = \mathcal{R}_{c12} = \mathcal{R}_{c1} + \mathcal{R}_{c2} = 1/\mathcal{P}_c. \tag{13}$$

The simplified equivalent circuit is shown in Figure 6. Here, the balanced representation is completely abandoned in order to simplify

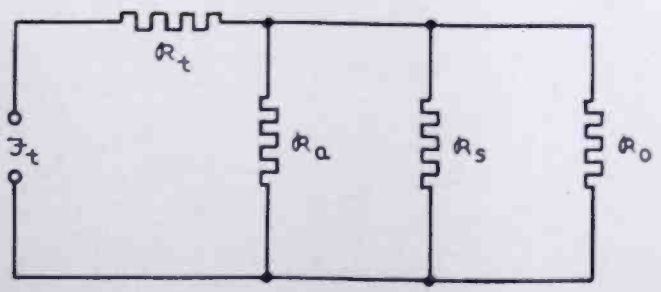

Fig. 7—Second simplification of equivalent circuit of magnetic playback head.

the circuit, since the change does not alter the computed transfer of magnetic energy to the reluctance $\mathcal{R}_0$.

It may be assumed that the values of reluctance are adjusted as functions of frequency so as to include all deviations produced by magnetic skin effects at each frequency which is considered. If laminations of .003 inch or less thickness are used, the low frequency reluctance values apply with sufficient accuracy, for most purposes, to maximum frequencies of at least 10 kilocycles, and usually to about 15 kilocycles when the common audio frequency core materials are used, and when $\mathcal{R}_0$ is relatively large.

The simplified circuit of Figure 6 may be evaluated in accordance with standard electrical circuit practice. The resultant value of magnetic flux which is computed to pass through the load reluctance ($\mathcal{R}_0$) is

$$\phi_0 = \frac{\mathcal{F}_t \mathcal{R}_a \mathcal{R}_s / (\mathcal{R}_a + \mathcal{R}_c + \mathcal{R}_s)}{\left[\frac{\mathcal{R}_a(\mathcal{R}_c+\mathcal{R}_s)}{\mathcal{R}_a+\mathcal{R}_c+\mathcal{R}_s} + \mathcal{R}_t\right]\left[\frac{\left(\frac{\mathcal{R}_t\mathcal{R}_a}{\mathcal{R}_t+\mathcal{R}_a} + \mathcal{R}_c\right)\mathcal{R}_s}{\frac{\mathcal{R}_t\mathcal{R}_a}{\mathcal{R}_t+\mathcal{R}_a} + \mathcal{R}_c + \mathcal{R}_s} + \mathcal{R}_0\right]}, \quad (14)$$

where $\mathcal{F}_t$ is the apparent value of magnetic exciting potential in the tape. Magnetic circuits of the general configuration indicated in Figure 4 usually allow the following simplifying assumptions:

$$\mathcal{R}_a \gg \mathcal{R}_c \ll \mathcal{R}_s, \quad (15)$$

so that

$$\mathcal{R}_a + \mathcal{R}_c + \mathcal{R}_s \doteq \mathcal{R}_a + \mathcal{R}_s, \quad (16)$$

and the maximum value of the exciting magnetic field intensity is

$$\hat{H}_0 = \hat{B}_0/\mu_0 = \frac{\hat{\phi}_0}{\mu_0 A_0} = \frac{\hat{\mathcal{F}}_t}{\mu_0 A_0} \times \frac{\left[\frac{\mathcal{R}_t\mathcal{R}_a}{\mathcal{R}_t+\mathcal{R}_a} + \mathcal{R}_s\right]\mathcal{R}_a\mathcal{R}_s}{[\mathcal{R}_a\mathcal{R}_s+\mathcal{R}_t(\mathcal{R}_a+\mathcal{R}_s)]\left[\left(\frac{\mathcal{R}_t\mathcal{R}_a}{\mathcal{R}_t+\mathcal{R}_a}\right)\mathcal{R}_s + \mathcal{R}_0\left(\frac{\mathcal{R}_t\mathcal{R}_a}{\mathcal{R}_t+\mathcal{R}_a} + \mathcal{R}_s\right)\right]}. \quad (17)$$

where

$\hat{\phi}_0$ = peak value of the sine wave of flux,

A_0 = sectional area of the active flux path in the magneto-optic medium of permeability μ_0 (i.e., the sectional area common to the light beam), and

$\hat{\mathcal{F}}_t$ = apparent peak value of the sine wave of magnetic potential in the tape.

Equation (17) indicates the complete absence of any dependence of $\hat{H}_0$ upon $\mathcal{R}_c$, in view of (15). Hence, a further simplified equivalent circuit diagram may be drawn, as shown in Figure 7. From Figure 7, or from (17), it may be shown that

$$\hat{H}_0 = \hat{\phi}_0/\mu_0 A_0 = \hat{\mathcal{F}}_0/\mathcal{R}_0 A_0 \mu_0 = \hat{\mathcal{F}}_t \mathcal{R}_2/\mathcal{R}_1 \mathcal{R}_0 A_0 \mu_0, \tag{18}$$

when

$$\mathcal{R}_1 = \mathcal{R}_t + \mathcal{R}_2, \tag{19}$$

and

$$\mathcal{R}_2 = \mathcal{R}_a \mathcal{R}_s \mathcal{R}_0/(\mathcal{R}_a \mathcal{R}_s + \mathcal{R}_s \mathcal{R}_0 + \mathcal{R}_a \mathcal{R}_0). \tag{20}$$

Precise computation of $\mathcal{F}_t$ (or $\hat{\mathcal{F}}_t$) from the actual value of magnetic intensity along the tape coating is somewhat involved and is not necessary here. A first order approximation which is usually sufficiently accurate, expresses the magnetic potential, applied to a magnetic circuit of the type shown in Figure 4, as

$$\hat{\mathcal{F}}_t = \hat{\phi}_t \mathcal{R}_t = 4\pi \hat{\mathcal{J}}_t A_t \mathcal{R}_t = 4\pi \hat{\mathcal{J}}_t s_t/\mu_t, \tag{21}$$

where

A_t = cross-sectional area of the coating of the tape (square centimeters),

s_t = longitudinal dimension (centimeters) in the direction of magnetization of the segment which produces the magnetic excitation,

μ_t = magnetic permeability of the magnetic coating on the record tape, and

$\hat{\mathcal{J}}_t$ = peak value of magnetic moment in the tape (e.m.u.).

Equation (10) may be simplified by consideration of only *alternating-current* components and *root-mean-square* values, and then combined with (18) and (21) to yield the completed expression for the plate current.

$$I_p = 4\pi abkmS_p s_t \mathcal{V} \mathcal{J}_t W_1 A_1 (\cos\theta_0) d\mathcal{R}_2/\mathcal{R}_1 \mathcal{R}_0 A_0 \mu_t \mu_0. \tag{22}$$

The magneto-optical and magnetic circuit geometry may be considered in terms of a geometrical function of effectiveness U, which may be defined from (22) in the form

$$U = d\mathcal{R}_2/\mathcal{R}_1\mathcal{R}_0A_0, \tag{23}$$

so that

$$I_p = 4\pi abkmS_ps_t\mathcal{V}\mathcal{J}_tW_1A_1(\cos\theta_0)U/\mu_t\mu_0. \tag{24}$$

It is interesting to investigate U as a design parameter. Immediately, it is noted that

$$\mathcal{R}_0 = d/A_0 = 1/\mathcal{P}_0, \tag{25}$$

so that

$$U = \mathcal{R}_2/\mathcal{R}_1 = [1 + \mathcal{R}_t(\mathcal{P}_a + \mathcal{P}_s + \mathcal{P}_0)]^{-1}, \tag{26}$$

or

$$U = [1 + \mathcal{R}_t(\mathcal{P}_a + \mathcal{P}_s + A_0/d)]^{-1}. \tag{27}$$

As A_0 and d vary, the value of

$$\mathcal{P}_s = \mu_sA_s/s_s = A_s/s_s \tag{28}$$

varies in approximate accordance with

$$\mathcal{P}_s = \mathcal{P}_s{}^*A_0{}^{1/2}d^*/A_0{}^{*1/2}d = \mathcal{R}_a\beta A_0{}^{1/2}/d, \tag{29}$$

where $\mathcal{P}_s{}^*$ is the value of $\mathcal{P}_s$ when $A_0 = A_0{}^* = 1$ cm.^{2}
and $d = d^* = 0.25$, so that $\mathcal{P}_0 = \mathcal{P}_0{}^* = A_0{}^*/d^* = 4$,
$\beta = d^*/A_0{}^{*1/2} = .25/1 = 1/4$, and $\mathcal{P}_s{}^* = \mathcal{P}_a$. (30)

Then

$$U = \{1 + \mathcal{R}_t[\mathcal{P}_a(1 + \beta A_0{}^{1/2}/d) + A_0/d]\}^{-1}. \tag{31}$$

It is obvious that U possesses no dimensions, and so is a pure numeric value.

In order that one may investigate the behavior of the function U, it is convenient to assign to certain of the parameters a particular set of practical values:

$$\mathcal{P}_a = \mathcal{P}_s{}^* = 4,\ \mathcal{R}_t = 2\mathcal{R}_a = 2/\mathcal{P}_a = 1/2, \text{ and } \beta = 1/4. \tag{32}$$

Then

$$U_1 = \left\{1 + \frac{1}{2}\left[4\left(1 + \frac{1}{4}A_0^{1/2}/d\right) + A_0/d\right]\right\}^{-1}, \tag{33}$$

or, after rearrangement,

$$U_1 = 2d/(A_0 + A_0^{1/2} + 6d). \tag{34}$$

A plot of U_1, from Equation (34), with d (the thickness of magneto-optic material in centimeters) as a parameter, is given in Figure 8. The cross (+) marked on the chart represents the operating point of

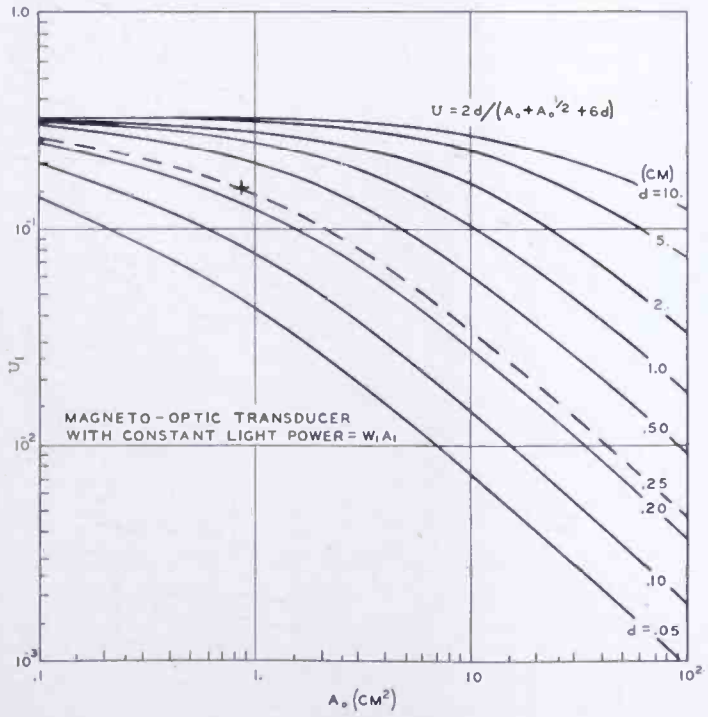

Fig. 8—U_1 as a function of A_0 and d.

a sample system (Figures 10, 11 and 12) which was constructed to test the operational results. If the average transmitted light power ($abkmW_1A_1$, from Equation (24)) is held constant, it is apparent, from Figure 8 and some additional consideration, that the best shape of magneto-optical element is approximately cubical or perhaps one which is symmetrical in cross section and of axial length (along the light beam) about 1 to 2 times the square root of the cross-sectional area ($A_0^{\frac{1}{2}}$) of the element.

If the area of the aperture A_1 is made equal to the area A_0, and if the *intensity* of the applied light is held constant, the signal output

becomes proportional to U_1A_0. This is plotted in Figure 9 as a function of A_0 with d as a parameter. In this case it is seen to be definitely advantageous to increase the cross section of the element to a maximum practical value and to make the value of d again equal to about 1 to 2 times $A_0^{\frac{1}{2}}$. In this case the only limitations to the available sensitivity are the practical values of A_0 and d and the maximum area of the available light beam. The photocell area is not critical, except in the limiting conditions, since an optical system may be used to bend the parallel rays of light onto the active surface of the cell, after they have passed through the analyzer. This arrangement is convenient for distribution of dissipated light energy over a large area in the polarizer, so that excessive heating may be avoided.

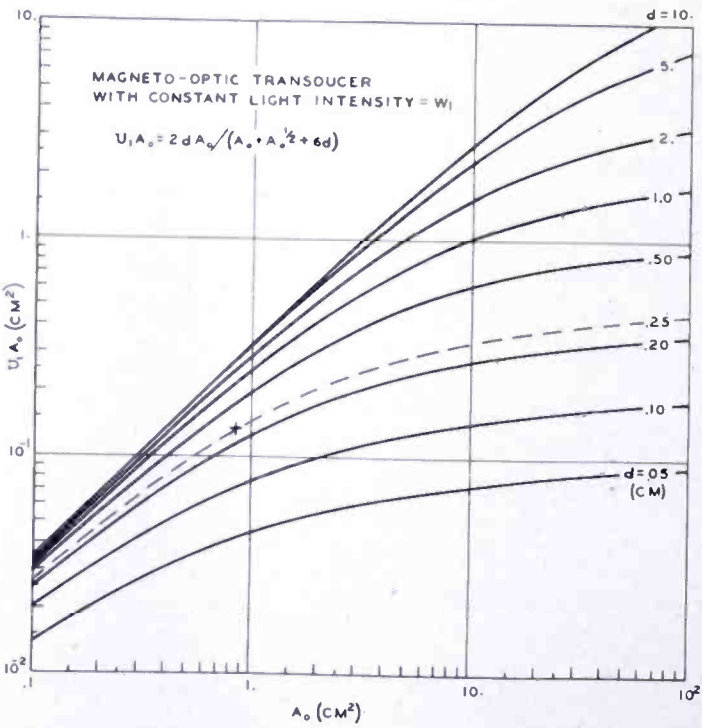

Fig. 9 — U_1A_0 as a function of A_0 and d.

Experimental Tests

A cross (+) is also used in Figure 9 to denote the operating point of the experimental test head of Figures 10, 11 and 12. This transducer was designed to operate with a magnetic tape record passing transversely over a magnetic pick-up gap in the manner customary in the playing of magnetic records. A piece of optically flat leaded X-ray shield glass (Pittsburgh Plate Glass Company) .100 inch (.254 centimeter) thick, and polished on both sides, was inserted between the pole pieces (Figure 10) to act as the magneto-optical material. All laminations were in place near the pick-up gap, but in the vicinity of

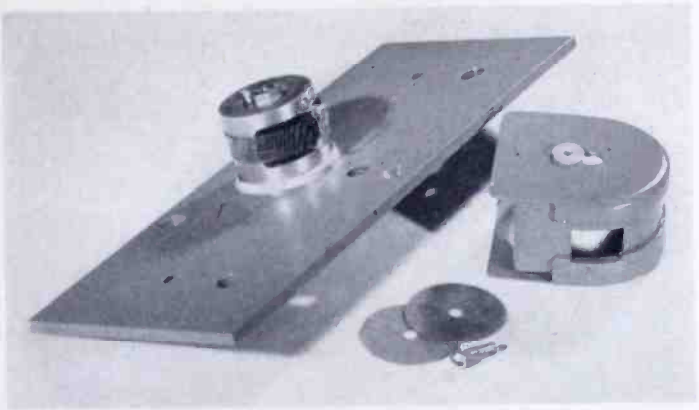

Fig. 10—Experimental magneto-optic playback head with shields removed.

the magneto-optical material only one of each four laminations continued to the opposite surfaces of the glass. The fringing flux was utilized to produce a substantially uniform magnetic field in the glass in the direction of the polarized light beam, which passes through the

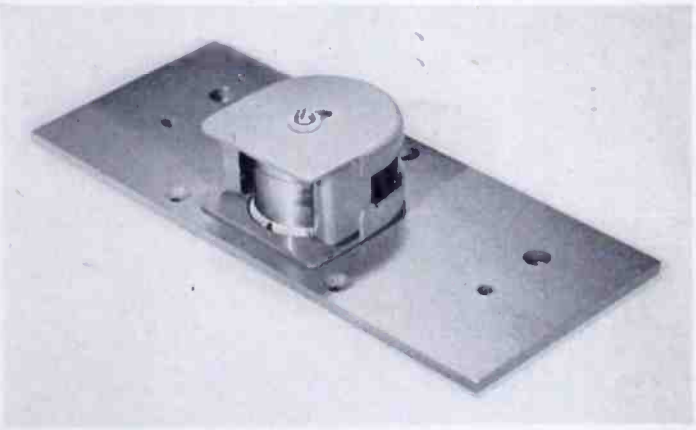

Fig. 11—Experimental magneto-optic playback head with magnetic shield in place.

core (where three quarters of the laminations were omitted) and through the magneto-optical glass. This glass was found to have a somewhat larger magneto-optical constant $\mathcal{V}$ (Verdet's constant) than the flint glass listed in Table I.

Initial tests of this magnetic pickup head were made with a Western Union Telegraph Co., No. K-300 AC, 300-watt, crater lamp as a plane

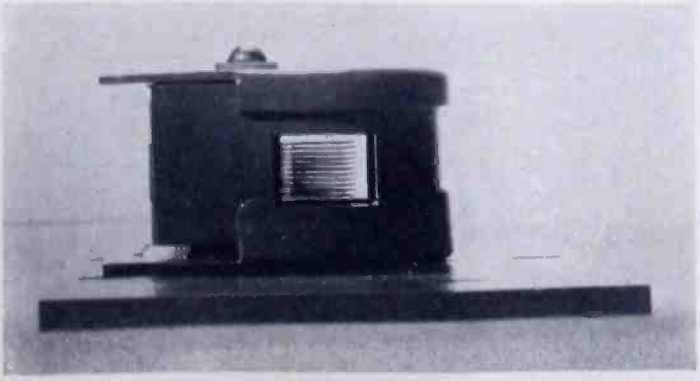

Fig. 12—Path of light through experimental magneto-optic head.

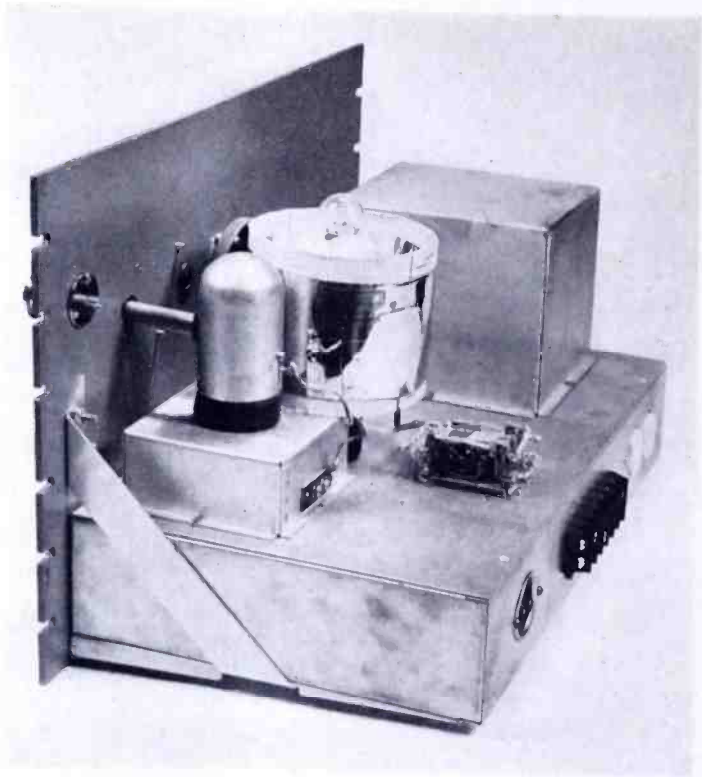

Fig. 13—Back view of magneto-optic test unit.

surface, "point" source of illumination. This lamp failed on account of overheating of the glass envelope before measurements could be made, because of operation with a heat shield with the forced ventilation turned off. The arrangement is shown in Figures 13, 14, 15 and 16. The condensing lens and panel aperture may be seen in front of the lamp in Figure 13. 45-degree front surfaced mirrors were used (Figures 14 and 15) to direct the light beam through the polarizer, the

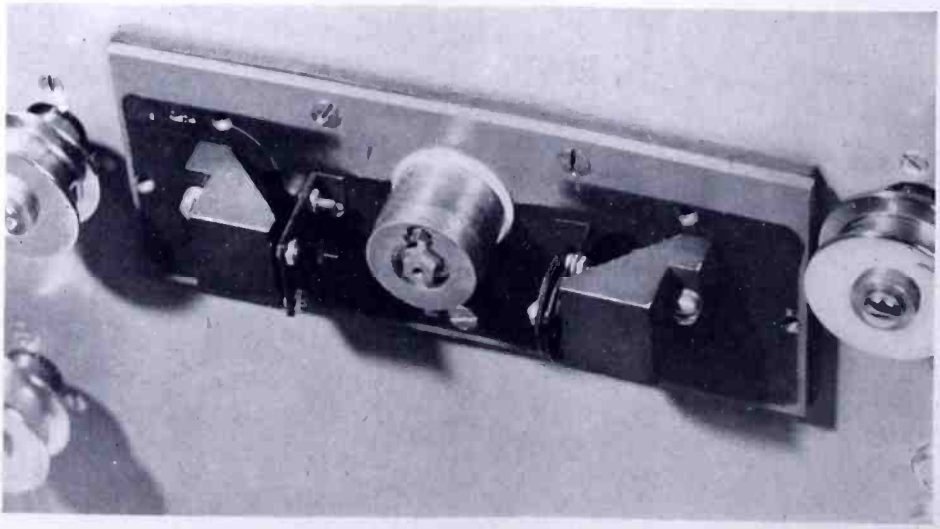

Fig. 14—Top view of magneto-optic system with shields removed.

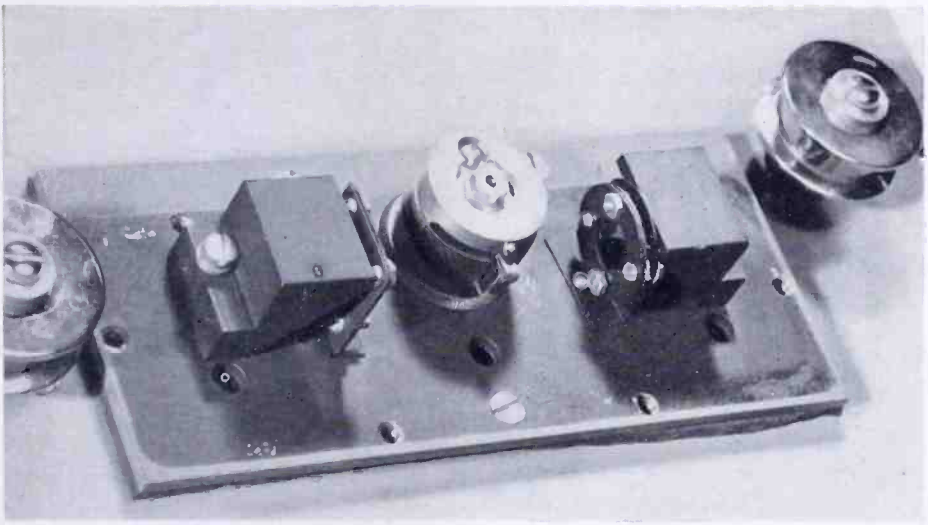

Fig. 15—Bottom view of magneto-optic system with shields removed.

magneto-optical system, and the analyzer, to a second mirror which reflected the resultant amplitude modulated light beam through a second panel aperture and light-tight enclosure, to a 931-A photomultiplier tube. The assembled system with the front light shield in place is shown in Figure 6. The 931-A tube was operated from a stabilized power supply, with variable output voltage. The schematic

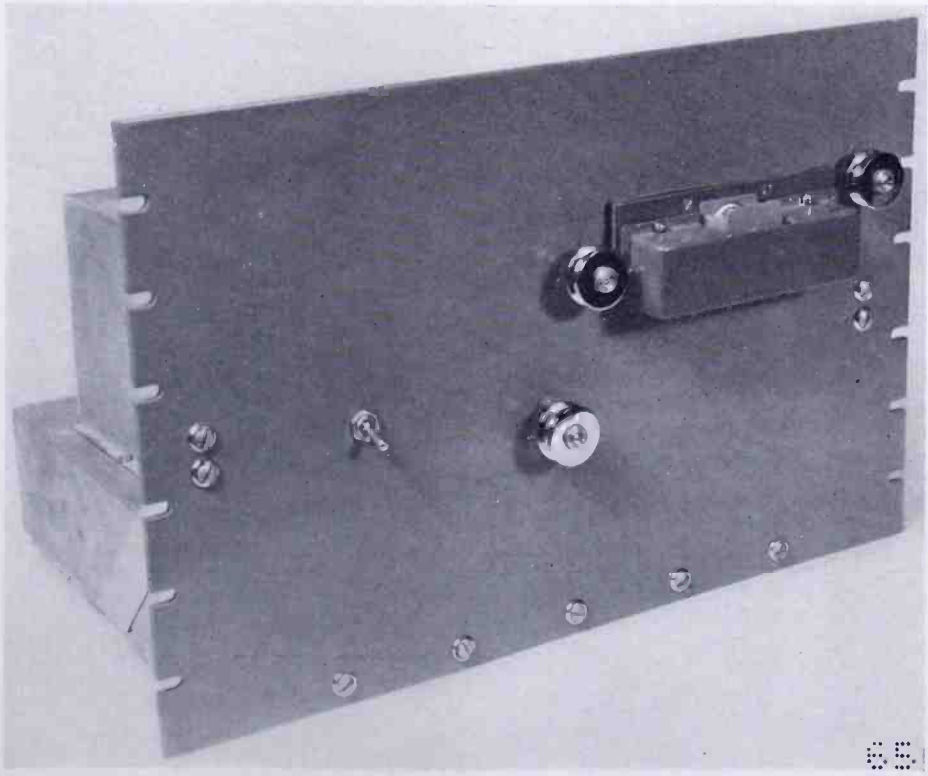

Fig. 16—Front view of magneto-optic test unit.

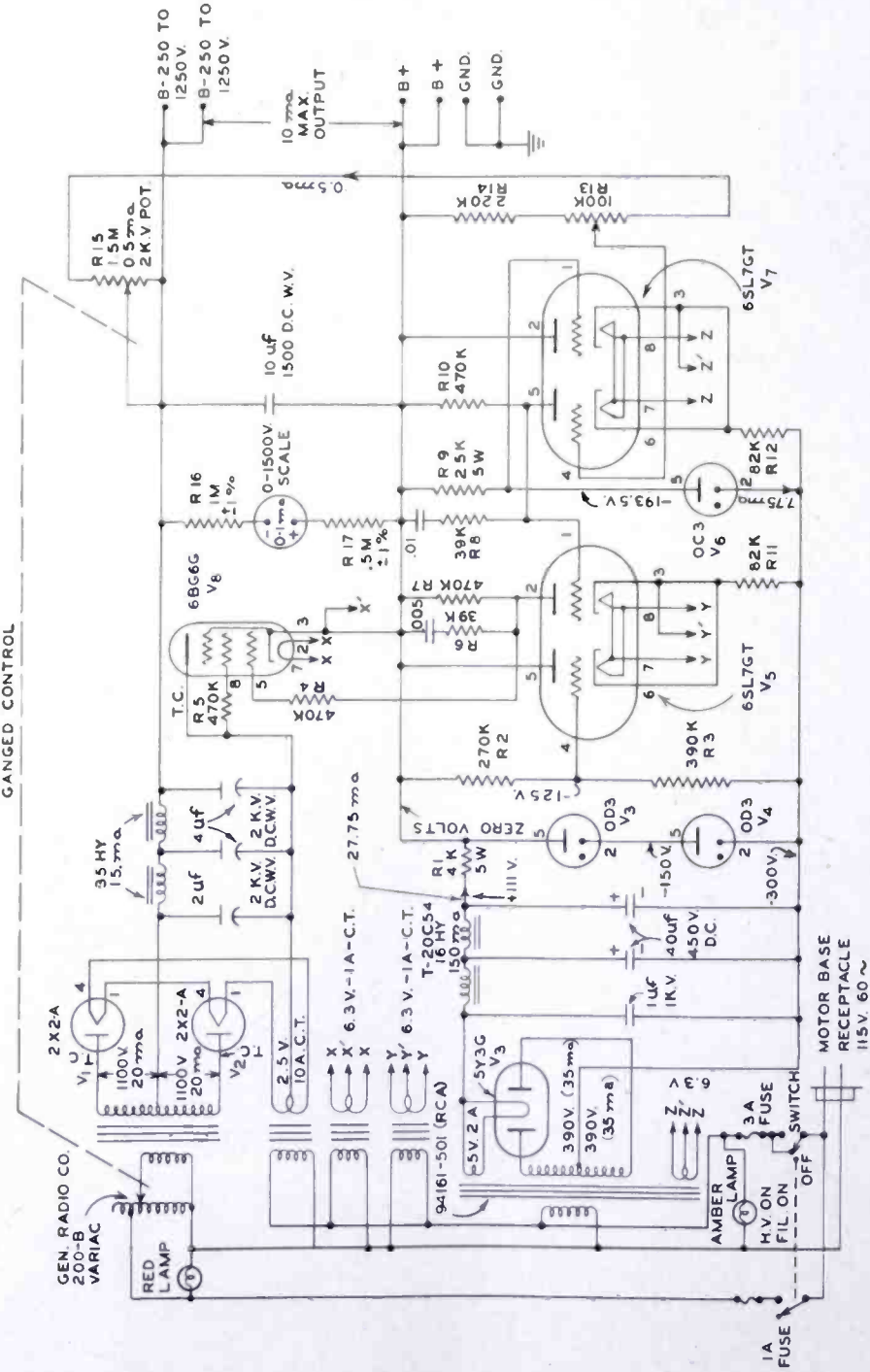

Fig. 17—Circuit diagram of power supply for photomultiplier tube.

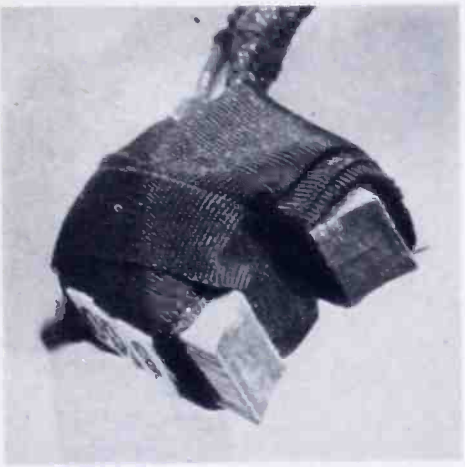

Fig. 18 — Enlarged view of magnetic exciter test unit for playback head.

circuit diagram of this power supply is given in Figure 17. A standard 931-A photomultiplier circuit was used with an output load resistance of about 11,000 ohms.

Tests were continued with a "Point-O-Light" 100 candle power omnidirectional light source. In addition to excitation from magnetic record tape, an exciter unit to provide sufficient excitation for *all* test purposes was arranged in the form of a small 500-turn coil on a special U-shaped core ($\frac{5}{8}$ inch wide), as shown in Figure 18. The plot of Figure 19 indicates the frequency response characteristic attained with the *complete* system. The low and high frequency deviations from uniform response were due entirely to the characteristics of the electrical circuits of the test arrangement. The output level could be varied at will by adjustment of the analyzer. A plot of output signal voltage versus the applied magnetic potential ($\mathcal{F}$), in gilberts, under approximately the same conditions, is given in Figure 20. An essentially linear dynamic response is indicated, over a very great range of amplitude, when the effects of noise from the photomultiplier tube are minimized. Narrow band operation has been employed for exploration of the linearity of response to quite low levels.

Approximate values of the constants and parameters of Equation

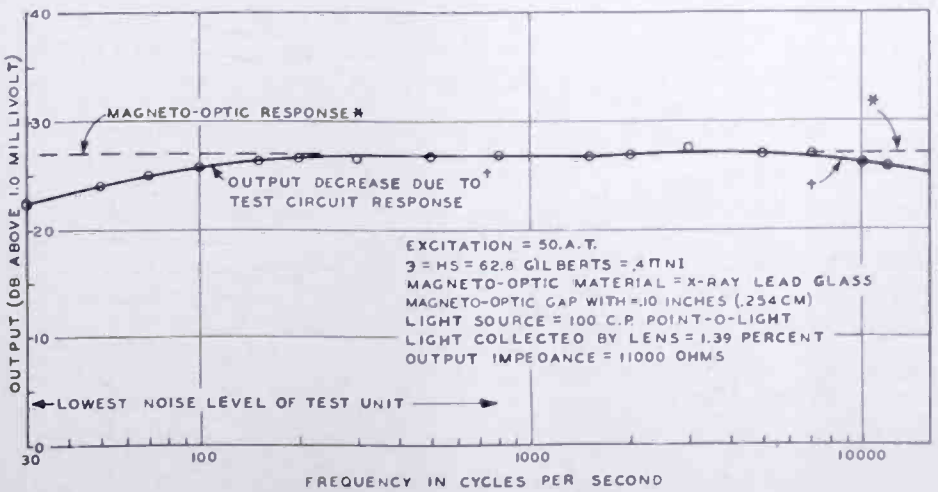

Fig. 19—Amplitude response characteristic of a magneto-optic playback head.

is *not* advocated. Thus a total increment in the signal-to-noise ratio of about 53 decibels would seem to be attainable by increasing the performance of the magneto-optic system when a bandwidth of 15 kilocycles is assumed.

The maximum signal level of present magnetic tapes is about 21 decibels *below* the noise level of Figures 19 and 20. Hence the net maximum signal-to-noise ratio for present magnetic tapes should be only about $53 - 21 = +32$ decibels.

It is possible to increase the signal-to-noise ratio by adding still more complications. Perhaps the most practical of these is an arrangement whereby the light is passed back and forth through the magneto-optic material to gain a limiting increase of 6 decibels in signal-to-noise increase for each passage through the material. It is conceivable that a 60-decibel signal-to-noise ratio might be attained in magnetic tape record playback by an optical arrangement to produce at least three extra transmissions of light in each direction.

A still more complicated method, which may, however, be more simple in certain special laboratory procedures, is the use of a refrigerated photomultiplier tube. The photomultiplier tube may be cooled to —160 degrees centigrade by means of liquid air. This expedient lowers the noise level by about 40 decibels. Therefore, a maximum signal to erased tape noise ratio of about $32 + 40 = 72$ decibels may possibly be attained by known procedures with a magneto-optic playback system in special laboratory test equipment. This is probably not fully attainable on account of the limitations due to tape noise. It is probable that some additional means may be found for enhancement of the performance of this system, but there may be counterbalancing deficiencies of various sorts.

It seems prudent to assume that no more than perhaps 30 decibels maximum signal-to-noise ratio is to be readily available in normal applications for operation directly from present magnetic record tapes, and that for any very special laboratory tests where multiple light transmission optical arrangements or perhaps liquid air cooling or both are used that figure could probably be increased to not more than about 70 decibels when even the best 931-A photomultiplier tube is assumed. It appears obvious that none of these systems is now competitive with present operating practice in the magnetic record playback field from the viewpoints of convenience and cost.

There are, however, a great many possibilities for utilization of magneto-optic transducer principles in special applications wherein independence of the output amplitude upon frequency is important. Within the scope of present knowledge, the constancy of amplitude

response as a function of frequency is limited by only the electrical circuits which are involved, plus the demagnetizing and gap geometry phenomena associated with magnetic record systems.

An application to which the system seems almost naturally adapted is that of the transfer of a magnetically recorded signal to any photographic recording medium. As an instance, suppose that in the motion picture industry the sound tracks are first recorded by magnetic means and that it is then desired to combine and convert them to the customary photographic sound track, before release of the finished product. The magneto-optic system of Figure 3 may be converted for this purpose by replacing the phototube with an optical mask containing a slit and the well known optical system for focussing the image of the slit upon the continuously moving unexposed film, as it passes the region of the image. No electrical circuits of any sort are involved in this transfer system. On account of its simplicity, this application may allow the use of the more complicated multiple-traverse light system and greater illumination in order to attain the required amplitude of modulated light signal. The restricted bandwidth of sound on film should also aid in improving the signal-to-noise ratio in this application.

There are other more specialized fields of application in which the method may be useful. For instance, very thin wafers of magneto-optic glass may be used as transducers to explore the external magnetic fields associated with magnetic record media when apparatus of maximum sensitivity is employed. Quite simple transducer systems may be employed in stronger magnetic fields for the investigation of complex alternating-current or direct-current magnetic field vector amplitudes and phases, when those fields are somewhat more intense than the earth's magnetic field.

In larger scale measurements it is also practical to use thicker sections of magneto-optic materials to increase the output amplitude and to attain increased sensitivity by multiple passage of the same beam of light back and forth through the magneto-optic medium. As previously stated, a limiting increment of 6 decibels per transit (in each direction) is available by this method.

A major possibility of employment lies in the field of measurement of magnetic fields in inaccessible regions, such as within the various particle accelerators connected with nuclear physics investigations. The only requirements are the availability of one or two small optically transparent ports, for the passage of a beam of light into and out of the device, the possibilities of constructing an optical path *through* the region of desired measurement, and of the insertion of a piece of

nonmagnetic insulating material, such as glass, at the point of the desired measurement.

Conclusion

A magneto-optical playback system and head have been developed for use with magnetic tape records. The signal amplitude is found to be constant with frequency, and it is linear over more than the desired amplitude range, as predicted, except as modified at high frequencies by tape and pickup-slot parameters. It is found that, with simple systems and presently available materials, the maximum signal-to-noise ratio is only about 30 decibels. This is considerably below the minimum desired value.

It is possible to increase the signal-to-noise ratio by adding still more complications. Perhaps the most practical of these is an arrangement whereby the light is passed back and forth through the magneto-optic material to gain a limiting increase of 6 decibels in signal-to-noise ratio for each passage through the material. It is conceivable that a 60-decibel signal-to-noise ratio might be attained in magnetic tape record playback by an optical arrangement to produce at least three extra transmissions of light in each direction.

A still more complicated method, which may however be applicable in certain special laboratory procedures, is the use of a refrigerated photomultiplier tube. If the photomultiplier tube of the system is cooled with liquid air, the potential signal-to-noise ratio may be increased by 40 decibels. When this and certain minor mechanical modifications are made, it appears that it should be possible to attain entirely satisfactory results and to produce a maximum signal to erased tape noise level of 70 decibels. The noise level of the tape may reduce this latter figure by several decibels, since it may become the controlling factor in this case.

It is concluded that in ordinary magnetic record playback applications the magneto-optic system is not now competitive with other available methods for performing the same task in magnetic record players. It is further concluded that the present system may possibly become more interesting if a somewhat more active magneto-optic material is found or produced, or possibly if a more quiet photomultiplier tube becomes available.* Presently available magneto-optic materials are found to be adequate for satisfactory operation in other applications wherein the cost and complexities of the system are not closely limited.

---

* Since this work was done, in 1948, better photomultiplier tubes have been made available.

It is possible that there may be at least one useful application in the motion picture industry, for the transfer of magnetic sound-track signals to optical sound tracks without any intermediate electrical circuits. The multiple light passage arrangement could be used to advantage in this application.

A system of this general nature may also afford a means for measuring the space vector magnitudes and phases of constant or varying magnetic fields *without* the introduction of either electrically conductive or ferromagnetic substances into the region of the field.

The theoretical treatment of the system was arranged so that the effects of any proposed new materials and of the variations of the system parameters may be readily evaluated.

ACKNOWLEDGMENT

The author wishes to acknowledge the assistance of R. N. Rhodes in the construction and testing of the unit shown in Figures 13 and 16.

TRANSMITTER DIVERSITY APPLIED TO MACHINE TELEGRAPH RADIO CIRCUITS*

By

GRANT E. HANSELL

Research Department, RCA Laboratories Division, Riverhead, New York

Summary—The communication system described in this paper makes use of transmitter diversity to overcome the effects of fading, as compared to receiver diversity on machine telegraph (printer) radio circuits. It has been determined experimentally that transmitter diversity is as effective as receiver diversity when appropriate receiving equipment is used. The gain has been determined to vary between 10 and 30 decibels. The system described here uses frequency shift keying, thereby realizing the advantages of frequency shift keying as well as the advantages of diversity.

The communication system described in this paper should be particularly well suited to a number of services where receiver diversity is not feasible or not economical, such as radio printer circuits from shore to ships or from ground to airplane or from one transmitter to a number of receiving locations situated in congested areas.

INTRODUCTION

THIS paper describes briefly the transmitter and receiver arrangements used for making use of transmitter diversity. Tests were made to determine whether or not separate transmitters connected to spaced antennas gave a diversity effect at the receiver. After this was determined, tests were made to determine the effectiveness of transmitter diversity compared to receiver diversity. Tests were also made to determine the effectiveness of transmitter diversity compared to a single transmitter.

OSCILLOSCOPE OBSERVATIONS OF TRANSMITTER DIVERSITY

In order to observe the effects of transmitter diversity, two transmitters were connected to separate antennas, on the same frequency, but keyed differentially with 60-cycle reversals. The per cent mark of the two transmitters was made unequal so that the transmitter and antenna combination could be identified at the receiver. With this arrangement, the diversity effect could be observed and still avoid the effects of phase cancellation because both transmitters were not on at the same instant. For this test a frequency of 15,457.5 kilocycles

* Decimal Classification: R423.21.

was used from Bolinas, California. The results were observed on an oscilloscope at Riverhead. Pictures were taken at the rate of one frame per second for a total of 4000 frames. The pictures were analyzed frame by frame to determine the effectiveness of transmitter diversity. This was done by arbitrarily deciding that when the signal dropped below a certain level it would result in an error. If it dropped below that same level on both transmitters at the same time it would mean an error on diversity. The results showed an error ratio of 407 to 61. An error ratio of 194 to 15 was measured on the same film when using a lower level for the error point. These figures show a calculated[1] improvement of 11 and 14.8 decibels respectively, when using the formula that errors are inversely proportional to the 0.75 power of the transmitter power.

Figure 1 is a sample reproduction of the pictures taken at one second intervals showing the diversity effect. The short dot is from one transmitter and the long dot from the other transmitter. In the top frame the short dot is at a minimum but rises to equality in the third frame. In the fourth frame the long dot has started to fade while the short dot has recovered to full amplitude.

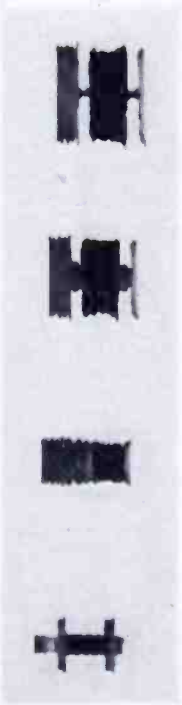

Fig. 1—Oscilloscope pictures taken at one frame per second, showing diversity effect.

Transmitter Arrangement

In practice, the two transmitters cannot be on the same frequency or it will result in phase cancellation. In order to overcome this objection is is necessary to use a small amount of frequency separation. In early work, a value of 200 cycles was used but a value of 90 cycles was used in later work. A discussion of frequency separation will be presented later in this paper.

The transmitter arrangement used in this system is shown in Figure 2. A teletype transmitter supplies a keyed tone signal to the tone-signal rectifier and then to a reactance tube which converts the

[1] H. O. Peterson, John B. Atwood, H. E. Goldstine, Grant E. Hansell, and Robert E. Schock, "Observations and Comparisons on Radio Telegraph Signalling by Frequency Shift and On/Off Keying", *RCA Review*, Vol. VII, No. 1, March 1946.

rectified tone to a frequency shift signal by its action on the 200-kilocycle oscillator. The output of the 200-kilocycle oscillator is combined in two mixers with the outputs of two crystal oscillators adjusted to be slightly off-set in frequency. The desired sideband output of each mixer is selected by frequency selective circuits and applied to frequency multipliers and power amplifiers to give the final transmitter output frequency and power. General practice has been to multiply the mixer output frequency by a factor of 4 or 8 depending on the output frequency desired. It will be noted that the frequency separation of the crystals would then be one fourth or one eighth of the

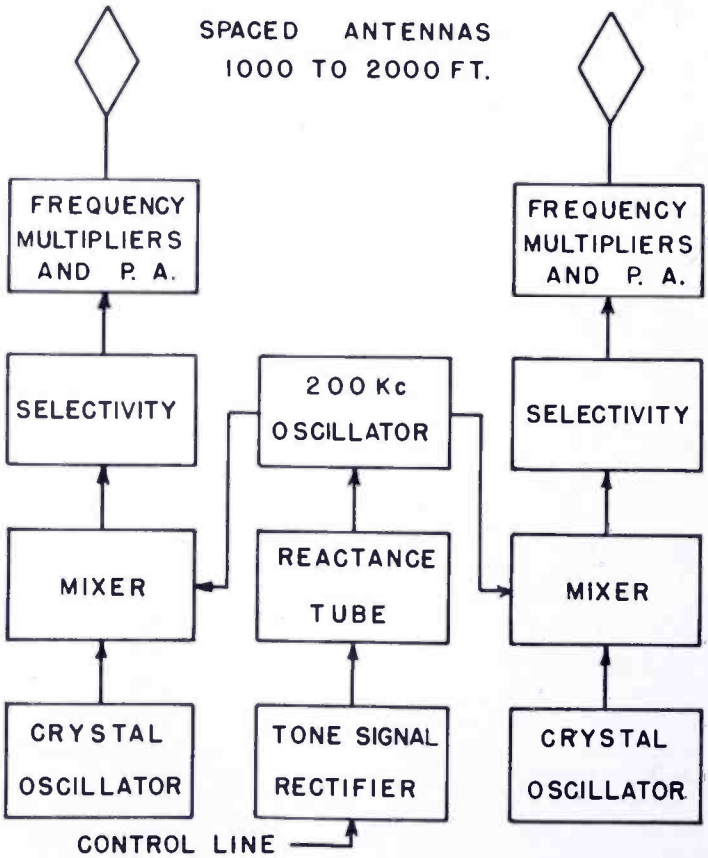

Fig. 2 — Block diagram of transmitting arrangement.

desired final separation. Some care is necessary in the design as well as in operation to maintain the frequency separation within reasonable limits. However experience has shown that this can be accomplished without undue difficulty.

A frequency shift of 850 cycles was used for all tests described in this paper. It is anticipated that other values of shift may be used at some later date.

Receiver Arrangement

Several factors are involved in the choice of the receiver arrange-

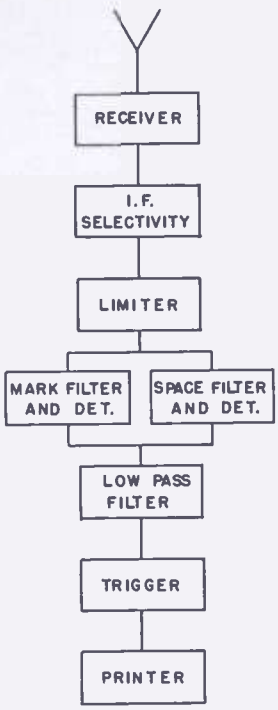

Fig. 3—Block diagram of receiving arrangement.

ment for use in the reception of transmitter diversity signals. Of several arrangements tested, the circuit indicated in block diagram, Figure 3, has given the best performance.

Following the receiver proper, the essential elements are selectivity, limiting, mark and space filters, differentially connected detectors, low pass filter, trigger circuit output control and a receiving printer. The intermediate-frequency selectivity serves as a roofing filter for the mark and space filters. The limiter serves to remove amplitude variations in the signal and to remove amplitude modulation components of noise and amplitude modulation beat components due to the presence of the two slightly different transmitter frequencies. The limiter further serves to select the stronger of the two transmitter frequencies present at any time. The mark and space filters separate the mark and space frequencies and their detected outputs are differentially connected to the low pass filter. The low-pass filter removes noise components as well as beat note components remaining as a result of the transmitter frequency differences. Selectivity curves of the intermediate-frequency roofing filter and the mark and space filters are shown in Figure 4. The selectivity characteristic of the low-pass filter used in these tests is shown in Figure 5.

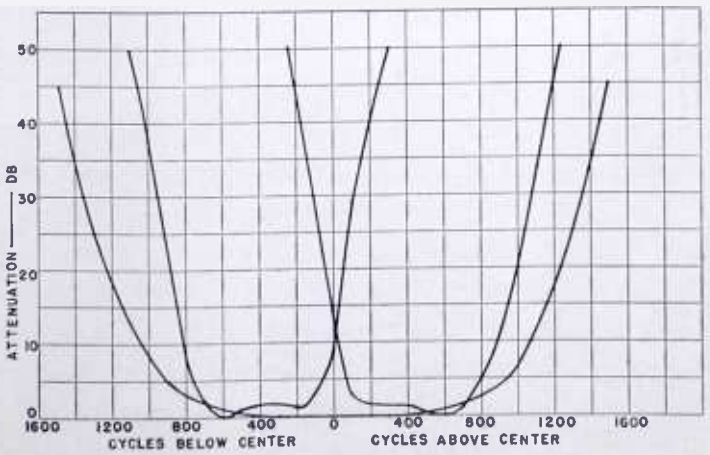

Fig. 4—Attenuation characteristics of i-f roofing filter, mark filter, and space filter.

Additional features of the receiver, not shown, are provisions for automatic gain control, and either or both automatic frequency control or crystal controlled high frequency oscillator.

Evaluation of Transmitter Diversity Gain

The most direct way to evaluate the effectiveness of transmitter diversity using the receiver arrangement shown in Figure 3, was to count errors using transmitter diversity compared to a single transmitter. This was done using a circuit from Bolinas, California to receiving locations in New York City. At San Francisco, a tape transmitter, provided with a repeating tape, fed 5-unit printer signals,

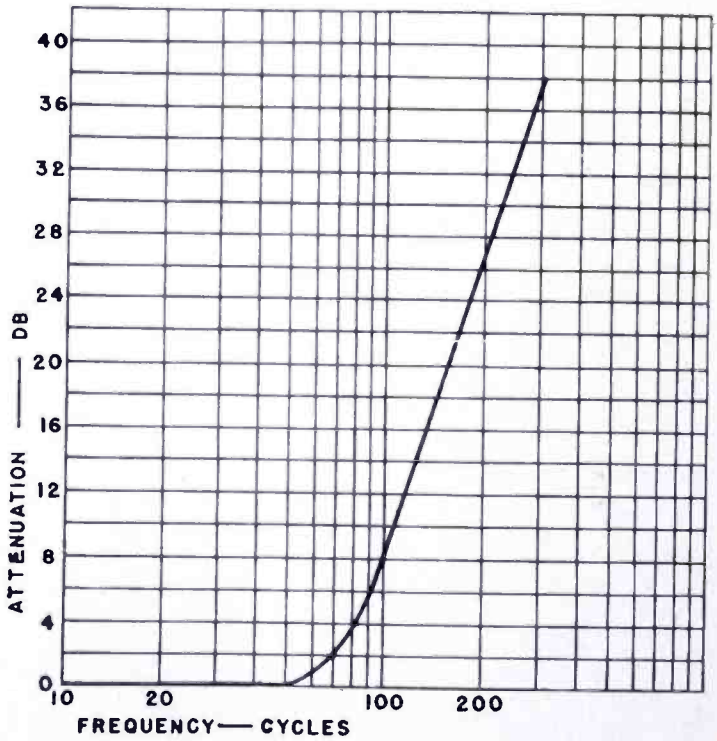

Fig. 5—Attenuation characteristic of low-pass filter.

over about 30 miles of land line to the transmitting site at Bolinas where they were fed to the transmitting equipment shown in Figure 2. This arrangement converted the printer signal to frequency shift keying for the operation of two 1-kilowatt transmitters. The transmitters were connected to separate rhombic antennas directed towards New York. These antennas had a power gain of about 12 decibels and were spaced about 1500 feet. Each transmitter used an assigned frequency of 15,490 kilocycles with 850 cycles shift and 200 cycles off-set.

It should be pointed out that the radio-frequency noise level in New York City is higher than one would generally expect to encounter elsewhere. Also, more power would be required for longer circuits,

particularly those whose great circle paths come closer to the magnetic poles where higher attenuation is encountered.

The results obtained at three receiver locations in New York City are shown in Table I.

Table I

Receiver Location	Hits Using 1 Trans.	Hits Using 2 Trans.	Letters	Error Ratio	S/N Ratio
60 Broad Street	201	13	10,000	15.5/1	−5 to −16 db
711 5th Avenue	409	25	45,000	16.3/1	+6 to − 6 db
22 William Street	65	2	8,000	32/1	+9 to 0 db

These measurements were obtained by providing an automatic timing unit at the transmitter to turn one of the transmitters off at alternate five minute intervals. This provided alternate five minute intervals of single transmitter and transmitter diversity. A "hit" is defined as either a single error or a series of errors resulting from the receiving printer being thrown out of synchronization. The signal-to-noise ratios are peak signal to peak noise ratios measured from time to time in a 1.7-kilocycle intermediate-frequency bandwidth and are only intended as a rough guide of the signal condition at the various locations. A simple half-wave horizontal dipole was used at each location. At 60 Broad Street the antenna was located approximately 25 stories above the street and very near to the dc elevator machinery. The building is surrounded by taller buildings. At 711 Fifth Avenue the antenna was located on the 12th floor almost directly above Fifth Avenue. Except for ignition noise from cars and buses, the location was fairly clear of local noise. At 22 William Street, the City Bank Farmers Trust Co. building, the antenna was located approximately 60 floors above the street and was well in the clear of other buildings, and the noise level was lower than at the other two sites.

An examination of Table I shows the ratio of errors without transmitter diversity to errors with transmitter diversity increased as the signal-to-noise ratio increased. This indicates that the gain due to diversity increases with higher signal-to-noise ratios. This effect has also been observed in more direct experimental results with receiver diversity in other work being conducted at Riverhead. These results indicate that the application of diversity produces a gain of from 12 to 30 decibels depending upon the signal-to-noise ratio.

A comparison of transmitter diversity and receiver diversity was made using three different receiver arrangements. In order to obtain

this comparison, one transmitter was turned on and off at alternate five minute intervals. When one transmitter was on, two receivers in diversity were used and when both transmitters were on, a single receiver was used. From these tests, the general conclusion was reached that the effectiveness of transmitter diversity is equal to that of receiver diversity if the receiving equipment is properly designed for the reception of transmitter diversity signals as, for example, the receiver arrangement of Figure 3.

Possible Uses for Transmitter Diversity

Obviously transmitter diversity will not replace receiver diversity for most point-to-point circuits because of the increased cost of a second transmitter and antenna compared to a second receiver and its antenna. However there are many circuits that can make use of transmitter diversity to advantage. These circuits fall into two general classifications; one type being any circuit where it is impossible or impractical to install two receivers with their associated spaced antennas, and the other being that of a broadcast service where it is more economical to install a second transmitter than a second receiver at a large number of locations. Some examples of possible uses are listed below:

1. Shore-to-ship transmission
2. Ground-to-airplane transmission
3. Fixed base to mobile vehicle transmission
4. Fixed base to undeveloped areas
5. Fixed base to city areas (building tops)
6. Broadcast transmission to many receiving stations

From the above it can be seen that transmitter diversity can provide better performance for many services.

Another advantage of transmitter diversity may be noted. Its use results in simplified installation and operation at the receiving location due to the fact that it is only necessary to have one receiver and receiving antenna. This simplification makes it less essential to have skilled technicians at the receiving location.

Analysis of Transmitter Off-Set

The use of transmitter diversity is made possible by offsetting the transmitters, by a small amount, in frequency to overcome the effects of phase cancellation. The amount of off-set required is a function of keying speed to be used. In 60 words per minute teletype, the duration of one keying element is about 22 milliseconds. If one transmitter is stronger than the other at the grid of the limiter, the weaker signal

is further rejected in the limiter output. The worst possible condition is when both frequencies are received with equal amplitudes. When this condition exists, the resultant varies between twice the amplitude of each signal and zero at the beat note or off-set rate as indicated in Figure 6. Calculations indicate that the time t_1 during which the amplitude of the resultant signal is less than the amplitude of one signal alone is ⅓ of the time for one cycle of the off-set frequency. If it is arbitrarily said that this time should be small compared to a keying element, say one fifth to one tenth, then t_1 would be equal to 4.4 to 2.2 milliseconds, and t would be three times these values or 13.2 to 6.6 milliseconds. The calculated off-set frequency would then be 76 to 152 cycles. Hence an off-set of 90 cycles appears to be a good choice for 60 words per minute teletype. This means that the signal drops below the value of a single signal for 3.7 milliseconds during each cycle when the two frequencies are received with exactly

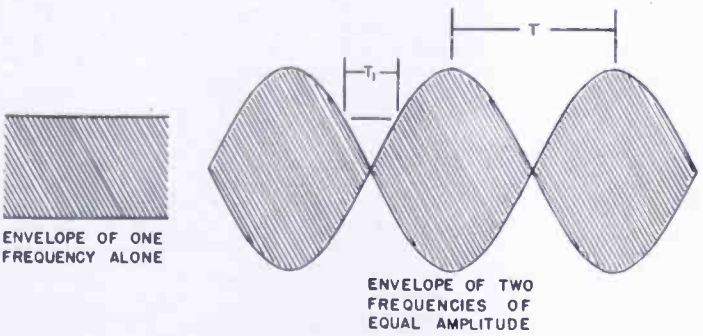

Fig. 6—Signal trace showing two signals of equal amplitude.

equal amplitude. There are two effects that occur during this time interval. One effect is the deterioration of the signal-to-noise ratio during this short interval. The other effect is that the signal will fall below the point where the limiter can maintain its full output. This effect is for even a much shorter time interval resulting in sharp peaks at the detector output. These peaks can easily be removed by the low pass filter. From this it can be seen that the low-pass filter need not reject the off-set frequency proper, but only the peaked wave that results from the beat note.

Factors in Receiver Design

The design factors for a receiver to receive transmitter diversity are fundamentally no different than a receiver used in receiver diversity. However, since transmitter diversity lends itself to somewhat special applications, there are certain factors that should be stressed for some particular services. If reception is desired on building tops or any location where impulse noise is encountered, the response to impulse noise and antenna input balance are important considerations.

Input balance is especially important if a long transmission line is used with a possible noise source near the transmission line between the antenna and the receiver. Experience has shown that receivers vary widely in their response to impulse noise. It has also been found that the low-pass filter is very effective in reducing the effect of impulse noise. Input balance can be provided external to a receiver by the use of a properly designed input transformer between the transmission line and the receiver input terminals.

The frequency shift portion of the receiver should be given careful consideration. The important factors are the use of mark and space filters, good limiting, and the low-pass filter.

Simplicity of operation is a very important factor for some applications. In order to require a minimum of attention with regard to tuning, the receiver should have exceptional frequency stability and possibly some means for automatic frequency control. A minimum of operating controls is a good feature for any receiver but this is of special importance in operations where a minimum of attention is required, or where operation by non-technical personnel is desired.

Conclusions

Transmitter diversity is not expected to replace receiver diversity for most point-to-point circuits, but it appears to offer a practical solution for a number of important services.

It is more economical to improve the single receiver reception of a given signal by the addition of a second transmitter, than to increase the power of the single transmitter to get the same results. The single transmitter would have to be increased 12 to 30 decibels or 16 to 1000 times the power required in each of two transmitters to obtain the same results at the receiver.

Transmitter diversity is as effective as receiver diversity in overcoming the effects of fading if a properly designed receiver is used.

Acknowledgments

The investigation of transmitter diversity described in this paper was initiated by H. O. Peterson, of the Riverhead Laboratory, under whose general direction the project was carried on.

The dual frequency shift equipment for the transmitter was designed and produced by H. E. Goldstine of the Rocky Point Laboratory.

The transmitting station facilities at Bolinas were provided by RCA Communications, Inc., and numerous test schedules were provided with excellent assistance and cooperation by various members of the RCA Communications staff.

A HIGH-PERFORMANCE TRANSISTOR WITH WIDE SPACING BETWEEN CONTACTS*

By

B. N. Slade

Tube Department, RCA Victor Division.
Harrison, N. J.

Summary—A number of transistors having contact spacings ranging between 0.010 inch and 0.020 inch have been made. Power gains of 20 to 30 decibels and current gains as high as 25 are obtained. These values are as good as or better than those previously reported for narrow-spaced units. An improvement in operational stability may result from the use of wide-spaced contacts through a reduction in the average value of the equivalent base resistance. Current gain falls off more rapidly with frequency in wide-spaced than in narrow-spaced transistors because of transit-time effects. These effects limit the usefulness of wide-spaced transistors to low-frequency applications. However, the technique of activating at wide spacing with an auxiliary contact, then operating with a close-spaced contact makes high current gains and reduced values of equivalent base resistance obtainable at frequencies of 1 to 5 megacycles per second.

Introduction

THE importance of maintaining close and accurate spacings between the emitter and collector contacts of the transistor has been emphasized in various published papers[1] discussing transistor characteristics. These papers stress that 0.002 inch is the maximum spacing for good transistor action, and any greater values would result in lower power gains and current gains. Curves in these papers show an almost exponential decrease in current gain and power gain as the spacing is increased. However, recent work reported here has indicated that transistors of considerably wider spacings may be made with no appreciable sacrifice in power gain. The use of wide contact spacings not only can simplify the assembly of transistors, but also may result in two improvements in electrical characteristics. These improvements are (1) a decrease in internal feedback which may result in better operational stability, and (2) higher current gain. These improvements are offset to some degree by a reduction in the

* Decimal Classification: R282.12.

[1] See for example J. Bardeen and W. H. Brattain, "Physical Principles Involved in Transistor Action", *Phys. Rev.*, Vol. 75, pp. 1208-1225, April 15, 1949.

frequency response, thus limiting wide-spaced transistors to low-frequency applications.

Equivalent Base Resistance as a Function of Contact Spacing

In order to study the phenomena involved in wide-spaced transistors, both the equivalent base resistance[2] and gain were measured as a function of contact spacing.

The equivalent base resistance, the mutual element of the T-network equivalent circuit of the transistor,[3] represents the internal impedances which are common to both input and output circuits. It will be shown that wide spacing of the transistor contacts results in a decrease of this resistance, thus resulting in a decrease of internal feedback.

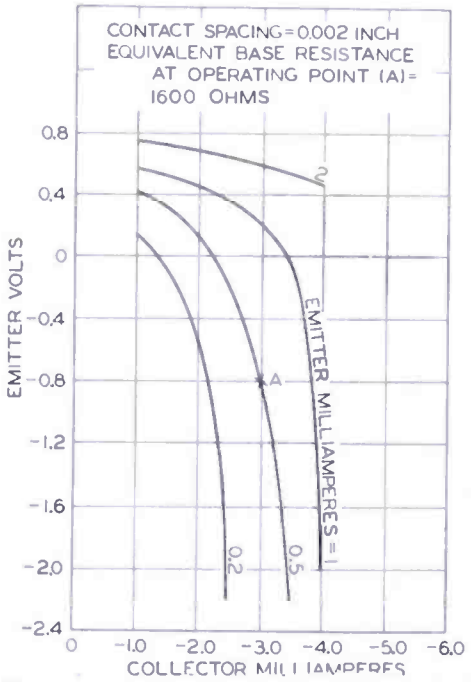

Fig. 1 — Static characteristic of narrow-spaced transistor having equivalent base resistance of 1600 ohms.

It is believed that the equivalent base resistance is composed of the bulk resistance of the germanium crystal, leakage between emitter and collector contacts, and electronic effects, the nature of which are not completely understood. High values of equivalent base resistance due to leakage and these electronic effects are illustrated in Figure 1 by the family of curves of emitter voltage versus collector current at constant emitter current for a narrow-spaced transistor. The equivalent base resistance, which is equal to the slope of these curves, is not only high at the operating point, A, but is also greatly dependent upon emitter and collector currents. Transistors with these characteristics have appreciable feedback since the equivalent base resistance at the operating point is approximately 1600 ohms. Shelf life tests on more than two hundred units have indicated that transistors having high and variable values of equivalent base resistance are quite unstable and have poor life.

---

[2] A committee of the I.R.E. is presently considering the use of the term "equivalent block resistance" to replace the term "equivalent base resistance."

[3] W. M. Webster, E. Eberhard and L. E. Barton, "Some Novel Circuits for the Three-Terminal Semiconductor Amplifier", *RCA Review*, Vol. X, No. 1, p. 5, March 1950.

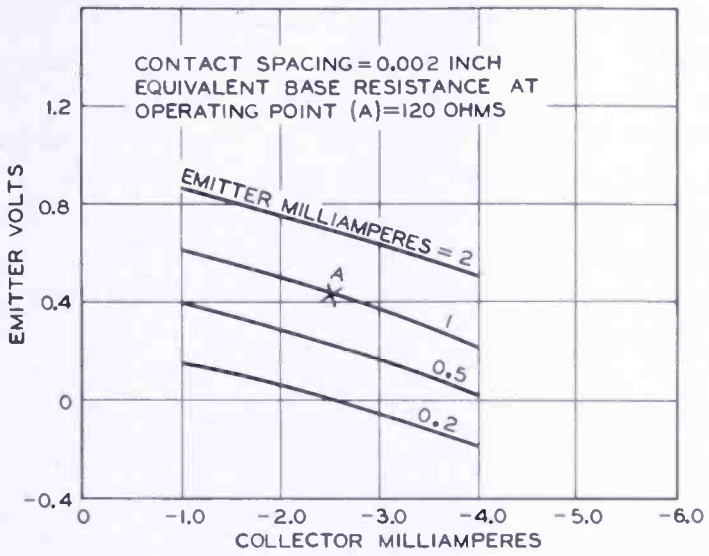

Fig. 2—Static characteristic of narrow-spaced transistor having equivalent base resistance of 120 ohms.

Figure 2 shows a similar set of curves for a narrow-spaced transistor having an equivalent base resistance varying from 100 to 200 ohms throughout the operating range. Leakage between the contacts has been reduced, but the electronic effects which cause the equivalent base resistance to vary with bias currents are still present to a small degree. Equivalent base resistance at the operating point, A, equals 120 ohms, and there is appreciable feedback in this transistor, though not as great as in the unit described in Figure 1. These curves are probably typical of many, if not most narrow-spaced transistors, although occasional narrow-spaced units have equivalent base resistance values as low as 30 ohms.

Figure 3 shows a family of curves for a wide-spaced transistor. It can be seen from these curves that the equivalent base resistance

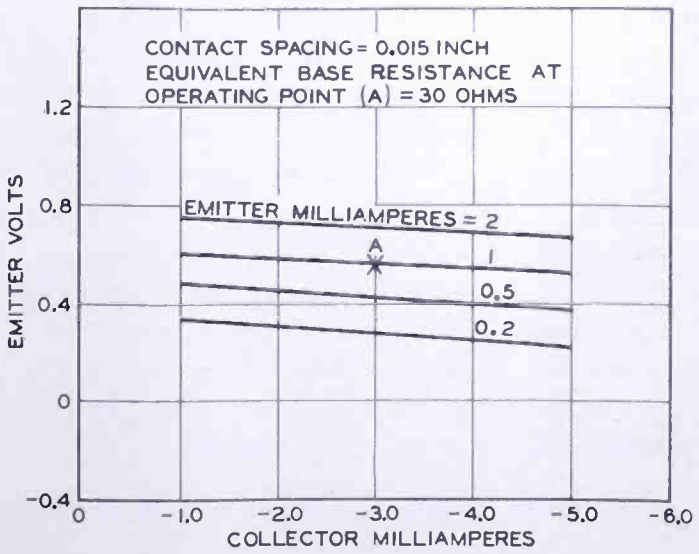

Fig. 3—Static characteristic of wide-spaced transistor having equivalent base resistance of 30 ohms.

is not only small, approximately 30 ohms at the operating point, A, but also practically independent of changes in emitter or collector currents. These curves are typical of almost all wide-spaced transistors. The extent to which the value of the equivalent base resistance decreases with increasing point spacing is shown in Figure 4.[4] In this curve, the equivalent base resistance decreases exponentially and approaches a value which is approximately equal to the bulk resistance of the crystal. Surface leakage and other effects appear to have been minimized at these wide spacings.

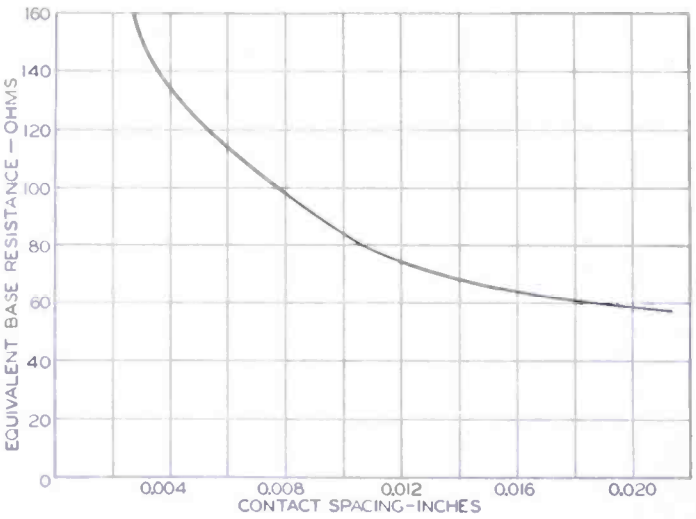

Fig. 4 — Effect of varying contact spacing on equivalent base resistance.

Power Gain and Current Gain as a Function of Contact Spacing

The effect of increased contact spacing on power gain is illustrated in Figure 5 which shows curves of power gain versus contact spacing for three crystals. Each unit was formed at a contact spacing of 0.016 inch. The collector remained fixed while the emitter was moved for each reading. All data were read at constant emitter and collector current conditions. It appears from these three curves that power gain is relatively independent of spacing up to approximately 0.015 inch.

If, however, a transistor is formed at 0.003 inch, as illustrated in Figure 6, current gain decreases fairly rapidly with increased spacing. A second curve in Figure 6 shows that if the same crystal is formed at 0.016 inch, the current gain remains fairly independent of the spacing. Significantly, the current gain of the unit formed at 0.016 inch is more than three times as great as the current gain for the same crystal formed at 0.003 inch. The third curve in Figure 6 shows a plot of current gain versus contact spacing published by Bardeen and

[4] Data provided by J. I. Pantchechnikoff, RCA Laboratories Division, Princeton, N. J.

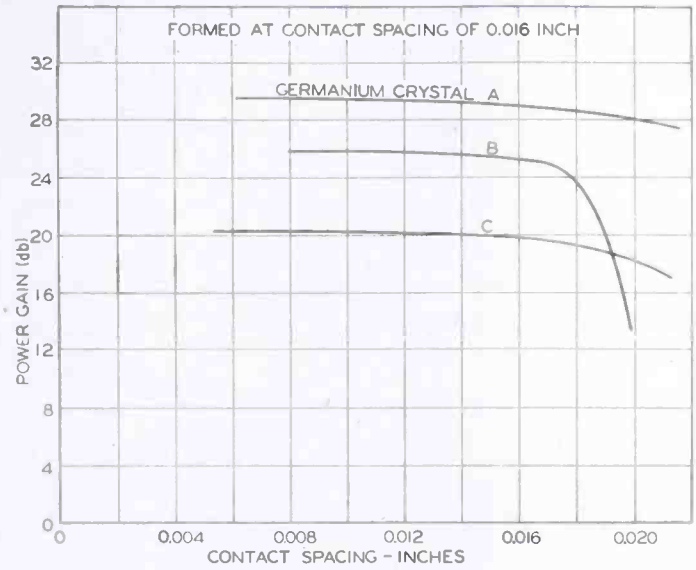

Fig. 5 — Effect of varying contact spacing on power gain.

Brattain.[1] This curve, like the curve of the unit formed at a spacing of 0.003 inch, decreases in gain with increased contact spacing.

Relation of Crystal Resistivity to Wide-Spaced Operation

In addition to the forming of the transistors, the crystal resistivity appears to be an important factor in the operation of wide-spaced transistors. The effect of crystal resistivity on the gain-versus-spacing characteristic is illustrated in Figure 7 which shows curves of power gain versus contact spacing for two high-resistivity crystals and one low-resistivity crystal. All three transistors were formed at a contact spacing of 0.016 inch. RCA germanium usually ranges from ½ to

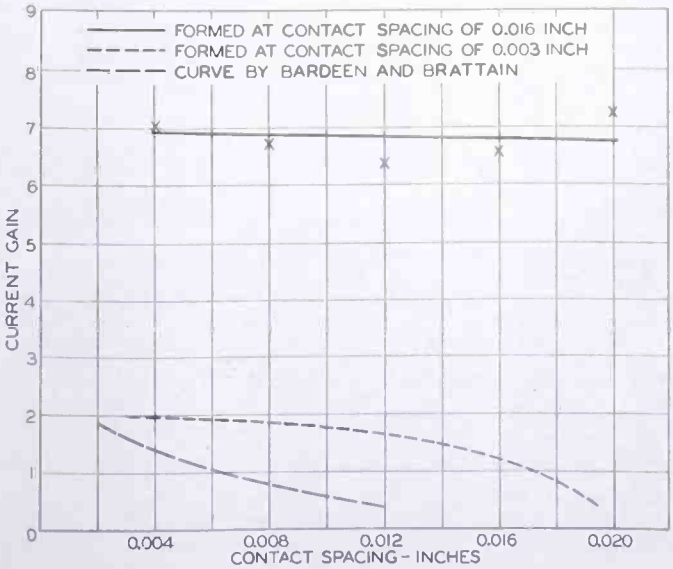

Fig. 6 — Effect of varying contact spacing on current gain.

15 ohm-centimeter in resistivity. Exact measurements of the resistivity of the germanium crystals which are best suited for wide spacing have not yet been made. However, high-resistivity germanium as discussed in this paper generally will include the upper portion of the ½ to 15 ohm-centimeter range while low-resistivity geranium will usually cover the lower part of this range. The transistor using the low-resistivity crystal shows a rapid decrease in gain with increasing point spacing. The gains of the two transistors having high-resistivity crystals are relatively independent of contact spacing up to 0.016 inch.

It appears that two requirements are necessary, therefore, in order that gain be relatively independent of contact spacing. First, the germanium must have relatively high resistivity, and secondly, the transistor should be formed with emitter and collector spaced far apart.

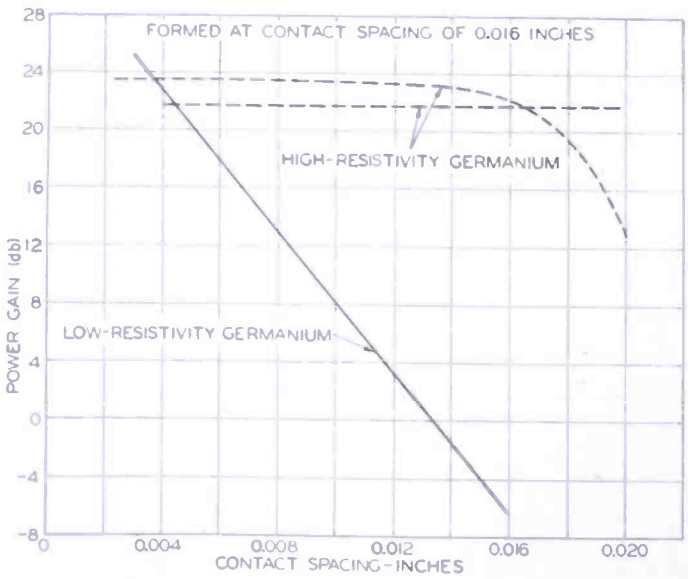

Fig. 7 — Effect of varying contact spacing on power gain of high- and low-resistivity germanium crystals.

Electrical Characteristics of Wide-Spaced Transistors

The gain and impedance characteristics of completed wide-spaced transistors are shown in Table I. Here four wide-spaced transistors are compared with four narrow-spaced units.

The average value of equivalent base resistance for the wide-spaced transistors listed in the table is 22.5 ohms as compared to 105 ohms for the narrow-spaced transistors. The significance of the equivalent base resistance in causing feedback may be appreciated by noting the difference between measured gain and calculated gain. Power gain, exclusive of feedback, is calculated from the expression

$$\text{Power Gain (db)} = 10 \log \left[(\text{current gain})^2 \times \frac{\text{output load resistance}}{4 \times \text{input load resistance}} \right]$$

where the input and output load resistances are adjusted for maximum output of the transistor. Table I shows that in the case of the narrow-spaced units the measured gain is approximately 4 decibels greater than the calculated value. This difference between the measured and calculated gain is approximately equal to the gain due to feedback. The gain due to feedback of the wide-spaced units is approximately 1.2 decibels.

Table I

Transistor No.	Contact Spacing Inches	RESISTANCES			Equiv. Base Resistance ohms	Current Gain	Power Gain	
		Input Load ohms	Transfer ohms	Output Load ohms			Meas. db	Calc. db
1	0.015	740	42000	5000	30	6.2	20.8	18.3
2	0.015	160	12000	2500	20	6.0	22.6	21.5
3	0.015	260	26000	5000	20	5.0	21.9	20.8
4	0.015	800	50000	9000	20	5.4	19.0	19.1
AVERAGE	——	490	32500	5375	22.5	5.65	21.1	19.9
1	0.002	320	42000	14000	80	2.8	22.8	19.3
2	0.002	440	60000	22000	180	2.8	27.8	19.9
3	0.002	320	44000	23000	100	1.8	18.8	17.6
4	0.002	360	45000	14000	60	3.2	23.5	19.9
AVERAGE	——	360	47750	18250	105	2.65	23.2	19.2

Table I shows that the output load resistance of the wide-spaced transistor is smaller, on the average, than that of the narrow-spaced transistor. Table I also shows that the current gain of the wide-spaced transistor is higher, on the average, than that of the narrow-spaced transistor. These higher values of current gain account for the high values of power gains.

Table II shows impedance and gain characteristics for three crystals. Each crystal was mounted as a transistor and formed at a spacing of 0.002 inch. After measurements were recorded, each crystal was remounted and formed at a contact spacing of 0.015 inch. The use of one crystal for tests at both 0.002 inch and 0.015 inch permits a comparison of wide and narrow spacings and minimizes the variables encountered when different pieces of germanium are used. Here, as in Table I, the output load resistance is considerably smaller in the case of the wide-spaced transistor. The current gains at 0.002 inch were 2.5 for all three samples, but at 0.015-inch spacing, current gains

Table II

Crystal No.	Contact Spacing Inches	RESISTANCES			Equiv. Base Resistance ohms	Current Gain	Power Gain	
		Input Load ohms	Transfer ohms	Output Load ohms			Meas. db	Calc. db
1	0.002	440	125000	45000	200	2.5	28.8	22.0
	0.015	140	42000	4000	10	10.0	27.8	28.5
2	0.002	520	45000	20000	320	2.5	24.0	17.8
	0.015	560	38000	2500	10	14.0	23.8	23.4
3	0.002	320	60000	25000	160	2.5	26.9	20.9
	0.015	500	42000	1000	10	26.0	25.2	25.3

were 10, 14, and 26. In the case of the wide-spaced transistors, because the calculated gains were practically equal to the measured gains, very little feedback was indicated. The calculated gains of the narrow-spaced transistors, however, averaged six decibels less than the measured gain. This large amount of feedback in the case of the narrow-spaced units may be attributed to the high values of equivalent base resistance which ranged from 160 to 320 ohms.

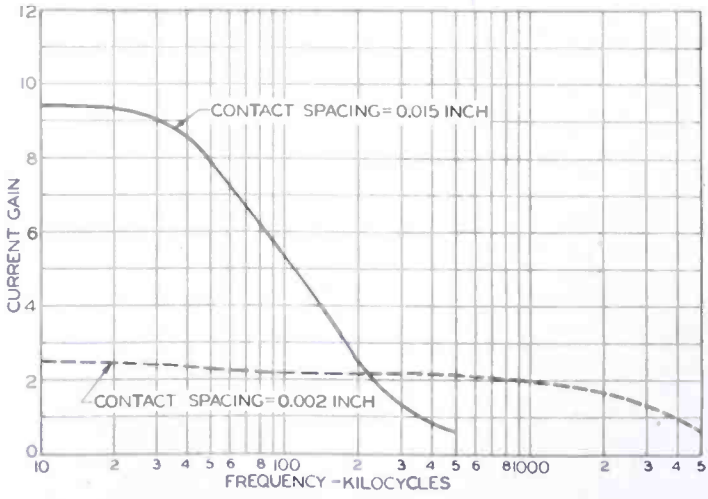

Fig. 8 — Frequency response of a wide-spaced and a narrow-spaced transistor.

Limitations of Wide Spacing of Contacts

The principal limitations of the wide-spaced transistors are apparent from Figure 8 which shows curves of current gain versus frequency for both a wide- and a narrow-spaced transistor.[5] Due to the effects of transit time, the frequency response of the wide-spaced transistors is poor at frequencies much greater than 100 kilocycles per second. Consequently, these transistors are limited to low-frequency applications.

[5] Data for transistor having contact spacing of 0.002 inch provided by G. Olive, RCA Laboratories Division, Princeton, N. J.

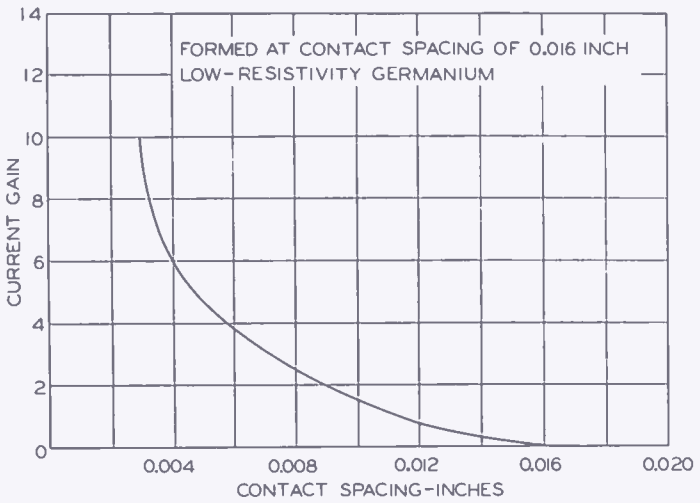

Fig. 9 — Effect of varying contact spacing on current gain for a low-resistivity germanium crystal.

Transistors Formed at Wide Spacing but Operated at Narrow Spacing

It has been found that a crystal of low resistivity may be formed at wide spacings, and even though its gain may be very small at these spacings, a high current gain and power gain will be obtained if the emitter is then moved to approximately 0.002 inch from the collector. Figure 9 shows a curve of current gain versus contact spacing for a low-resistivity crystal formed at 0.016 inch spacing. As the emitter is moved toward the collector, the current gain increases. At 0.003-inch spacing a current gain of ten is obtained. Due to the limitations of the equipment used for taking these measurements, current gain at spacings smaller than 0.003 inch were not measured. If a crystal of high resistivity is used, excessive feedback usually occurs if the emitter is moved close to the collector after forming at wide spacings; consequently it is necessary to use fairly low-resistivity germanium for this transistor. A transistor which is formed at wide spacing and operated at narrow spacing may be assembled with three contacts as illustrated in Figure 10. Emitter 2, which is spaced 0.015 inch from the collector, draws approximately three milliamperes of current during forming. Emitter 1 is out of the circuit. After forming, the unit

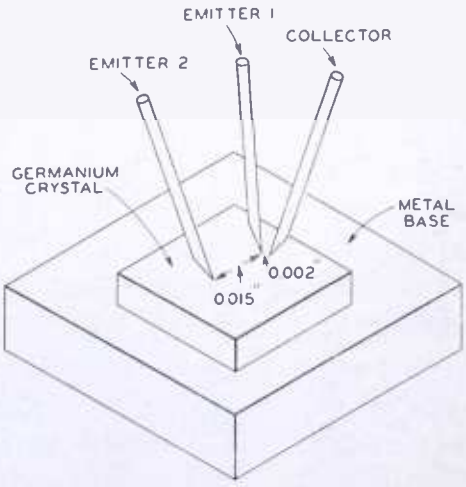

Fig. 10—Contact arrangement of transistor formed at wide spacing and operated at narrow spacing.

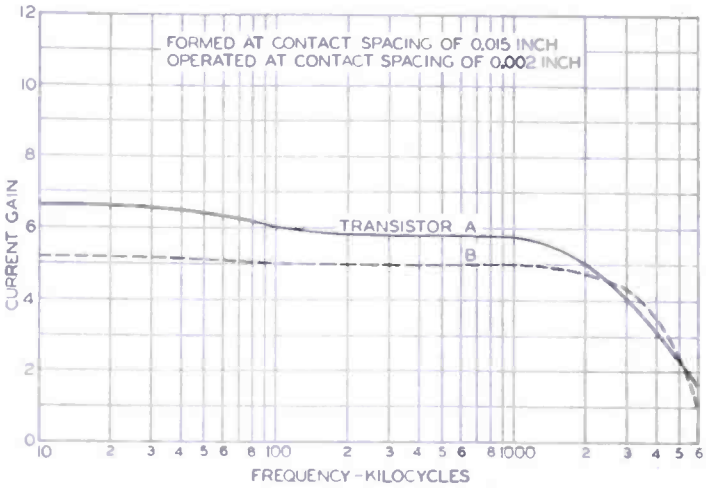

Fig. 11—Frequency response of a transistor formed at wide spacing and operated at narrow spacing.

is operated as a narrow-spaced transistor with emitter 1. Emitter 2 is no longer used and may be removed. Values of current gain for these units have ranged from 4 to 20. Power gain ranges from 20 to 30 decibels. Because only low-resistivity germanium is used, the equivalent base resistance averages about 75 ohms as compared to over 100 ohms for conventional transistors.

Figure 11 shows two typical frequency-response curves of transistors formed at 0.015 inch and operated at 0.002 inch. These curves are only three decibels down at approximately three megacycles per second. The frequency response of these transistors is, therefore, comparable to conventional narrow-spaced transistors; in addition, the current gains are comparable to the current gains of wide-spaced transistors.

Conclusions

It is possible to make transistors with contact spacings of 0.015 inch or greater. These transistors, compared with narrow-spaced transistors, have higher current gain, lower equivalent base resistance, and approximately the same power gain. These advantages, in addition to the obvious simplification in manufacture of transistors, are obtained at the expense of good frequency response. However, the process used in the forming of wide-spaced transistors may be used to obtain high current gains and good frequency response at narrow contact spacings if the germanium crystal material is properly selected. Transistors which are processed in this manner have higher values of equivalent base resistance than are obtained with the use of wide-contact spacings.

DEFLECTION OF CATHODE-RAY TUBES IN SEQUENCE*

By

G. W. Gray and A. S. Jensen

Research Department, RCA Laboratories Division, Princeton, N. J.

Summary—*The resolution of a cathode-ray-tube system, for example one employing storage tubes or switching tubes, can be increased if a number of such tubes are deflected in parallel. If their deflection plates are biased differently so that only in one tube at a time is the beam on the target, they each may be deflected successively, or sequentially, as the signal amplitude varies. This paper describes a circuit which enables such a multiplicity of tubes to be deflected in sequence with many advantages including reduced power and tube requirements over a conventional direct driving circuit. Since only one tube is being deflected at any one time, a saving in power by a factor 5 is attained in the example shown. Details are given of the design of such a circuit operable for ten beam tubes with a frequency response flat beyond 5 megacycles. A circuit diagram and oscillograms indicating its operation are included.*

Introduction

IN electronics systems using cathode-ray tubes for display, switching, memory, etc., it is often found that one of the limitations of the system is the finite resolution of the cathode-ray tube. Increasing this resolution can always be reduced to the problem of increasing the ratio of the deflection sensitivity to the beam width. This is so since increasing the distance between the deflection system and the target can always increase the deflection per unit input voltage but increases the spot size in practically the same proportion. An increase in the deflection angle or an increase in the current density by redesigning the electron gun are possible approaches but are subject to the limitations of the electron optics in the tube.

This paper describes a circuit approach which increases the possible cathode-ray-tube resolution by an order of magnitude and yet requires a minimum of additional equipment. This is a problem which arises in a multitude of electronic systems and it is felt that this solution may be applicable in many systems. The deflection-input-signal wave form will, of course, depend upon the system, but the circuit described will accept any input signal within its bandwidth limitation. In illustration of this approach, two applications are

* Decimal Classification: R138.312.

described below: the first, employing a storage tube for electronic memory, would most likely use a sawtooth deflection signal with deflection being a simple function of time; the second, employing switching tubes, would use a series of randomly spaced pulses of arbitrarily varying amplitude as an input deflection signal.

In general it is found in beam type storage tubes, such as the Radechon or barrier grid storage tube[1] that the amount of information which can be stored is inversely proportional to the fidelity with which it can be reproduced. The product of these quantities is limited by the spot size and the deflection angles. Electronic systems requiring information storage can be improved if this product is made higher. One approach to the problem is the arrangement of several storage tubes in parallel. The tubes are sequentially deflected so that the number of storage elements in the system is increased by a factor equal to the number of tubes. These elements are available one after the other with no spaces, just as if they were all in one tube. There are several objections to this proposal, but all are related to the large deflection power and deflection driver tubes which are required if such a number of beam tubes are to be deflected by a conventional circuit. So far, at least, systems engineers do not object to the increased input and output capacitance in the signal circuit, this being considered a proper price to pay for the increase in storage elements.

In nuclear research, the energy spectra of elemental particles from nuclear disintegrations are of considerable interest. One approach to the measurement of these spectra uses a proportional counter detector, either of the gaseous or crystal variety, the output of which is a pulse whose amplitude is proportional to the energy of the particle detected. A device which records the number of such pulses as a function of their amplitude (this is exactly the energy spectrum of the group of particles detected) is called in the literature a pulse amplitude analyzer. Several devices of this type have been described, some using conventional tubes,[2,3] others with special single tubes having a multiplicity of targets.[4,5] These references do not exhaust the literature. All of

---

[1] A. S. Jensen, J. P. Smith, M. H. Mesner and L. E. Flory, "The Barrier Grid Storage Tube and Its Operation", *RCA Review*, Vol. IX, pp. 112-135, March 1948.

[2] H. F. Freundlich, E. P. Hincks and W. J. Ozeroff, "Pulse Analyzer for Nuclear Research", *Rev. Sci. Instr.*, Vol. 18, pp. 90-100, February 1947.

[3] C. H. Westcott and G. C. Hanna, "A Pulse Amplitude Analyzer for Nuclear Research Using Pretreated Pulses", *Rev. Sci. Instr.*, Vol. 20, pp. 181-188, March 1949.

[4] D. A. Watkins, "The Ten Channel Electrostatic Pulse Analyzer", *Rev. Sci. Instr.*, Vol. 20, pp. 495-499, July 1949.

[5] W. E. Glenn, Jr., "Pulse Height Distribution Analyzer", *Nucleonics*, Vol. 4, pp. 50-61, June 1949.

the systems described have limitations, particularly with respect to the pulse repetition rate, the discrimination between amplitude channels, and the driving requirements.

A pulse amplitude analyzer can be built which comprises several beam deflection tubes, each having a collecting target structure behind a limiting slit. The input pulse deflects the beams sequentially across their targets, with only one tube conducting at any one time. Here, as in the storage tube system, the deflecting circuits can be improved and simplified if direct deflection drive can be eliminated. Moreover, since each amplitude channel of an analyzer of this design is controlled by its own individual beam tube, the ratio of the sensitive portion of the amplitude gate to the twilight zone is very high. This results in apparatus in which the regions of amplitude where there is doubt as to which channel should count the pulse are very small. Furthermore, since each such beam tube is considerably less complicated in design than one with a multiplicity of targets, some complication may be incorporated in the tubes in order to prevent two adjacent channels from counting the same pulse, to simplify the output circuits, or to assure that the amplitude gates are of equal width.

Advantages

There is no fundamental problem involved in deflecting a number of cathode-ray tubes in parallel where each tube is so biased that only one beam is on its target at any one instant and the tubes are therefore deflected successively, or sequentially. However, the deflection driver required is awesome in size and power requirements. This article describes a circuit for sequentially deflecting a number of beam tubes with the following advantages over a conventional deflection circuit:

1. No large B supply is required. (Direct drive of 10 levels would require nearly a 1500-volt supply.)
2. No large driving tubes are required (such as 4X150A, two of which would be required to replace the circuit shown in Figure 1).
3. The driving power (including both B supply and heater power) is less.
4. 10 beam tubes together with this circuit can be driven with the conventional circuit required for one tube.
5. Separate centering is provided for each beam tube.
6. Push-pull anastigmatic operation is provided.
7. DC coupling or dc restoration is simple. This is important in computer type circuits (pulse height analysis) where the deflection signal is arbitrary.

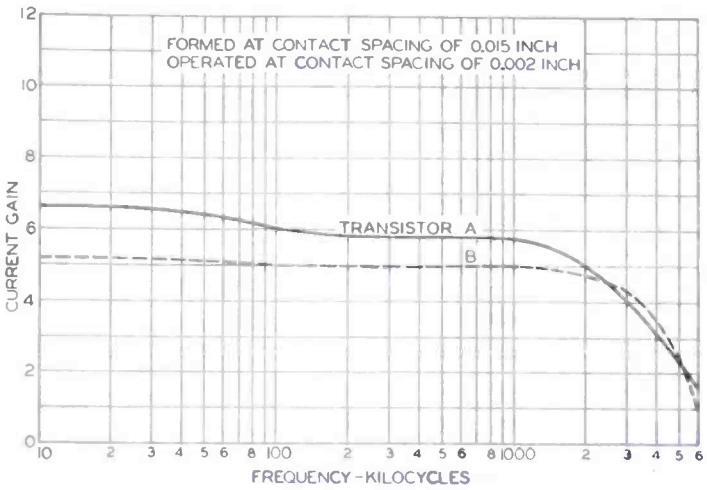

Fig. 11—Frequency response of a transistor formed at wide spacing and operated at narrow spacing.

is operated as a narrow-spaced transistor with emitter 1. Emitter 2 is no longer used and may be removed. Values of current gain for these units have ranged from 4 to 20. Power gain ranges from 20 to 30 decibels. Because only low-resistivity germanium is used, the equivalent base resistance averages about 75 ohms as compared to over 100 ohms for conventional transistors.

Figure 11 shows two typical frequency-response curves of transistors formed at 0.015 inch and operated at 0.002 inch. These curves are only three decibels down at approximately three megacycles per second. The frequency response of these transistors is, therefore, comparable to conventional narrow-spaced transistors; in addition, the current gains are comparable to the current gains of wide-spaced transistors.

Conclusions

It is possible to make transistors with contact spacings of 0.015 inch or greater. These transistors, compared with narrow-spaced transistors, have higher current gain, lower equivalent base resistance, and approximately the same power gain. These advantages, in addition to the obvious simplification in manufacture of transistors, are obtained at the expense of good frequency response. However, the process used in the forming of wide-spaced transistors may be used to obtain high current gains and good frequency response at narrow contact spacings if the germanium crystal material is properly selected. Transistors which are processed in this manner have higher values of equivalent base resistance than are obtained with the use of wide-contact spacings.

DEFLECTION OF CATHODE-RAY TUBES IN SEQUENCE*

By

G. W. Gray and A. S. Jensen

Research Department, RCA Laboratories Division,
Princeton, N. J.

Summary—The resolution of a cathode-ray-tube system, for example one employing storage tubes or switching tubes, can be increased if a number of such tubes are deflected in parallel. If their deflection plates are biased differently so that only in one tube at a time is the beam on the target, they each may be deflected successively, or sequentially, as the signal amplitude varies. This paper describes a circuit which enables such a multiplicity of tubes to be deflected in sequence with many advantages including reduced power and tube requirements over a conventional direct driving circuit. Since only one tube is being deflected at any one time, a saving in power by a factor 5 is attained in the example shown. Details are given of the design of such a circuit operable for ten beam tubes with a frequency response flat beyond 5 megacycles. A circuit diagram and oscillograms indicating its operation are included.

Introduction

In electronics systems using cathode-ray tubes for display, switching, memory, etc., it is often found that one of the limitations of the system is the finite resolution of the cathode-ray tube. Increasing this resolution can always be reduced to the problem of increasing the ratio of the deflection sensitivity to the beam width. This is so since increasing the distance between the deflection system and the target can always increase the deflection per unit input voltage but increases the spot size in practically the same proportion. An increase in the deflection angle or an increase in the current density by redesigning the electron gun are possible approaches but are subject to the limitations of the electron optics in the tube.

This paper describes a circuit approach which increases the possible cathode-ray-tube resolution by an order of magnitude and yet requires a minimum of additional equipment. This is a problem which arises in a multitude of electronic systems and it is felt that this solution may be applicable in many systems. The deflection-input-signal wave form will, of course, depend upon the system, but the circuit described will accept any input signal within its bandwidth limitation. In illustration of this approach, two applications are

* Decimal Classification: R138.312.

described below: the first, employing a storage tube for electronic memory, would most likely use a sawtooth deflection signal with deflection being a simple function of time; the second, employing switching tubes, would use a series of randomly spaced pulses of arbitrarily varying amplitude as an input deflection signal.

In general it is found in beam type storage tubes, such as the Radechon or barrier grid storage tube[1] that the amount of information which can be stored is inversely proportional to the fidelity with which it can be reproduced. The product of these quantities is limited by the spot size and the deflection angles. Electronic systems requiring information storage can be improved if this product is made higher. One approach to the problem is the arrangement of several storage tubes in parallel. The tubes are sequentially deflected so that the number of storage elements in the system is increased by a factor equal to the number of tubes. These elements are available one after the other with no spaces, just as if they were all in one tube. There are several objections to this proposal, but all are related to the large deflection power and deflection driver tubes which are required if such a number of beam tubes are to be deflected by a conventional circuit. So far, at least, systems engineers do not object to the increased input and output capacitance in the signal circuit, this being considered a proper price to pay for the increase in storage elements.

In nuclear research, the energy spectra of elemental particles from nuclear disintegrations are of considerable interest. One approach to the measurement of these spectra uses a proportional counter detector, either of the gaseous or crystal variety, the output of which is a pulse whose amplitude is proportional to the energy of the particle detected. A device which records the number of such pulses as a function of their amplitude (this is exactly the energy spectrum of the group of particles detected) is called in the literature a pulse amplitude analyzer. Several devices of this type have been described, some using conventional tubes,[2,3] others with special single tubes having a multiplicity of targets.[4,5] These references do not exhaust the literature. All of

---

[1] A. S. Jensen, J. P. Smith, M. H. Mesner and L. E. Flory, "The Barrier Grid Storage Tube and Its Operation", *RCA Review*, Vol. IX, pp. 112-135, March 1948.

[2] H. F. Freundlich, E. P. Hincks and W. J. Ozeroff, "Pulse Analyzer for Nuclear Research", *Rev. Sci. Instr.*, Vol. 18, pp. 90-100, February 1947.

[3] C. H. Westcott and G. C. Hanna, "A Pulse Amplitude Analyzer for Nuclear Research Using Pretreated Pulses", *Rev. Sci. Instr.*, Vol. 20, pp. 181-188, March 1949.

[4] D. A. Watkins, "The Ten Channel Electrostatic Pulse Analyzer", *Rev. Sci. Instr.*, Vol. 20, pp. 495-499, July 1949.

[5] W. E. Glenn, Jr., "Pulse Height Distribution Analyzer", *Nucleonics*, Vol. 4, pp. 50-61, June 1949.

the systems described have limitations, particularly with respect to the pulse repetition rate, the discrimination between amplitude channels, and the driving requirements.

A pulse amplitude analyzer can be built which comprises several beam deflection tubes, each having a collecting target structure behind a limiting slit. The input pulse deflects the beams sequentially across their targets, with only one tube conducting at any one time. Here, as in the storage tube system, the deflecting circuits can be improved and simplified if direct deflection drive can be eliminated. Moreover, since each amplitude channel of an analyzer of this design is controlled by its own individual beam tube, the ratio of the sensitive portion of the amplitude gate to the twilight zone is very high. This results in apparatus in which the regions of amplitude where there is doubt as to which channel should count the pulse are very small. Furthermore, since each such beam tube is considerably less complicated in design than one with a multiplicity of targets, some complication may be incorporated in the tubes in order to prevent two adjacent channels from counting the same pulse, to simplify the output circuits, or to assure that the amplitude gates are of equal width.

Advantages

There is no fundamental problem involved in deflecting a number of cathode-ray tubes in parallel where each tube is so biased that only one beam is on its target at any one instant and the tubes are therefore deflected successively, or sequentially. However, the deflection driver required is awesome in size and power requirements. This article describes a circuit for sequentially deflecting a number of beam tubes with the following advantages over a conventional deflection circuit:

1. No large B supply is required. (Direct drive of 10 levels would require nearly a 1500-volt supply.)
2. No large driving tubes are required (such as 4X150A, two of which would be required to replace the circuit shown in Figure 1).
3. The driving power (including both B supply and heater power) is less.
4. 10 beam tubes together with this circuit can be driven with the conventional circuit required for one tube.
5. Separate centering is provided for each beam tube.
6. Push-pull anastigmatic operation is provided.
7. DC coupling or dc restoration is simple. This is important in computer type circuits (pulse height analysis) where the deflection signal is arbitrary.

8. There is no beam-current loading of the deflection plates, and there are no glancing angle secondaries from the deflection plates to reach the target and give a spurious output signal.
9. The frequency characteristic is flat beyond 5 megacycles for 10 beam tubes, each using a pair of 6J6's.

Circuit Operation

The sequential deflection circuit is shown in the circuit diagram of Figure 1. This figure also shows the last stage of the deflection amplifier circuit and the dc clamp which would be required to deflect

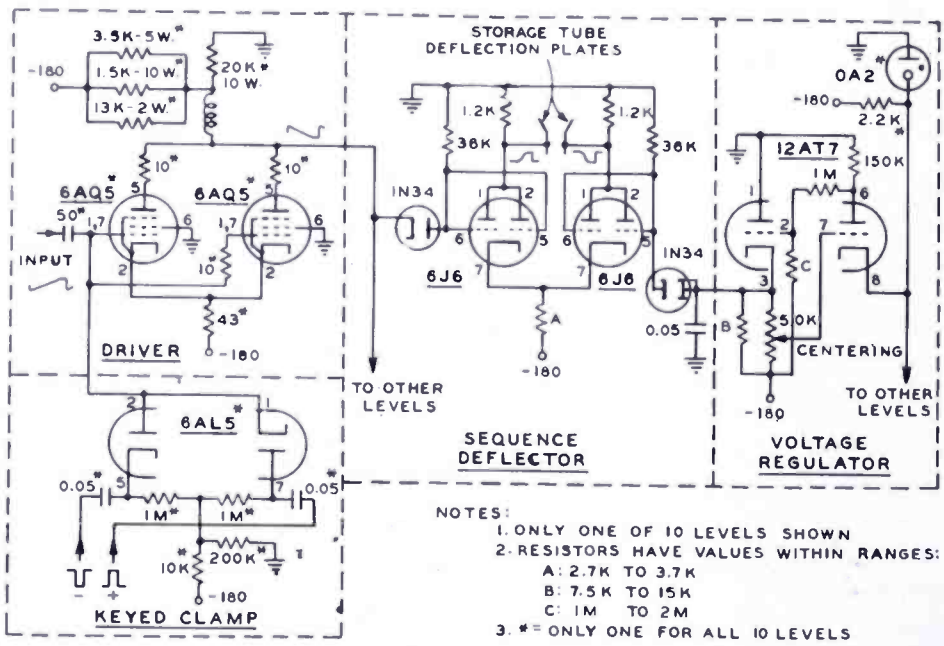

Fig. 1—Sequential deflection circuit (schematic).

one tube alone in the conventional manner. Only one such driver and one clamp are required for all ten levels. There are ten sequential deflectors each with its own voltage regulator. Only one level is shown in Figure 1. It consists of two 6J6 triodes, each having its two halves connected in parallel, connected in a standard cathode-coupled phase splitting circuit, designed for a push-pull gain of 10. The input is dc coupled to the driver, and the plates feed the beam-tube deflection plates in push-pull directly, so that the one keyed clamp suffices for the entire network.

In operation the beam of the deflection tube is on the center of its target when the deflection plates are both at the same poential. This occurs for both 6J6's conducting the same plate current; that is, both grids are at the same potential. One grid is the input; the other then controls the centering. Since ten levels are to be deflected sequen-

tially, to minimize the current drain from the B supply, each deflector circuit is designed so that it either cuts off or saturates shortly after its deflection-tube beam has been deflected beyond the target. This also means that the beam does not strike the deflection plates due to excessively large deflection. In this mode of operation, usually only the deflectors of the conducting deflection tube and of adjacent levels are not saturated. However, since either grid of any one deflector can draw grid current when its half is saturated, both are protected by crystal diodes which open circuit when the input is above cathode potential, leaving the grid at the same potential as the cathode without drawing grid current. Since the diode provides only a one-way path for electrons into the grid, the grid resistor must be returned to a high potential in order to remove these electrons. This resistor must be of low enough impedance to keep the time constant of the circuit formed by this resistor and the stray capacitance of the grid low for

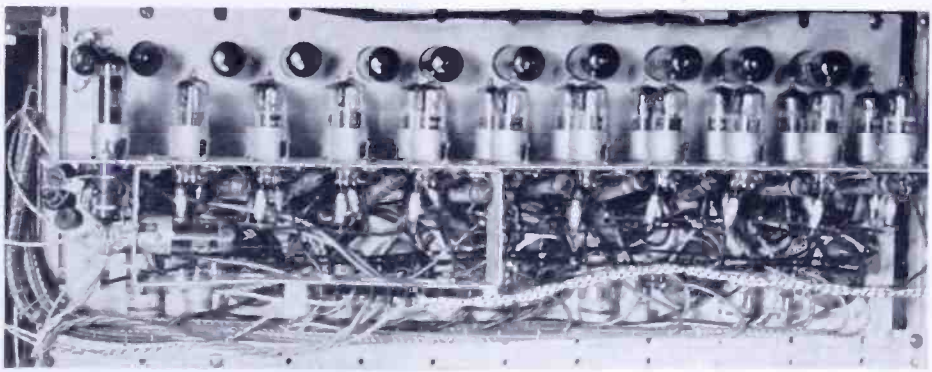

Fig. 2—Sequential deflection circuit.

high frequency operation. This low impedance requires a much lower impedance voltage source for centering, hence the electronic voltage regulator. For a repetitive deflection signal, a conventional voltage divider of higher impedance would be satisfactory.

When the deflection input is an arbitrary video signal, its dc level is lost in the ac stages preceding the driver. In order to maintain the deflection centering properly, it is necessary to restore the dc level by any one of a variety of dc clamps.[6] The clamp adjusts the dc potential of any reproducible signal level which has been previously chosen as a reference. It will be noted that as long as the operating range of the driver is properly chosen by adjusting the dc bias potential to which it is restored, and the individual sequence deflectors are properly centered, the actual signal value chosen as a reference is

[6] K. R. Wendt, "Television DC Component", *RCA Review*, Vol. IX, pp. 85-111, March 1948.

immaterial. Thus this circuit is not limited in the signal polarity acceptable.

It must be noted that the plate resistor of the 6J6 must be chosen so that the bandwidth of the sequence deflector is greater in proportion to the number of levels than that of the driver.

Figure 2 is a photograph of the sequential deflection circuit in the equipment for which it was built. The two 6AQ5's are at right angles at the left. The 6J6 tubes are shown in side view while the

(a) Signal on plates of one 6J6 of level #5 showing saturation and cut off characteristic.

(b) Multiple exposure: signals on plates of each 6J6 of level #5 showing push-pull operation. Output signal from beam deflection tube #5 indicating portion of deflection when beam is on target. Note high flat to rise ratio.

(c) Multiple exposure: signals on plates of one 6J6 of each of levels #2 to #8 indicating effect of centering.

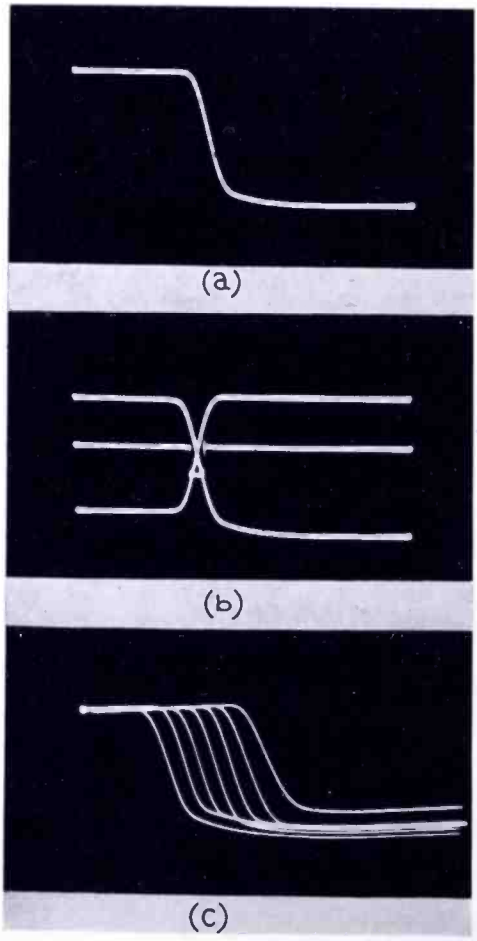

Fig. 3—Deflection plate signal with sawtooth input.

12AT7 tubes are shown in top view. The large 17-pin cinch sockets used for the button stems of the Radechon storage tubes can be seen through the wiring at the center.

Figure 3 shows three oscillograms of the deflection plate signal for a sawtooth input. Part (a) is the signal on one deflection plate of level #5, showing the effect of saturation and cutoff. The beam is on the target only during the linear portion of this characteristic. Part (b) shows, in multiple exposure, the signals on each deflection plate

of level #5. The push-pull operation can be seen, the beam being in the center of the target when the two traces cross. The output of the collector of secondary electrons from the target of the deflection tube is superimposed to show exactly when it is conducting (the signal is negative during conduction). Part (c) shows, in multiple exposure, the signals on one deflection plate of each level from #2 to #8, inclusive, to illustrate the effect of centering. Note that the beams traverse their targets sequentially.

To measure the frequency response of the circuit as shown, a sine-wave input, dc restored to the bottom of level #1, was used with amplitude just sufficient to extend to the top of level #10 for the middle frequency region. The number of targets traversed indicated the response amplitude. At 5 megacycles, level #10 was still being traversed.

DESIGN OF HIGH-PASS, LOW-PASS AND BAND-PASS FILTERS USING R-C NETWORKS AND DIRECT-CURRENT AMPLIFIERS WITH FEEDBACK*†

By

C. C. Shumard

Research Department, RCA Laboratories Division,
Princeton, N. J.

Summary—The construction of band-pass filters with relatively low cutoff frequencies is described. The filters consist of a combination of R-C networks and a direct-current amplifier with feedback.

Introduction

IT HAS BEEN necessary to use band-pass (B.P.) filters with relatively very low cutoff frequencies. Three ranges were required: .005 to 0.5, .01 to 1, and 0.03 to 3 cycles per second. To build filters of the conventional L-C type would require impractically large if not unrealizable values. On the other hand a filter using a combination of R-C networks and a direct-current (dc) amplifier with feedback, it has been found, results in a relatively small, practical unit.

The fundamental principle** involved is operation of the dc amplifier near the 1,0 point of the Nyquist loop, resulting in controlled regeneration without oscillation. In conjunction with external filtering the combination then is made to give a pass band comparable to the L-C filter used at higher frequencies.

Several configurations may be used to obtain the above results but this investigation has been limited to one in which only one dc amplifier is required and the new combination has the output characteristics of a normal feedback amplifier. This means that the output circuit is independent of load up to the power handling limits of the output tube.

This configuration in its simplified low-pass, high-pass and band-pass forms is shown respectively in Figures 1a, 1b, 2 and 3.

Low-Pass Filter Design Considerations

The prototype configuration may be considered that of Figure 1(a),

* Decimal Classification: R386.

† This work was done under contract for the Special Devices Center of the Naval Office of Research.

** Suggested by A. W. Vance of these laboratories.

which is the unmodified original version of the low-pass (L.P.) type. This has proved useful in the derivation and use of the high-pass (H.P.) and B.P. types. A solution* of the mesh equations for the ratio of the output voltage, e_o, to the input voltage, e_i, yields the relation

$$\frac{e_o}{e_i} = \frac{1}{-A + B_1 m^2 - j m [C_1 - D_1 m^2]}, \tag{1}$$

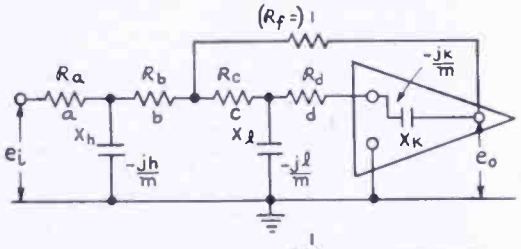

Fig. 1(a) — Low pass.

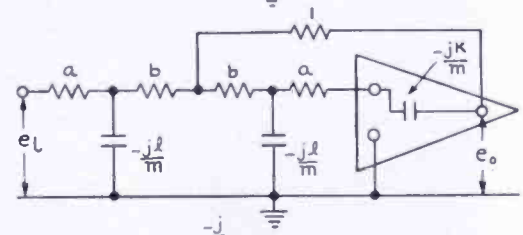

Fig. 1(b) — Low pass.

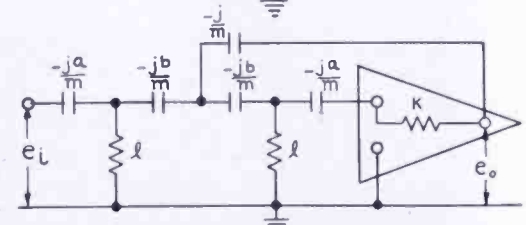

Fig. 2 — High pass.

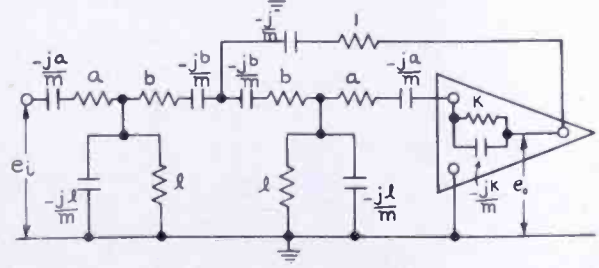

Fig. 3 — High pass.

R-C network and dc feedback amplifier filters.

where m = the frequency ratio f/f_0, the reference frequency, f_0, being chosen as desired,

$$A = a + b, \tag{1a}$$

$$B_1 = \frac{d}{kl}[a\,(1+c) + (1-d)\,(b+c) - c^2] + \frac{a}{hk}[b + (1+b)\,(c+d)], \tag{1b}$$

* See Appendix II, for B.P. filter, as illustration of method followed.

$$C_1 = \frac{a+b+(1+a+b)\,(c+d)}{\mathrm{k}} + \frac{ab}{h}, \tag{1c}$$

and $$D_1 = \frac{ad}{hkl}\,[\,(1+c)\,(b+c) - a\,c^2\,\mathrm{d}\,], \tag{1d}$$

in terms of the reference unit resistance used for external feedback.

Letting θ represent the phase angle between e_i and e_o,

$$\theta = \tan^{-1}\frac{m\,[C_1 - D_1\,m^2]}{-A + B_1\,m^2}. \tag{2}$$

Investigating the possibility of a solution with $d = a$, $h = l$ and $b = c$, it was found that

$$g = \frac{e_o}{e_i} = \frac{1}{-A + B_2\,m^2 - j\,m\,[C_2 - D_2\,m^2]}, \tag{3}$$

where $A = a + b$, (3a)

$$B^2 = \frac{2a\,(a+2b)}{kl} = \frac{2a\,(2A-a)}{kl}, \tag{3b}$$

$$C_2 = \frac{(a+b)\,(2+a+b)\,l + abk}{kl} = \frac{A\,(2+A)\,l + a\,(A-a)\,k}{kl}, \tag{3c}$$

and $$D_2 = \frac{a^2 b}{kl^2}\,[2 + b\,(2-a^2)\,] = \frac{a^2\,(A-a)}{kl^2}\,[2 + (A-a)\,(2-a^2)\,]. \tag{3d}$$

Here $$\theta = \tan^{-1}\frac{m\,[C_2 - D_2\,m^2]}{-A + B_2\,m^2}. \tag{3e}$$

In rationalized form,

$$|g| = \frac{1}{\sqrt{A^2 + m^2\,(C_2^2 - 2AB_2) + m^4\,(B_2^2 - 2C_2\,D_2) + m^6\,D_2^2}}. \tag{4}$$

It will be noticed that if in Equation (4)

$$C_2^2 - 2A\,B_2 = 0, \tag{5}$$

and $$B_2^2 = 2C_2 D_2 = 0, \tag{6}$$

then $$|g| = \frac{1}{\sqrt{A_1^2 + D_2^2 m^6}}. \tag{7}$$

Equation (7) is of the same form as that obtainable in a dissipationless low-pass single-section L-C filter terminated in its characteristic impedance $R = \sqrt{L/C}$, and therefore gives the same rate of attenuation.

The conditions expressed by Equations (5) and (6) may be fulfilled if

$$B_2 = C_2 = 2A, \tag{8}$$

and $$D_2 = A. \tag{9}$$

Then Equation (7) becomes

$$\left| \frac{e_o}{e_i} \right| = \frac{1}{A} \frac{1}{\sqrt{1 + m^6}} \quad \text{or} \quad |g| = G_o / \sqrt{1 + m^6}, \tag{10}$$

where g is the gain variation with frequency, and G_o is the low frequency gain $\frac{1}{A} = \frac{1}{a+b}$. Equation (3e), for the phase angle θ, becomes

$$\theta = \tan^{-1} \frac{m(2-m^2)}{2m^2-1}. \tag{11}$$

However, the values of a, b, k and l which fulfill these conditions must still be found using the above relations. (See Appendix I.)

The values of a for different values of $A = a + b$, may be found from the relation

$$2A(2A-a)^2[2 + (A-a)(2-a^2)]$$
$$-A^2(2+A)(A-a)[2 + (A-a)(2-a^2)]^2 - (2A-a)^3 = 0. \tag{12}$$

Then $$b = A-a, \tag{13}$$

$$k = \frac{a(2A-a)}{Al}, \tag{14}$$

and $$l = \frac{a(A-a)[2 + (A-a)(2-a^2)]}{2A-a}. \tag{15}$$

Values of a, b, k and l were determined for a number of values of A. Some of these are given in Table I below.

Table I

$A=a+b$	$G_o=1/A$	a	b	b/a	k	l
0.1	10.0	.012	.088	7.3333	1.76029	0.012483
0.2	5.0	.05	.15	3.0	1.77552	0.049275
0.45	2.222	.208	.242	1.16346	1.770328	0.180309
0.52	1.923077	.26	.26	1.0	1.798635	0.216853
1.0	1.0	.65	.35	.538461	2.0395	0.430175
2.0	.5	1.436	.564	.393728	2.96977	0.62039

In Figure 4 is shown a partial plot of the above values. The curves are indicative only, however, since the scale is insufficient for exact interpolation. Exact values should be calculated from Equations (12), (13), (14), and (15).

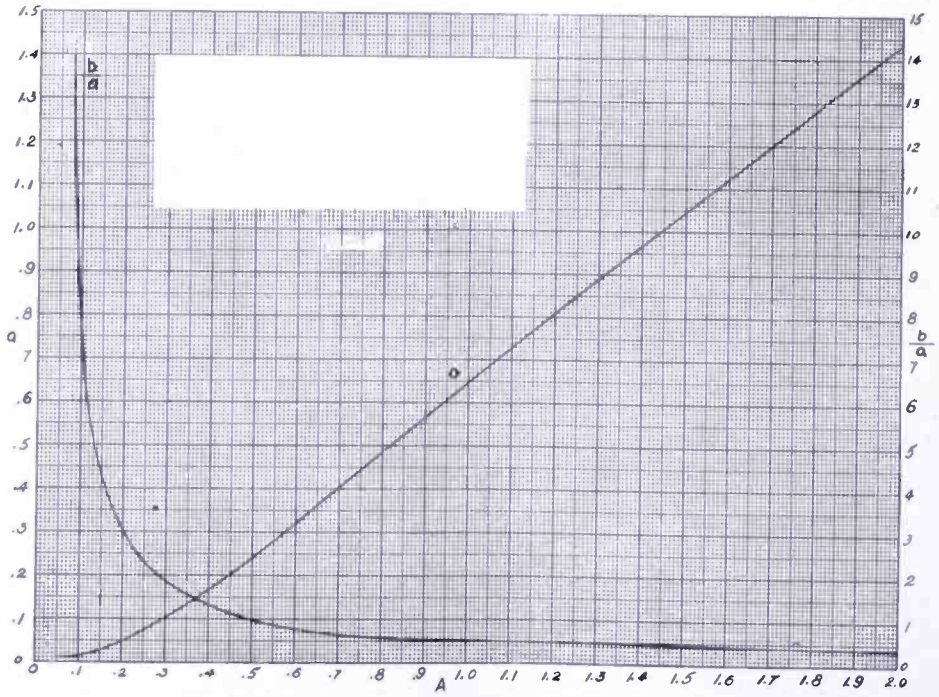

Fig. 4—Low- and high-pass filters. Values of a versus A for the maximum rate of change of attenuation.

Since the rate of attenuation in Equation (10) is fixed, it now remains only to fix the frequency at which the attenuation is the desired value. For simplicity of manipulation it is convenient to select a frequency, which will be called the cutoff frequency, at which $m=1$. If the reactances of the capacitors C_k and C_l are then made such that

X_{c_k}/R_f and X_{c_l}/R_f equal k and l respectively at this frequency, the ratio of the output voltage, e_o, to the input voltage, e_i, will be 0.70711, i.e., $e_o/e_i = 0.70711$, or $g = 0.70711\, G_o$. This of course is equivalent to the voltage attenuation of 3 decibels. The curve of Figure 5 shows the relative amplitude with frequency $(m = f/f_0)$.

As an example of specific design, suppose the cutoff frequency, f_c, is chosen as one cycle per second. Then $m = 1$ at one cycle per second. If the gain (or loss) of the filter is of no particular interest, it is convenient to make $a = b$. For these values of a and b there is only one set of values meeting the maximum rate of change of attenuation

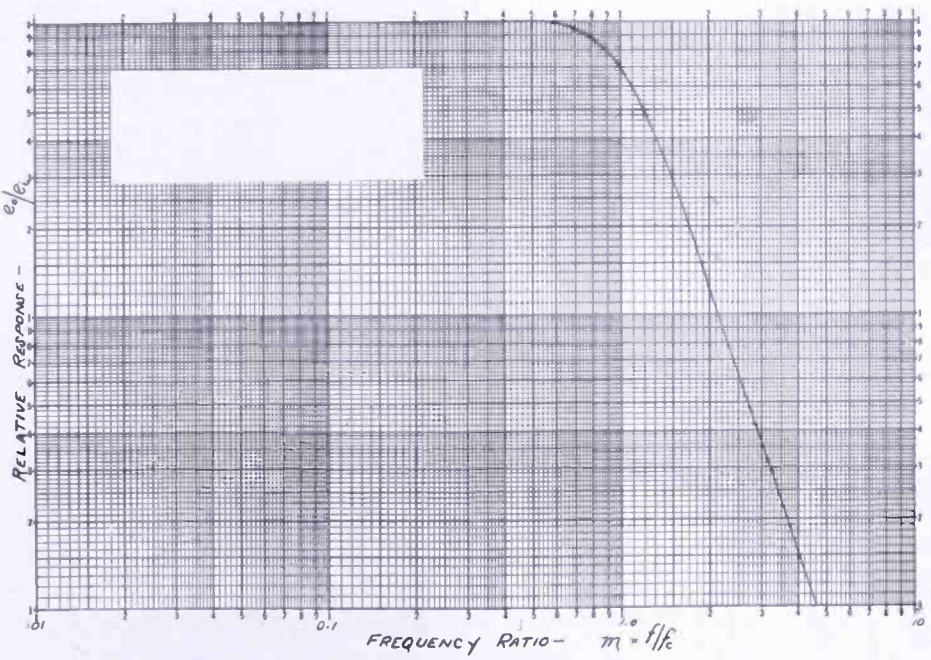

Fig. 5—Low-pass filter with maximum rate of change of attenuation, using values of a, b, k, and l from Table I.

conditions. These are (See Table I) $a = b = 0.26$, $k = 1.79863$ and $l = 0.216853$. If it is desired to use a particular one of the parameters as the reference the others are then established from it. Thus if it is convenient to make $C_l = 1$ microfarad, then at one cycle per second, $X_{c_l} = 159{,}155.1$ ohms. R_f will then be $R_f = X_{c_l}/l = 159{,}155.1/0.216853 = 733{,}931$ ohms. Also $R_a = R_b = aR_f = 0.26\,(733{,}931) = 190{,}822$ ohms and $X_{c_k} = k\,R_f = 1.79863\ (733{,}931) = 1{,}320{,}074$ ohms or $C_k = 0.120565$ microfarad. In summation then, the configuration is that of Figure 1b, a gain $g = 1/(a+b) = 1/0.53 = 1.9231$ will be obtained at 0 frequency $(m = 0)$ and the relative frequency response will be as shown in Figure 5, with the relative response at 1 cycle per second $(m = 1)$ down to 70.711 per cent and the actual response down to 0.70711

(1.9231) = 1.35984. In Figure 6 the phase angle, θ, is plotted versus the relative frequency ratio, m. This is a representative curve for any values of a, b, k and l giving the maximum rate of change of attenuation.

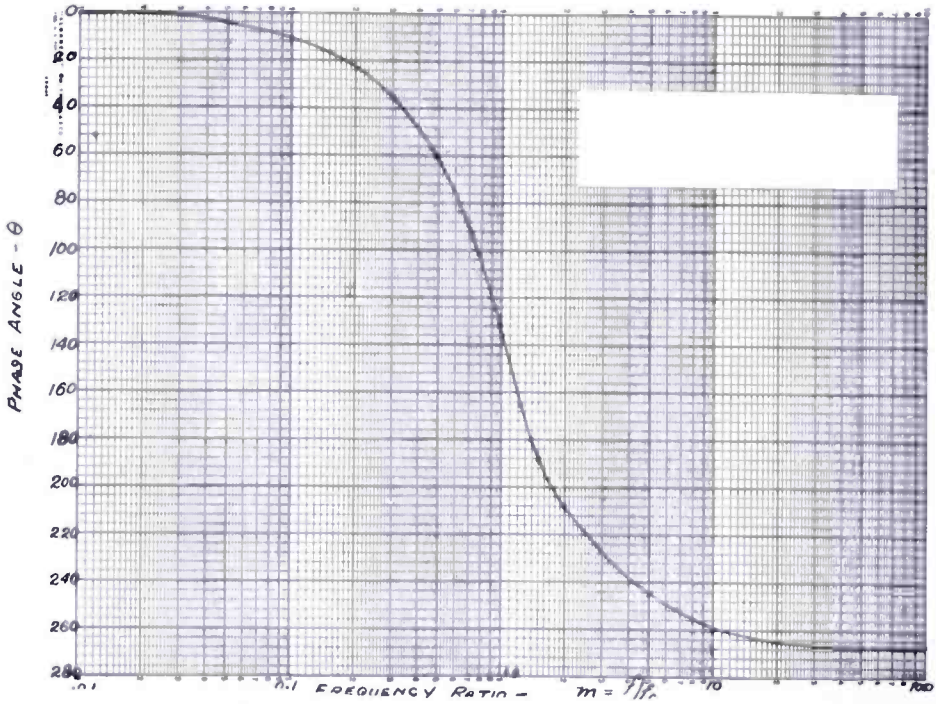

Fig. 6—Low-pass filter. Phase angle θ for maximum rate of change of attenuation.

High-Pass Filter Design Considerations

The H.P. filter design formulas may be derived at once from the L.P. ones by substituting a new variable $\mu = 1/m$ in the L.P. formulas and taking the sign of the phase relation into account. This has been done in the formulas below but the symbol m has been retained since it has the same meaning.

Thus Equation (1) for the L.P. yields, for the high-pass configuration of Figure 2, the relation

$$g = \frac{e_o}{e_i} = \frac{m^3}{m\,[-A\,m^2 + B_1] + j\,[m^2 C_1 - D_1]}, \tag{16}$$

where, as for Equation (1),

$$A = a + b, \tag{16a}$$

$$B_1 = \frac{a}{kl}[a(1+c) + (1-d)(b+c) - c^2]$$

$$+ \frac{a}{hk}[b + (1+b)(c+d)]. \tag{16b}$$

$$C_1 = \frac{a+b+(1+a+b)(c+d)}{k} + \frac{ab}{h}, \tag{16c}$$

and

$$D_1 = \frac{ad}{hkl}[(1+c)(b+c) - ac^2 d]. \tag{16d}$$

Here, however, the feedback capacitive reactance $-j/m$, (external feedback) has been taken as reference.

For the phase angle, θ, between the output voltage, e_o, and input voltage, e_i,

$$\theta = \tan^{-1} \frac{-(m^2 C_1 - D_1)}{(-Am^2 + B_1)m}. \tag{16e}$$

Similarly (3) becomes

$$g = \frac{m^3}{m[-A m^2 + B_2] + j[m^2 C_2 - D_2]}, \tag{17}$$

where, as in Equation (3),

$$A = a + b, \tag{17a}$$

$$B_2 = 2a(2A-a)/kl, \tag{17b}$$

$$C_2 = \frac{A(2+A)l + a(A-a)k}{kl}, \tag{17c}$$

and

$$D_2 = \frac{a^2(A-a)}{kl^2}[2 + (A-a)(2-a^2)]. \tag{17d}$$

However

$$\theta = \tan^{-1} \frac{-(m^2 C_2 - D_2)}{(-A_1 m^2 + B_2)m}. \tag{17e}$$

Because of the reciprocal frequency relations existing between the H.P. and L.P. filters, the same optimum parameters holding for the L.P. hold for the H.P.

Thus when Equation (17) is rationalized, it becomes

$$|g| = \frac{m^3}{\sqrt{A^2m^6 + (C_2^2 - 2AB_2)m^4 + (B_2^2 - 2C_2D_2)m^2 + D_2^2}}. \tag{18}$$

The substitution of the optimizing conditions $C_2 = B_2 = 2A$ and $D_2 = A$ into Equations (18) and (17e) yields

$$|g| = \frac{1}{A} \cdot \frac{m^3}{\sqrt{m^6 + 1}}, \tag{19}$$

and

$$\theta = \tan^{-1} \frac{(1 - 2m^2)}{m\,(2 - m^2)}. \tag{19e}$$

It is now necessary to remember only that the frequency at which $m = 1$ is selected as the low-frequency cutoff.

Thus, if the values of a, b, k and l giving optimum relation for the L.P. filter are made to be valid at a particular frequency, $m = 1$ at that frequency, and the transmission will be 70.71 per cent of the high-frequency ($f = f_\infty$) transmission where $g = 1/(a+b) = 1/A = G_\infty$.

As an example, and referring to Figure 2, let the external feedback capacitor C_f have the value of 0.1 microfarad. It will then have a reactance of 1,591,551 ohms at a cutoff frequency of 1 cycle per second, i.e., $-jX_{Cf}/m = 1{,}591{,}551$ ohms at $m = 1 = m_c$. The values of a, b, k and l are $a = b = 0.26$, $l = 0.216853$ and $k = 1.798635$ as for the L.P. filter.

Hence

$$R_l = 0.216853\ (1{,}591{,}551) = 345{,}133 \text{ ohms},$$

$$R_k = 1.798635\ (1{,}591{,}551) = 2{,}862{,}619 \text{ ohms}.$$

and

$$X_{Ca} = X_{Cb} = 0.26\ (1{,}591{,}551) = 413{,}803 \text{ ohms}.$$

Then

$$C_a = C_b = 1/\omega X_{Ca} = 1/[2\pi(1)\,413{,}803] = 0.384615 \times 10^{-6}$$

farads. In the circuit configuration of Figure 2 the response with frequency for the above example, as for any other properly related values, will be as shown in Figure 7, where it will be seen that the gain at 1 cycle per second is 0.7071 times the gain at high frequency. The actual value of the gain at f_c ($m = 1$) is $G_c = 0.7071\ [1/(a+b)] = 0.7071$

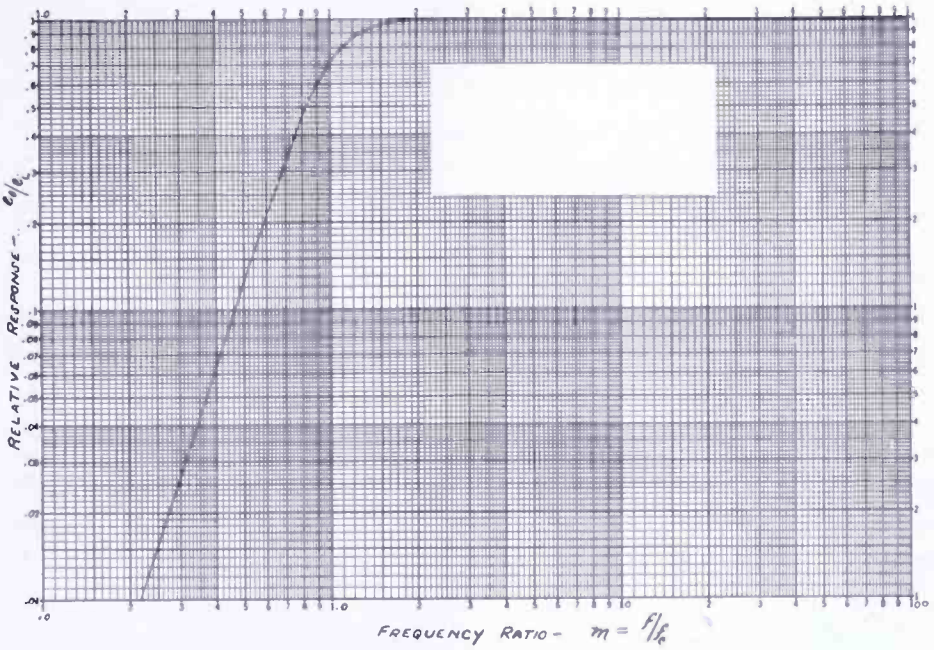

Fig. 7—High-pass filter. Maximum rate of change of attenuation using values of a, b, k, and l of Table I.

$(1/0.52) = 0.7071$ $(1.9231) = 1.3598$. In Figure 8 the phase angle θ is plotted versus the relative frequency ratio m. This is a representative curve for any values of a, b, k and l giving the maximum rate of change of attenuation.

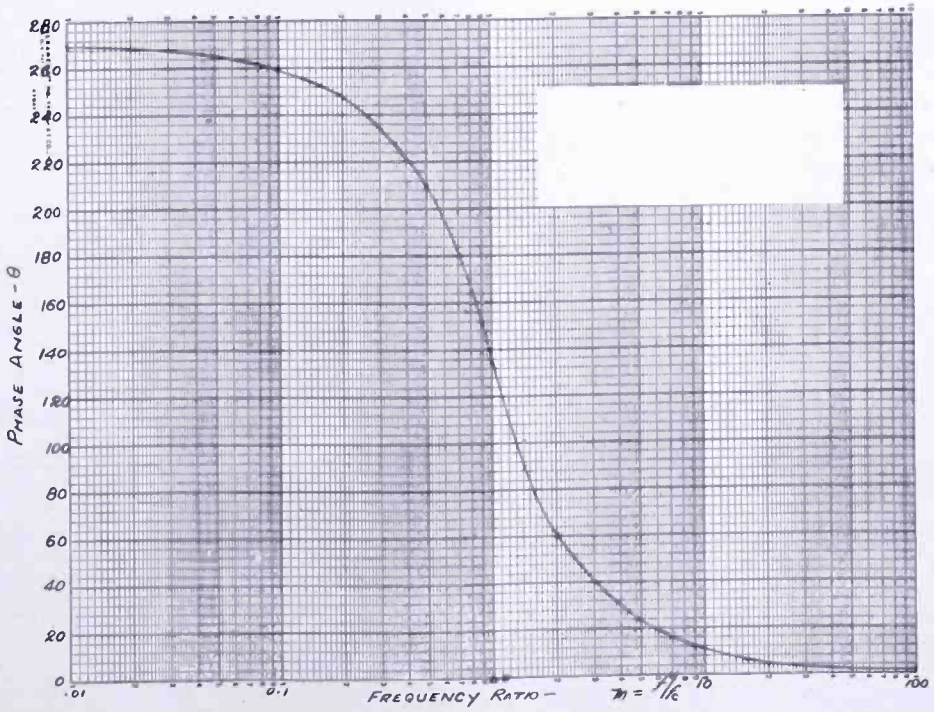

Fig. 8—High-pass filter. Phase angle θ for maximum rate of change of attenuation.

Band-Pass Filter Design Considerations

If the pass band is wide enough, a band-pass filter may be designed using the design data for the low-pass and high-pass filters. The series arms would be composed of the series arms of the component L.P. and H.P. filters and the shunt arms would consist of the shunt arms of the component L.P. and H.P. filters in parallel. In addition the component reactances of each arm would have the same value at the mid-frequency and of course the cutoff frequency of the L.P. portion would bear the same ratio to the mid-frequency as the mid-frequency would to the cutoff frequency of the H.P. portion.

However, even with a ratio of cutoff frequencies as large as 100 to 1, there is some interaction which prevents the obtaining of as great a rate of change of attenuation as for each of the component filters, and bars a clean cut definition of the pass band. Moreover, this interaction is not subject to simple analysis.

For these reasons an independent solution was obtained for the band-pass configuration. This configuration, however, was retained in the form of the L.P. and H.P. combination, and the same parameter designation a, b, k and l was used. (See Figure 3.) It was then possible to compare the results with the ideal case of cascaded L.P. and H.P. filters where there would be no interaction. The relationship between parameters necessary to obtain the exact pass band, and to obtain the same optimum rate of change of attenuation as obtained with the separate optimized L.P. and H.P. filters, was then found.

For the circuit of Figure 3, as determined* directly from the determinants of the equations for this configuration,

$$g = \frac{e_o}{e_i} = \frac{-kl^2 m^3 (m-j)}{\alpha - \beta m^2 + \gamma m^4 - \delta m^6 - jm(\alpha m^6 - \beta m^4 + \gamma m^2 - \delta)}, \tag{20}$$

where

$$\alpha = a^2 b (b+2), \tag{20a}$$

$$\beta = 21\alpha + 10\lambda + \phi, \tag{20b}$$

$$\gamma = 35\alpha + 20\lambda + 3\phi + kl^2 (a+b), \tag{20c}$$

$$\delta = 7\alpha + 2\lambda, \tag{20d}$$

$$\lambda = al[a(b+1) + b(b+2)], \tag{20e}$$

and

$$\phi = l^2 (a+b)(a+b+2) + abkl. \tag{20f}$$

* See Appendix II.

Equation (20) may be rewritten**

$$g = \frac{kl^2m^3}{m\,[(m^4+1)\,(\delta-\alpha) + m^2(\alpha+\beta-\gamma-\delta)\,]}$$

$$+ j(m^2-1)\,\{\alpha(m^4+1) + m^2(\delta-\beta)\,\}} \qquad (21)$$

$$\text{Then } \theta = \tan^{-1}\frac{-(m^2-1)\,\{\alpha(m^4+1) + m^2(\delta-\beta)\,\}}{m\,[m^4+1)\;\;(\delta-\alpha) + m^2\;(\alpha+\beta-\gamma-\delta)\,]}. \qquad (22)$$

Equations (21) and (22) then apply for all values of the parameters.

It was desired, however, as stated above, to obtain for this band-pass case the conditions which would give the same maximum rate of change of attenuation at each end of the pass band as obtained indi-

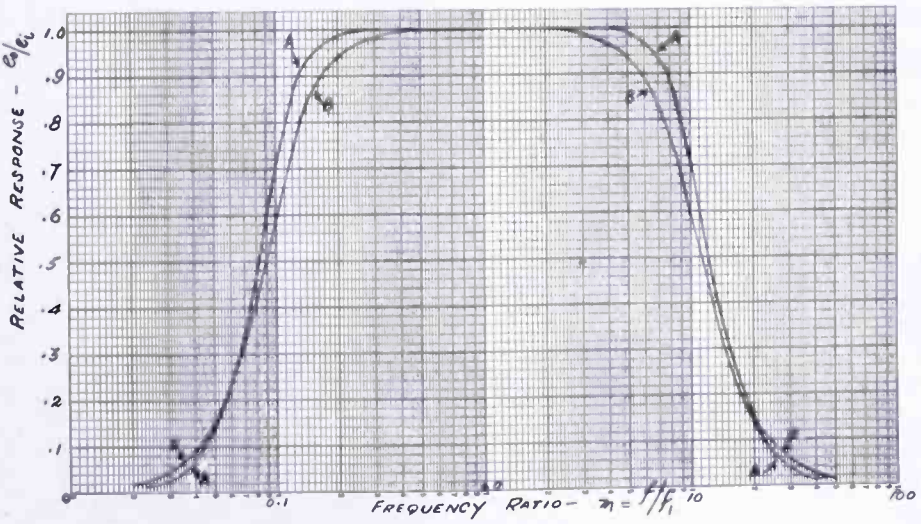

Fig. 9—Band-pass filters. Curve A: Direct band pass optimum derivation; $\sigma^2 = 100$. Curve B: Composite filter of L.P. and H.P. optimum design; $\sigma^2 = 100$ nominal.

vidually near cutoff frequencies in the L.P. and H.P. cases. Before the manner in which this was done is described, however, an example will be given showing the effect of interaction when it is attempted to form directly a B.P. filter based on parameters calculated for the individual cases of L.P. and H.P. filters for the maximum rate of change of attenuation. Curve B of Figure 9 shows the results of the composite case of combined L.P. and H.P. filter elements. (Configuration Figure 3; $a = b = 0.26$, $k = 1.798635$ and $l = 0.2168529$.) The cutoff frequency for the separate L.P. filter was one cycle per second

** See Appendix III.

and that for the H.P. filter was 0.01 cycle per second; the cutoff frequency ratio was therefore equal to 100. The curve shape that might be expected with no interaction is shown as Curve A on Figure 9. This is the band-pass curve desired.

Curve B was experimentally obtained and mathematically checked by Equation (20) ($a=b=0.26$, $k=17.98635$, $l=2.168529$ for $m=1$ at 0.1 cycle per second). The experimental check at these low frequencies was made by means of a special sine-wave generator.

If Equation (20) has the potentiality of providing the desired curve shape of Curve A when the proper relations are known, then it is clear how these conditions may be obtained. For if L.P. and H.P. configurations are theoretically combined to form a B.P. filter without interaction, a formula* will result for the optimum conditions which will disclose the nature of the optimum relations necessary for inclusion in the general formula, Equation (20). Practically, such a combination, if one were necessary, could take the not uncommon form of a cascaded amplifier where the L.P. filter section would be isolated from the H.P. filter section by an amplifier. A general unoptimized formula could be obtained in the same manner but would be no more amenable, presumably, to simple analysis than Equation (20).

However, only the optimized relationship is generally required and this relation is**

$$g=\frac{kl^2}{a^2b\,(b+2)}\cdot\frac{\sigma^3m^3}{(\sigma^2+1)\,m\,\{2\sigma^2(m^4+1)-m^2(\sigma^4+3\sigma^2+1)\}}$$

$$\frac{}{+j\sigma(m^2-1)\,\{\sigma^2(m^4+1)-m^2[2(\sigma^4+1)+3\sigma^2]\}}, \tag{23}$$

giving the phase angle

$$\theta=\tan^{-1}\frac{-\sigma(m^2-1)\,\{m^2[2(\sigma^4+1)+3\sigma^2]-\sigma^2(m^2+1)\}}{(\sigma^2+1)\,m\,\{m^2(\sigma^4+1+3\sigma^2)-2\sigma^2(m^4+1)\}}. \tag{24}$$

When Equation (23) is rationalized,†

$$|g|=\frac{kl^2}{a^2b\,(b+2)}\cdot\frac{1}{\sqrt{m^6+\sigma^6+m^{-6}+\sigma^{-6}}}, \tag{25}$$

* See Appendix IV.
** See Appendix V.
† See Appendix V.

where

b is determined from the relation

$$b(b+2)^2 + \frac{H_1 F^3}{H_2^3 H_4^2 (H_4+2)} = \frac{H_3 (b+2) F^2}{H_2^2 H_4 (H_4+2)}, \tag{26}$$

$$H_1 = (\sigma^6 - 4\sigma^5 + 8\sigma^4 - 10\sigma^3 + 8\sigma^2 - 4\sigma + 1)/\sigma^3$$
$$= \sigma^3 - 4\sigma^2 + 8\sigma - 10 + 8\sigma^{-1} - 4\sigma^{-2} + \sigma^{-3}, \tag{27}$$

$$H_2 = (\sigma^2 - 3\sigma + 1)/\sigma = \sigma - 3 + \sigma^{-1}, \tag{28}$$

$$H_3 = (2\sigma^4 - 8\sigma^3 + 13\sigma^2 - 8\sigma + 2)/\sigma^2$$
$$= 2\sigma^2 - 8\sigma + 13 - 8\sigma^{-1} + 2\sigma^{-2}, \tag{29}$$

$$H_4 = H_1/G_1 \sqrt{2 + \sigma^6 + \sigma^{-6}}, \tag{30}$$

G_1 = filter gain desired at $m = 1$,

σ^2 = band width, ratio of the cutoff frequencies f_{c_1} to f_{c_2},

and $$F = (H_4 - b)(b+1) + b(b+2). \tag{31}$$

Since $$a = H_4 - b, \tag{32}$$

and $$\alpha = a^2 b (b+2),$$

then $$l = \frac{\alpha H_2}{aF}, \tag{33}$$

and $$k = \frac{\alpha H_1}{l^2 (a+b)}. \tag{34}$$

Thus the independent parameters selected are the band width, σ^2, and the gain, G_1, desired for the filter at the frequency for which $m = 1$, i.e., the midband frequency, f_1. The factors H_1, H_2, H_3 and H_4 may then be computed. Equation (26) now becomes an equation in which b is the only variable. Finding a real value of b which will satisfy both sides of this equation constitutes most of the labor of the computation. Any one of a number of methods may be used. The values herein obtained were computed by finding roughly the intersection of the plots of the right and left sides of Equation (26) and narrowing down the value to at least four places.

As an example of the procedure, take the case where a band width $\sigma^2 = 100$ is desired and the gain is taken as $G_1 = 1$. Then

$$H_1 = 670.761,$$

$$H_2 = 7.1,$$

$$H_3 = 132.22,$$

and $$H_4 = \frac{670.761}{1\sqrt{1{,}000{,}002}} = \frac{670.761}{1000.001} = 0.6707603.$$

Then $F = 0.67076\,(b+1) + b(b+2)$,

$$\frac{H_1}{H_2^3 H_4^2 (H_4+2)} = \frac{670.7603}{(7.1)^3\,(0.6707603)^2\,(2.67076)}$$

$$= \frac{1000}{(7.1)^3\,(.6707603)\,(2.67076)},$$

$$= \frac{1000}{357.911\,(.670761)\,(2.670761)} = \frac{1000}{240.0727\,(2.67076)},$$

$$= 1000/641.1769,$$

$$= 1.559631.$$

$$\frac{H_3}{H_2^2 H_4\,(H_4+2)} = \frac{132.22}{(7.1)^2\,(.6707603)\,(2.6707603)}$$

$$= \frac{132.22}{50.41\,(1.79144232)} = \frac{132.22}{90.3066},$$

$$= 1.464123.$$

In order to obtain b, these values are substituted in Equation (26) giving

$$b\,(b+2)^2 + 1.559631\,F^3 = 1.464123\,(b+2)\,F^2.$$

Trial values of b indicate that a value of b which will satisfy Equation (26) falls between $b = 0.5$ and $b = 0.4$. The value of b must

be less than 0.67076 to make a real. The right hand side of Equation (26) gives 8.0303 + and 6.300 + respectively for these values of b and the left hand side the respective values of 8.4536 + and 6.0487 +. Plotting these values versus b, as straight lines, indicates a value of $b = 0.47$. This turns out to be slightly high; plotting the values obtained for the value of b gives a more accurate curve intersection and now indicates a value of $b = 0.465$. This value of b indicates a final value which is taken as $b = 0.4665$. This gives a difference only in the fifth place.

Using $b = 0.4665$, $a = H_4 - b = 0.67076 - 0.4665 = 0.20426$.

Then $\alpha = a^2 b(b+2) = 0.048007$,

$l = \alpha H_2 / aF = 1.150687$,

and $k = \alpha H_1 / l^2 (a+b) = 36.25676$.

Checking the gain at $m = 1$, $|G_1| = \dfrac{kl^2}{\sigma^3 \alpha} = \dfrac{48.0069}{10^3\ (.0480069)} = 1$. For the values a, b, k and l given above, and with $\sigma^2 = 100$ and $G_1 = 1$, Equation (25) becomes

$$|g| = \frac{1}{\sqrt{m^6 + 10^6 + m^{-6} + 10^{-6}}},$$

$$= \frac{1}{\sqrt{m^6 + m^{-6} + 10^6}}.$$

Curve A of Figure 9 or that for $\sigma = 10$ of Figure 11 shows a plot of this equation.

In applying the above findings to the evaluation of the constants of the B.P. configuration, it is only necessary to choose the mid-band frequency for which $m = 1$, fix one of the impedances of the circuit and compute the others, maintaining the ratios a, b, k and l.

Suppose the mid-band frequency is chosen as 0.1 cycle per second. The pass band is then from 0.01 to 1 cycle per second for $\sigma^2 = 100$. The relative response and the actual response are the same for $G_1 = 1$; at the cutoff frequencies 0.01 and 1 cycle per second these will have the value 0.7071. If the external feedback resistor is chosen arbitrarily as one megohm, the external feedback capacitor, C_f, will be adjusted to have a reactance value of one megohm also at 0.1 cycle per second.

Similarly the values of the reactances of C_a, C_b, C_k and C_l will be adjusted to have values of a, b, k, and l times respectively that of C_f, or 204,261, 466,500, 36,256,760 and 1,150,690 ohms at 0.1 cycle per second. Also the values of R_a, R_b, R_k and R_l will have the respective resistance values of 204,260, 466,500, 36,256,760 and 1,150,690 ohms. The circuit configuration for any pass band and gain will, of course, be that of Figure 3.

For values of $G_1 = 1.0$ and $G_1 = 2.0$ the values of b, a, k and l have been calculated for some widely different values of pass-band ratios σ^2. The values of b obtained have been plotted against σ^2 in Figure 10. It should be immediately noted that the curve is indicative only since the accuracy of the plot is insufficient for the accuracy of the calculations. Accurate values of b as well as a, k, l and α are given in Table

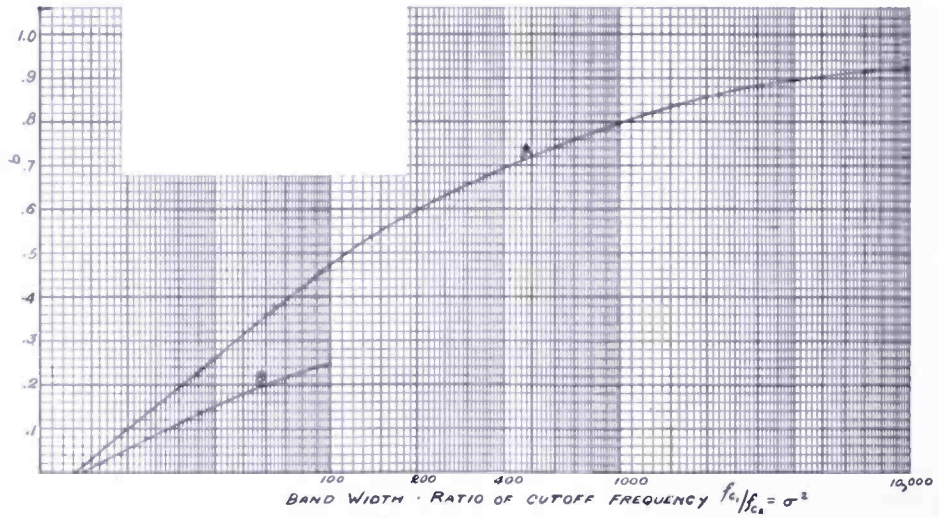

Fig. 10—Band-pass filter. Values of b giving maximum rate of change of attenuation for different band widths. Curve A; $G_1 = 1.0$. Curve B; $G_1 = 2.0$.

II for the corresponding values of σ^2. For other values of σ^2 the curves of Figure 10 serve as a guide to the approximate values; exact values should be calculated by means of Equations (26) to (31). It will be noted that σ^2 can be decreased slightly below 16 and still maintain the usually desired maximum rate of change of attenuation. In Figure 11 have been plotted the lower halves of the symmetrical pass bands of optimum attenuation for the band-width ratios $\sigma^2 = 16$, 100, 1000 and 10,000 or $\sigma = 4$, 10, $\sqrt{1000}$ and 100. Here $G_1 = 1.0$ so the actual and relative response are the same. Equation (25) was used with values obtained from Table II.

For any values of a, b, k and l giving this optimum rate of attenuation for a given pass band σ^2, the phase angle between the output and

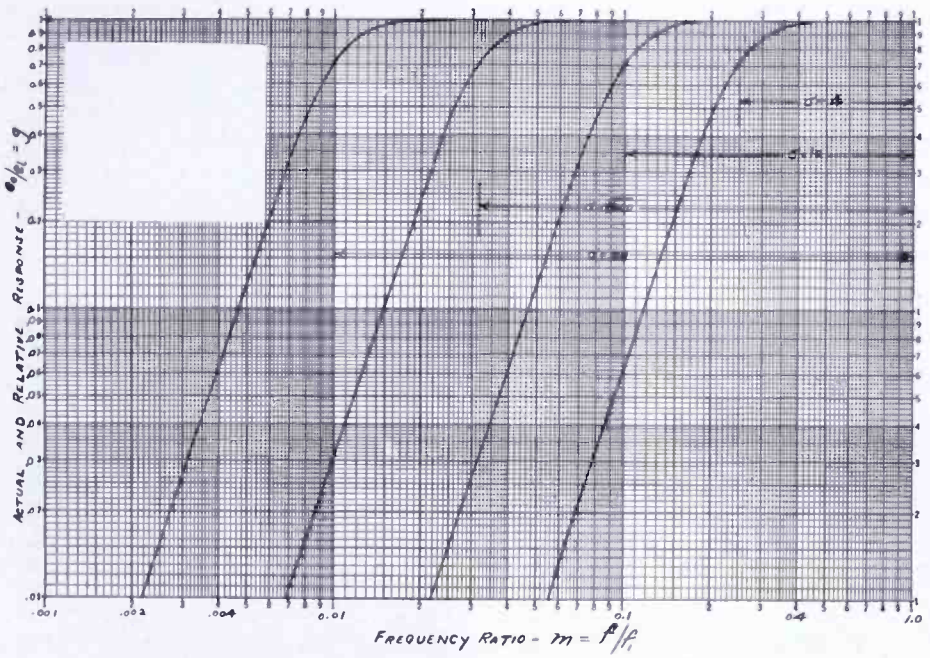

Fig. 11—Band-pass filter. Lower half of pass band for four values of σ. $G_1 = 1.0$.

input voltages may be computed using Equation (24). Thus for $\sigma^2 = 100$, the phase angle θ is that plotted in Figure 12.

Table II — Band-Pass Filters.

Values of parameters giving maximum rate of attenuation for different pass-band ratios σ^2.

σ^2	b	a	l	k	α
			$G_1 = 1.0$		
16	0.03535	0.335897	0.0719755	100.3133	0.008117858
36	0.23832	0.276608	0.533412	30.98489	0.04081431
64	0.37225	0.23505131	0.8823513	32.08552	0.0487888
100	0.4665	0.204261	1.150687	36.25676	0.480069
1000	0.79801	0.08319052	2.234112	97.90288	0.01545273
10000	0.93218	0.02861	2.687202	306.0464	0.00221
			$G_1 = 2.0$		
16	0.019054	0.1665696	0.0384706	92.338712	0.001067396
36	0.12612	0.1313440	0.2680608	27.81115	0.00462586
100	0.2425	0.0928805	0.5440042	31.70398	0.00469125

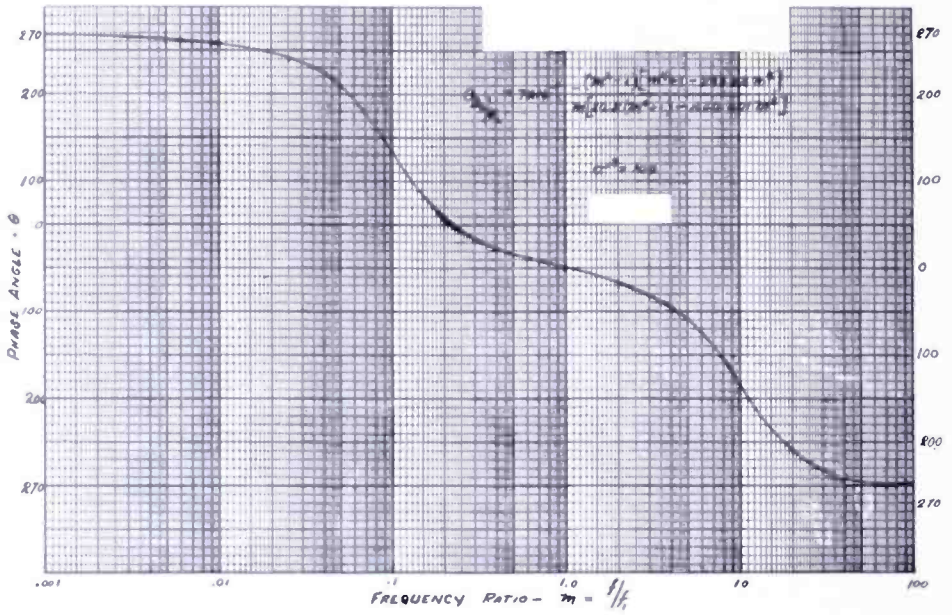

Fig. 12—Band-pass filter. Phase angle θ for maximum rate of change of attenuation. $\sigma^2 = 100$.

Departure from Conditions of Maximum Rate of Change of Attenuation

When a rate of change of attenuation other than the maximum is desired, an infinite variety of curves may be obtained for the L.P., H.P. or B.P. types. No criteria have been developed for obtaining a certain curve shape but large significant trends may be plotted and interpolation attempted. This method is illustrated by the curves of Figures 13 and 14 for the L.P. Filter. The H.P. counterparts are plotted in Figures 15 and 16. Thus decreasing l or increasing k gives a rise in relative response as the cutoff frequency is approached. The pass band however is narrowed in the former case and widened in the latter since in the first instance the shunt arm impedance is decreased and in the second the impedance of the internal feedback path is raised. Increasing l or decreasing k has contrariwise effect. It will be noted that relatively small decreases in k are necessary to obtain relatively flat curves such as (f) and (g); they are nowise equivalent however.

Except for frequency inversion, curves of the same shape are obtained for the H.P. case as for the L.P. for the same values of k and l. Figures 15 and 16 illustrate this point.

For the band-pass case, shapes similar to those obtained for the L.P. and H.P. cases will be obtained with variations of k and l, but the variations will appear symmetrically in the neighborhood of both the cutoff frequencies.

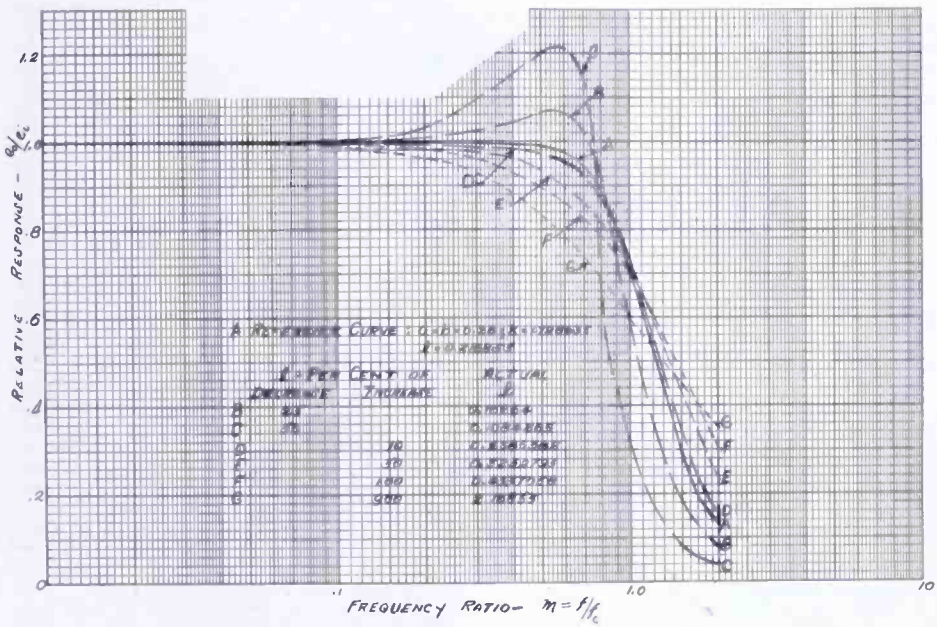

Fig. 13—Low-pass filter. Relative response with different values of l.

Curve A: Reference curve (a=b=0.26; k=1.798635; l=0.216853)

Curve	Increase in l (per cent)	l	Curve	Increase in l (per cent)	l
B	—25	0.16264	E	50	0.3252793
C	—50	0.1084265	F	100	0.4337058
D	10	0.2385382	G	900	2.16853

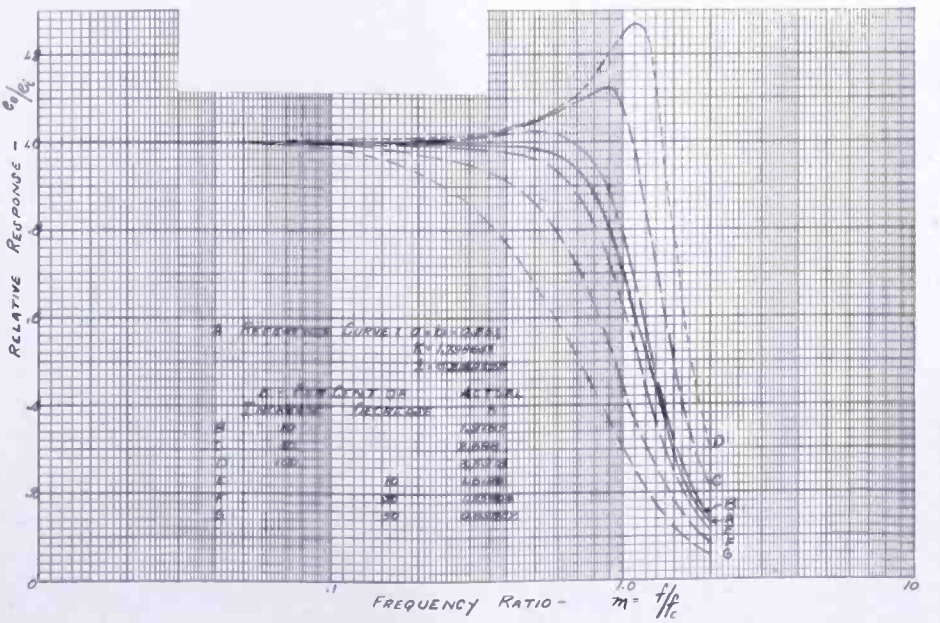

Fig. 14—Low-pass filter. Relative response with different values of k.

Curve A: Reference curve (a=b=0.26; k=1.798635; l=0.2168529)

Curve	Increase in k (per cent)	k	Curve	Increase in k (per cent)	k
B	10	1.9785	E	—10	1.6188
C	50	2.698	F	—30	1.25904
D	100	3.5973	G	—50	0.89932

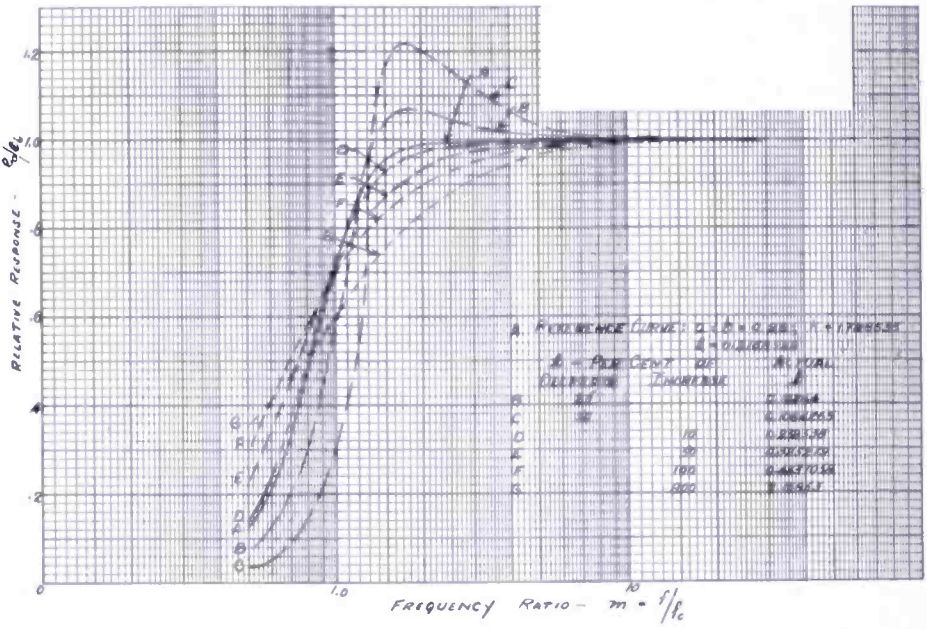

Fig. 15—High-pass filter. Relative response with different values of l.

Curve A: Reference curve (a=b=0.26; k=1.798635; l=0.2168529)

Curve	Increase in l (per cent)	l	Curve	Increase in l (per cent)	l
B	—25	0.16264	E	50	0.325279
C	—50	0.1084265	F	100	0.4337058
D	10	0.238538	G	900	2.16853

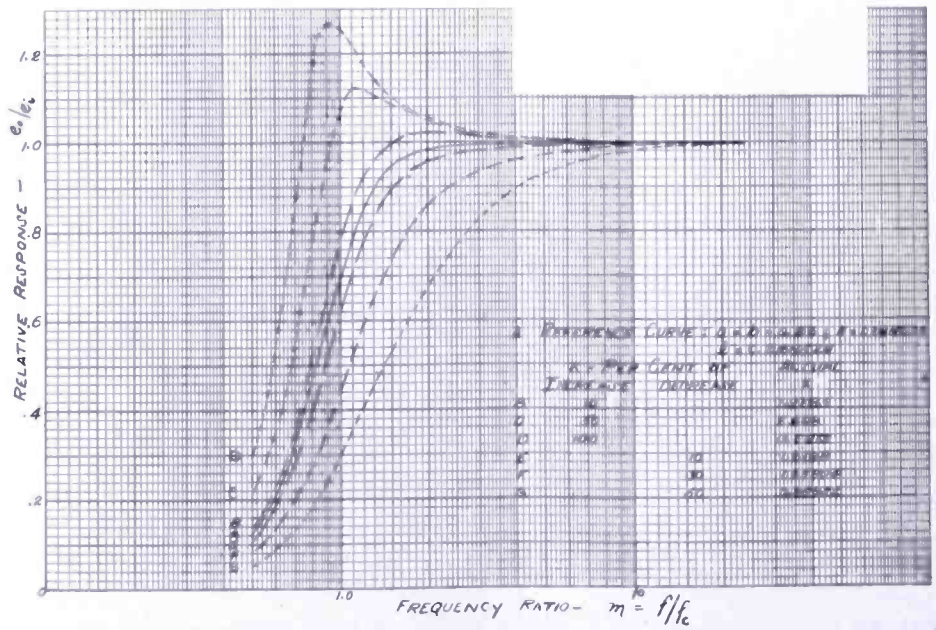

Fig. 16—High-pass filter. Relative response with different values of k.

Curve A: Reference curve (a=b=0.26; k=1.798635; l=0.2168529)

Curve	Increase in k (per cent)	k	Curve	Increase in k (per cent)	k
B	10	1.9785	E	—10	1.6188
C	50	2.698	F	—30	1.25904
D	100	3.5973	G	—50	0.89932

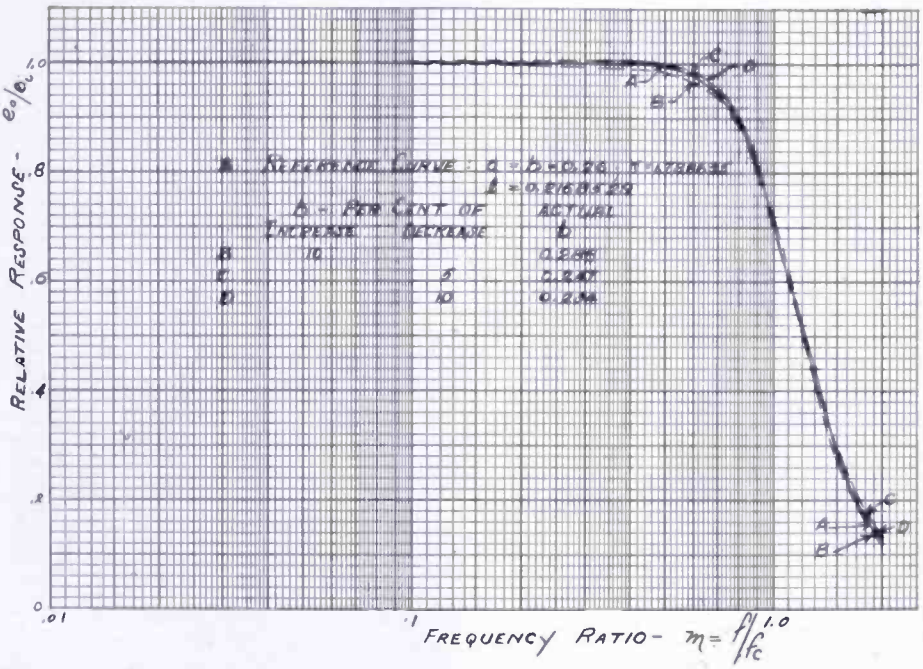

Fig. 17—Low-pass filter. Relative response with different values of b.

Curve A: Reference curve (a=b=0.26; k=1.798635; l=0.2168529)

Curve	Increase in b (per cent)	b
B	10	0.286
C	—5	0.247
D	—10	0.234

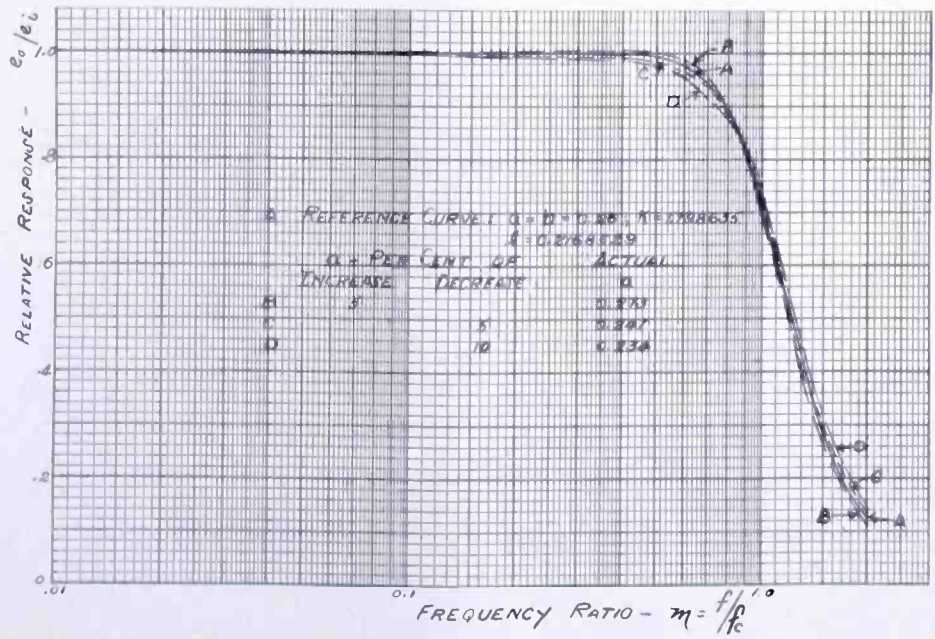

Fig. 18—Low-pass filter. Relative response with different values of a.

Curve A: Reference curve (a=b=0.26; k=1.798635; l=0.2168529)

Curve	Increase in a (per cent)	a
B	5	0.273
C	—5	0.247
D	—10	0.234

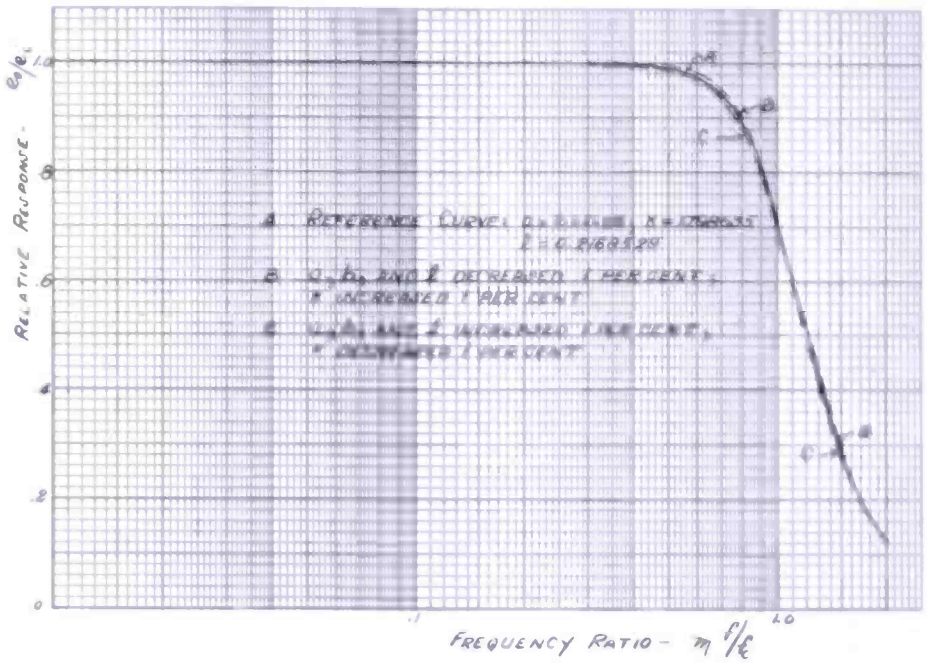

Fig. 19 — Low-pass filter. Curve A: Reference curve (a=b=0.26; k=1.798635; l=0.2168529). Curve B: a, b, and l decreased 1 per cent; k increased 1 per cent. Curve C: a, b, and l increased 1 per cent; k decreased 1 per cent.

Another factor of interest is the error involved in departure from the values of computed constants. While all constants should be computed accurately, once all of them are determined slight departure in the practical application of any one of them may not be serious. Figures 13 and 14 show the variation of curve shape with 10 per cent change in the value of l and k for the L.P. filter. Figure 17 shows curves for the L.P. filter in which the constant b has been varied up to ±10 per cent. In Figure 18, a has been varied from −10 to +5 per cent. It is seen that the relative seriousness of any departure from the ideal response curve would depend on the individual application and the actual adjustments of all circuit constants. Figure 19 shows curves for the L.P. case computed with all constants changed one per cent in the direction which causes a decrease or increase in the resultant response curve at certain intervals. Thus for curve (C) a, b and l have been increased and k has been decreased one per cent. This results primarily in a lowered cutoff frequency. Decreasing a, b, and l and increasing k one per cent extends the cutoff frequency slightly, as shown in curve (B) Figure 19. At frequencies more remote from the cutoff frequency, the slight rise in response due to decrease in b, as illustrated by curves (C) and (D) of Figure 17, is compensated for by the decrease in a. The rise in this interval would apparently be accentuated by an increase in the value of a.

APPENDIX I

From values of B_2 in Equations (3b) and (9),

$$2A = \frac{2a\,(2A-a)}{kl},$$

or

$$k = \frac{a\,(2A-a)}{Al}. \tag{14}$$

From values of C_2 in Equations (3c) and (9),

$$2A = \frac{A\,(2+A)\,l + a\,(A-a)\,k}{kl},$$

or

$$2Akl - A\,(2+A)\,l - a\,(A-a)\,k = 0. \tag{I_1}$$

Substituting values of k from (14) in (I_1),

$$\frac{2Al\,a\,(2A-a)}{Al} - A\,(2+A)\,l - \frac{a\,(A-a)\,a\,(2A-a)}{Al} = 0,$$

or

$$2aA\,(2A-a)\,l - A\,(2+A)\,l^2 - a^2\,(A-a)\,(2A-a) = 0. \tag{I_2}$$

From values of D_2 in Equations (3d) and (10),

$$A = \frac{a^2\,(A-a)}{kl^2}\,[2 + (A-a)\,(2-a^2)],$$

or

$$kl^2A - a^2\,(A-a)\,[2 + (A-a)\,(2-a^2)] = 0, \tag{I_3}$$

Substituting the value of k from (14) in (I_3),

$$\frac{l^2Aa\,(2A-a)}{Al} - a^2\,(A-a)\,[2 + (A-a)\,(2-a^2)] = 0,$$

or

$$l = \frac{a\,(A-a)\,[2 + (A-a)\,(2-a^2)]}{2A-a}. \tag{15}$$

Substituting value of l from Equation (15) in (I_2),

$$\frac{2aA(2A-a)a(A-a)[2+(A-a)(2-a^2)]}{2A-a}$$

$$-\frac{A^2(2+A)a^2(A-a)^2[2+(A-a)(2-a^2)]^2}{(2A-a)^2}-a^2(A-a)(2A-a)=0,$$

or

$$2A(2A-a)^2[2+(A-a)(2-a^2)]$$

$$-A^2(2+A)(A-a)[2+(A-a)(2-a^2)]^2-(2A-a)^3=0. \qquad (12)$$

Appendix II

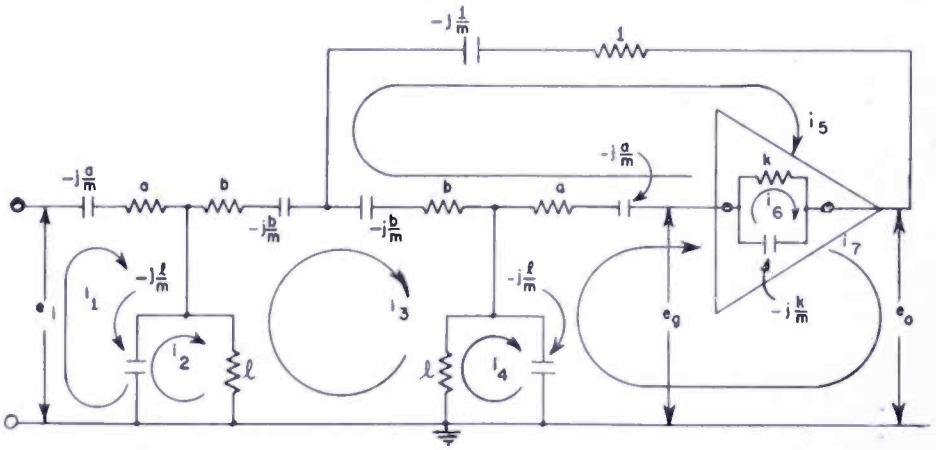

$$e_g=e_i-i_1\,a\left(1-\frac{j}{m}\right)-i_3\,2b\left(1-\frac{j}{m}\right)+i_5\,(a+b)\left(1-\frac{j}{m}\right)$$

$$-i_7\,a\left(1-\frac{j}{m}\right)=e_i-\left(1-\frac{j}{m}\right)\{ai_1+2bi_3-(a+b)\,i_5+ai_7\}.$$

But $i_1=\dfrac{e_id_1}{\Delta}-\dfrac{e_od_1'}{\Delta}$; $i^3=\dfrac{1}{\Delta}\{e_id_3-e_od_3'\}$;

$$i_5=\frac{1}{\Delta}\{e_id_5-e_od_5'\} \text{ and } i_7=\frac{1}{\Delta}\{e_id_7-e_od_7'\},$$

where Δ is the determinant of the system and d_1, d_1', d_3, d_3', etc. are minors.

$$\text{Then } e_g = e_i - \frac{e_i}{\Delta}\left(1-\frac{j}{m}\right)\{a\,d_1 + 2b\,d_3 - (a+b)\,d_5 + a\,d_7\}$$

$$+\frac{e_o}{\Delta}\left(1-\frac{j}{m}\right)\{a d_1' + 2b\,d_3' - (a+b)\,d_5' + a d_7'\}.$$

$$\text{Letting } K_1 = \frac{1}{\Delta}\left(1-\frac{j}{m}\right)\{a\,d_1 + 2b\,d_3 - (a+b)\,d_5 + a\,d_7\},$$

$$K_2 = \frac{1}{\Delta}\left(1-\frac{j}{m}\right)\{a\,d_1' + 2b\,d_3' - (a+b)\,d_5' + a\,d_7'\}$$

and $e_g = e_o/\mu$ since it is stipulated that $\mu\, e_g = -e_o$ where μ is the amplification factor of the amplifier without feedback;

$$\text{then } e_o\left[-\frac{1}{\mu} - K_2\right] = e_i\,[1-K_1] \text{ or } e_o\left[\frac{-1-\mu K_2}{\mu}\right] = \frac{\mu\, e_i\,[-1-K_1]}{\mu}.$$

$$\text{Hence } \frac{e_o}{e_i} = \frac{\mu\,[1-K_1]}{-1-\mu K_2}.$$

If $\mu \gg 1$, so that $\mu K_2 \gg 1$,

$$\text{then } \frac{e_o}{e_i} = \frac{1-K_1}{-K_2} = \frac{\Delta - \left(1-\frac{j}{m}\right)[a\,d_1 + 2b\,d_3 - (a+b)\,d_5 + a\,d_7]}{-\left(1-\frac{j}{m}\right)[a\,d_1' + 2b\,d_3' - (a+b)\,d_5' + a\,d_7']}.$$

Appendix III

Multiplying the numerator and denominator of Equation (20) by $(m+j)$,

$$g = \frac{-kl^2 m^3 (m^2+1)}{m\,[\alpha - \beta m^2 + \gamma m^4 - \delta m^6] - j m^2\,[\alpha m^6 - \beta m^4 + \gamma m^2 - \delta]}$$

$$+ j\,[\alpha - \beta m^2 + \gamma m^4 - \delta m^6] + m\,[\alpha m^6 - \beta m^4 + \gamma m^2 - \delta]$$

Regrouping and factoring out the term $-(m^2+1)$,

$$g = \frac{kl^2 m^3}{m\left[(m^4+1)(\delta-\alpha)+m^2(\alpha+\beta-\gamma-\delta)\right] + j(m^2-1)\left[\alpha(m^4+1)+m^2(\delta-\beta)\right]}. \qquad (III_1)\ (21)$$

Appendix IV

Appendix IV is a derivation of the band-pass filter formula in terms of the band width, using optimized L.P. and H.P. filters in cascade, for comparison with the general formula, Equation (21).

For the L.P. filter, let $m = m_1 = \omega/\omega_{01} = f/f_{01}$ where $f =$ any frequency and f_{01} is the cutoff frequency. Then, when the optimum conditions that $B_2 = C_2 = 2A$ and $D_2 = A$ are substituted, Equation (3) becomes

$$g_1 = \frac{1}{A} \cdot \frac{1}{2m_1^2 - 1 - j(2m_1 - m_1^3)}. \qquad (IV_1)$$

For the H.P. filter, let $m = m_2 = \omega/\omega_{02} = f/f_{02}$ where $f =$ any frequency and f_{02} is the cutoff frequency. Then, when the optimum conditions that $B_2 = C_2 = 2A$ and $D_2 = A$ are substituted, Equation (18) becomes

$$g_2 = \frac{1}{A} \cdot \frac{m_2^3}{2m_2 - m_2^3 + j(2m_2^2 - 1)}. \qquad (IV_2)$$

For the cascaded B.P. form, the product of Equations (IV_1) and (IV_2) will be

$$g_1 g_2 = \frac{1}{A^2} \cdot \frac{m_2^3}{(2m_1^2-1)(2m_2 - m_2^3) + (2m_1 - m_1^3)(2m_2^2 - 1) + j\{(2m_1^2-1)(2m_2^2-1) - (2m_2 - m_2^3)(2m_1 - m_1^3)\}},$$

$$= \frac{1}{A^2} \cdot \frac{m_2^3}{4m_1^2 m_2 - 2m_1^2 m_2^3 - 2m_2 + m_2^3 + 4m_1 m_2^2 - 2m_1 - 2m_1^3 m_2^2 + m_1^3 + j\{4m_1^2 m_2^2 - 2m_1^2 - 2m_2^2 + 1 - 4m_1 m_2 + 2m_1^3 m_2 + 2m_1 m_2^3 - m_1^3 m_2^3\}}. \qquad (IV_3)$$

Now let $\omega_{01}/\omega_{02} = f_{01}/f_{02} = \sigma^2$ and m

$= \sqrt{m_1 m_2}$ where σ^2 is the band width.

Then $m = \sqrt{\frac{f}{f_{01}} \cdot \frac{f}{f_{02}}} = f/\sqrt{\sigma^2 f_{02}^2} = f/\sigma f_{02} = m_2/\sigma$

or $\quad m = f/\sqrt{f_{01}^2 \sigma^2} = \sigma f/f_{01} = \sigma m_1$

and $m_1 = m/\sigma$ and $m_2 = m\sigma$. Hence

$$g_1 g_2 = \frac{1}{A^2} \cdot \frac{m^3\sigma^3}{4m^2m\sigma^{-1} - 2m^4m\sigma - 2m\sigma + m^3\sigma^3 + 4m^2m\sigma}$$

$$\frac{}{- 2m\sigma^{-1} - 2m^4m\sigma^{-1} + m^3\sigma^{-3} + j\{4m^4 - 2m^2\sigma^{-2}}$$

$$\frac{}{- 2m^2\sigma^2 + 1 - 4m^2 + 2m^2m^2\sigma^{-2} + 2m^2m^2\sigma^2 - m^6\}}.$$

Multiplying numerator and denominator by σ^3 and regrouping,

$$g_1 g_2 = \frac{1}{A^2} \cdot \frac{m^3\sigma^6}{m\{(m^4+1)(-2\sigma^2)(\sigma^2+1) + m^2[\sigma^6 + 4\sigma^2(\sigma^2+1) + 1]\}}$$

$$\frac{}{+ j(m^2-1)\{-\sigma^3(m^4+1) + m^2(2\sigma + 3\sigma^3 + 2\sigma^5)\}} \qquad (IV_4)$$

$$g_1 g_2 = \frac{1}{A^2} \cdot \frac{m^3\sigma^6}{m(\sigma^2+1)\{m^4+1)(-2\sigma^2) + m^2(\sigma^4 + 3\sigma^2 + 1)\}} \qquad (IV_5)$$

$$\frac{}{+ j(m^2-1)\sigma\{m^2[2(\sigma^4+1) + 3\sigma^2] - \sigma^2(m^4+1)\}},$$

where $\sigma^2 =$ the band width.

The phase angle, θ, is

$$\theta = \tan^{-1} \frac{-\sigma(m^2-1)\{m^2[2(\sigma^4+1) + 3\sigma^2] - \sigma^2(m^4+1)\}}{(\sigma^2+1)m\{(m^4+1)(-2\sigma^2) + m^2(\sigma^4 + 3\sigma^2 + 1)\}}. \qquad (IV_6)$$

APPENDIX V

Equations (IV_4) and (III_1) are of the same form. The relation with respect to relative gain is indefinite and unimportant. However, if the ratios of the coefficients of m are made the same, the relative response will be of course identical. Thus, if α is taken for reference,

$$\frac{\delta-\alpha}{\alpha}=\frac{-2\sigma^2(\sigma^2+1)}{-\sigma^3}=\frac{2(\sigma^2+1)}{\sigma}, \qquad (V_1)$$

$$\frac{\delta-\beta}{\alpha}=\frac{2\sigma+3\sigma^3+2\sigma^5}{-\sigma^3}=\frac{-(2+3\sigma^2+2\sigma^4)}{\sigma^2}, \qquad (V_2)$$

and

$$\frac{\alpha+\beta-\gamma-\delta}{\alpha}=\frac{-(\sigma^2+1)(\sigma^4+3\sigma^2+1)}{\sigma^3}. \qquad (V_3)$$

If the numerator and denominator are divided by α, Equation (III_1) becomes

$$g=\frac{kl^2}{\alpha}\cdot\frac{m^3}{m\left[(m^4+1)\frac{(\delta-\alpha)}{\alpha}+m^2\frac{(\alpha+\beta-\gamma-\delta)}{\alpha}\right]+j(m^2-1)\left[(m^4+1)+m^2\frac{(\delta-\beta)}{\alpha}\right]} \qquad (V_4)$$

When the relations expressed by Equations (V_1), (V_2) and (V_3) are substituted into Equation (V_4) there results for a given chosen band width, σ^2, an expression for the optimum rate of attenuation (Equations (20), (21) and (V_4) are for the general cases). Making this substitution and multiplying through by σ^3 gives

$$g=\frac{kl^2}{\alpha}\cdot\frac{\sigma^3m^3}{m[(m^4+1)(2\sigma^2)(\sigma^2+1)-m^2(\sigma^2+1)(\sigma^4+3\sigma^2+1)]+j(m^2-1)\sigma[(m^4+1)\sigma^2-m^2(2+3\sigma^2+2\sigma^4)]}$$

$$= \frac{kl^2}{\alpha} \frac{\sigma^3 m^3}{(\sigma^2+1)\, m \{2\sigma^2 (m^4+1) - m^2 (\sigma^4+3\sigma^2+1)\}}$$

$$\overline{+ j\sigma (m^2-1) \{\sigma^2 (m^4+1) - m^2 (2+3\sigma^2+2\sigma^4)\}} \qquad (V_5) \quad (23)$$

After Equation (V_5) is rationalized

$$|g| = \frac{kl^2}{a^2 b (b+2)} \frac{1}{\sqrt{m^6 + m^{-6} + \sigma^6 + \sigma^{-6}}}. \qquad (V_6) \quad (25)$$

Equation (25) is the general optimized expression for the standardized maximum rate of change of attenuation obtainable for any selected passband. However, the proper values of the parameters a, b, k and l must yet be determined to make Equation (25) valid. This is done by using the Equations (V_1), (V_2), (V_3) and (V_6).

Thus from Equations (V_1), (V_2) and (V_3) it is found that

$$\beta = \frac{2 (\sigma^2+1) (\sigma^2+\sigma+1) \alpha}{\sigma^2}, \qquad (V_7)$$

$$\gamma = \frac{(\sigma^2+1) (\sigma^4+2\sigma^3+3\sigma^2+2\sigma+1) \alpha}{\sigma^3} \qquad (V_8)$$

and

$$\delta = \frac{(2\sigma^2+\sigma+2) \alpha}{\sigma}. \qquad (V_9)$$

Then from Equations (20b), (20c), (20d), (20e) and (20f) three relations are found expressing a, b, k and l in terms of the pass-band width σ^2. These are

(1) $$kl^2(a+b) = (\sigma^6-4\sigma^5+8\sigma^4-10\sigma^3+8\sigma^2-4\sigma+1)\alpha/\sigma^3 \qquad (V_{10})$$

or $$k = \frac{H_1 \alpha}{l^2 (a+b)} \qquad (V_{11})$$

where $$H_1 = (\sigma^6-4\sigma^5+8\sigma^4-10\sigma^3+8\sigma^2-4\sigma+1)/\sigma^3, \qquad (V_{12})$$

(2) $$al\,[a(b+1)+b(b+2)] = (\sigma^2-3\sigma+1)\alpha/\sigma$$

or $l = \alpha H_2 / a[a(b+1)+b(b+2)]$ (V_{13})

where $H_2 = (\sigma^2 - 3\sigma + 1)/\sigma$, (V_{14})

and (3) $l^2(a+b)(a+b+2)+abkl = (2\sigma^4 - 8\sigma^3 + 13\sigma^2 - 8\sigma + 2)\alpha/\sigma^2$

or $l^2(a+b)(a+b+2)+abkl - H_3\alpha = 0$ (V_{15})

where $H_3 = (2\sigma^4 - 8\sigma^3 + 13\sigma^2 - 8\sigma + 2)/\sigma^2$. (V_{16})

Equation (V_6) gives the gain G_1 at $m = 1$ to be

$$G_1 = \frac{kl^2}{\alpha} \frac{1}{\sqrt{2+\sigma^6+\sigma^{-6}}}. \qquad (V_{17})$$

It seems essential to make the gain at $m = 1$ and the pass band, σ^2, the independent parameters.

So from (V_{11}) and (V_{17})

$$a = \frac{H_1}{G_1\sqrt{2+\sigma^6+\sigma^{-6}}} - b$$

$$= H_4 - b \qquad (V_{18})$$

where $H_4 = H_1/G_1\sqrt{2+\sigma^6+\sigma^{-6}}$ (V_{19})

or $a+b = H_4$. (V_{20})

Using the value of (V_{11}) in (V_{15}), then (V_{13}) in the result and then (V_{18}) and (V_{20}) in that result, remembering that $\alpha = a^2b(b+2)$, yields after rearranging, the expression

$$b(b+2)^2 + \frac{H_1F^3}{H_3^3H_4^2(H_4+2)} = \frac{H_3(b+2)F^2}{H_2^2H_4(H_4+2)} \qquad (V_{21})$$

where $F = (H_4 - b)(b+1) + b(b+2)$. (V_{22})

Equation (V_{21}) is an expression in b after the values of σ and G_0 are substituted.

RCA TECHNICAL PAPERS†

Third Quarter, 1950

Any request for copies of papers listed herein should be addressed to the publication to which credited.

"Analysis of the Sampling Principles of the RCA Color Television System", Bulletin, RCA Laboratories Division (July 28) 1950

"An Analysis of the Sampling Principles of the Dot-Sequential Color Television System", *RCA Review* (September) 1950

"Automatic Audio Gain Controls", J. L. Hathaway, *Audio Engineering* (September) 1950

"Blower Selection for Forced-Air Cooled Tubes", A. G. Nekut, *Electronics* (August) 1950

"The Brief Case Field Amplifier", J. L. Hathaway and R. C. Kennedy, *RCA Review* (September) 1950

"Circuit Diagram and Description of a Receiver Sampler for Dot-Sequential Color Television", *RCA Licensee Bulletin LB-799* (August 18) 1950

"Ferromagnetic Spinels for Radio Frequencies", R. L. Harvey, I. J. Hegyi and H. W. Leverenz, *RCA Review* (September) 1950

"Flying Spot Camera, Type TK-3A", C. R. Monro, *Broadcast News* (September-October) 1950

"Flying Spot Cameras", C. R. Munro, *TV Engineering* (September) 1950

"How to Modify RCA Cameras for Setting Correct Target Voltage", J. H. Roe, *Broadcast News* (July-August) 1950

"How to Plot TV Studio Lighting", W. C. Eddy and H. Duszak, *Broadcast News* (July-August) 1950

"Improved Ultra-Thin Sectioning of Tissue for Electron Microscopy", J. Hillier and M. S. Gettner, *Jour. Appl. Phys.* (September) 1950

"Industrial Television and the Vidicon", V. K. Zworykin, *Elec. Eng.* (July) 1950

"An Intermodulation Analyzer for Audio Systems", Roy S. Fine, *Audio Eng.* (July) 1950

"A Laboratory Television System", R. L. Hucaby, *Audio Eng.* (September) 1950

"Light-Transfer Characteristics of Image Orthicons", R. B. Janes and A. A. Rotow, *RCA Review* (September) 1950

"Linear Phase Shift Video Filters", G. L. Fredendall and R. C. Kennedy, *RCA Review* (September) 1950

"Low-Frequency Discone", A. M. Seybold, *CQ* (July) 1950

"Mass Spectrometric Study of Solids — I. Preliminary Study of Sublimination Characteristics of Oxide Cathode Materials", R. H. Plumlee and L. P. Smith, *Jour. Appl. Phys.* (August) 1950

"Microwave Propagation Experiments", L. E. Thompson, *Proc. I.R.E.* (Australia) (August) 1950

† Report all corrections or additions to RCA Review, Radio Corporation of America, RCA Laboratories Division, Princeton, N. J.

"Mixed Highs in Simultaneous Color Television", Bulletin, RCA Laboratories Division (July 28) 1950

"Mixed Highs in Color Television", A. V. Bedford, *Proc. I.R.E.* (September) 1950

"A New Deluxe 35-Mm. Motion Picture Projector Mechanism", H. J. Benham and R. H. Heacock, *Jour. S.M.P.T.E.* (September) 1950

"New Television Camera Tubes and Some Applications Outside the Broadcasting Field", V. K. Zworykin, *Jour. S.M.P.T.E.* (September) 1950

"Open Field Test Facilities for Measurement of Incidental Receiver Radiation", C. G. Seright, *RCA Licensee Bulletin LB-802* (September 22) 1950

"On the Nature of a Soldered Contact on a Semiconductor", J. I. Pantchechnikoff, (Letter to the Editor), *Phys. Rev.* (September) 1950

"The Orthogam Amplifier", E. D. Goodale and C. L. Townsend, *RCA Review* (September) 1950

"The Orthogam Amplifier", E. Dudley Goodale, *TV Engineering* (September) 1950

"Permanent Magnet Electron Microscope for General Laboratory Services", J. H. Reisner, E. G. Dornfeld and S. W. Pike, *Electrical Manufacturing* (October) 1950

"Practical Television Lighting, Part I", C. A. Rackey, *Audio Eng.* (July) 1950

"Practical Television Lighting, Part II", C. A. Rackey, *Audio Eng.* (September) 1950

"Progress Report of RCA on Color Television and U-H-F", Bulletin, RCA Laboratories Division (July 31) 1950

"Pulse Measuring of Deionization Time", H. W. Wittenberg, *Elec. Eng.* (September) 1950

"Recording and Fine-Groove Technique", H. E. Roys, *Audio Eng.* (September) 1950

"Recording and Fine Groove Technique", H. E. Roys, *Broadcast News* (July-August) 1950

"A Removable Intermediate Lens for Extending the Magnification Range of an Electron Microscope", J. Hillier, *Jour. Appl. Phys.* (August) 1950

"RF Tests and Noise Measurements of Secondary-Emission Tubes of the Directly Exposed Dynode Type", R. P. Stone, *RCA Licensee Bulletin LB-800* (August 28) 1950

"Slot Antenna Development and Basic Principles", P. S. Carter, *Proc. I.R.E.* (August) 1950

"Small Short-Run Parts Made by Rubber-Die Process", William J. Bachman, *American Machinist* (August 21) 1950

"Some Design Considerations of Ultra-High Frequency Converters", W. Y. Pan, *RCA Review* (September) 1950

"Some Design Considerations of U-H-F Converters", W. Y. Pan, *RCA Licensee Bulletin LB-801* (September 22) 1950

"Specifications for Motion Picture Films Intended for Television Transmission", C. L. Townsend, *Jour. S.M.P.T.E.* (August) 1950

"Television Service. Part X—More on Horizontal-Deflection Troubles", J. R. Meagher, *RCA Rad. Serv. News* (September-October) 1950

"Test and Alignment Procedures for Video Amplifiers", F. E. Cone and N. P. Kellaway, *Broadcast News* (September-October) 1950

"Transient Testing of Loudspeakers", M. S. Corrington, *Audio Eng.* (August) 1950

"The Trigger-Grid Thyratron", M. R. Boyd and L. Malter, *RCA Licensee Bulletin LB-797* (August 7) 1950

"TV Studio Illumination", H. M. Gurin and R. L. Zahour, *Broadcast News* (July-August) 1950

"Uniform Speech-Peak Clipping in a Uniform Signal-to-Noise Spectrum Ratio", D. W. Martin, *Jour. Acous. Soc. Amer.* (September) 1950

"Unobtrusive Pressure Microphone", H. F. Olson and J. Preston, *Audio Eng.* (July) 1950

"Variable-Area Sound Track Requirements for Reduction Printing onto Kodachrome", R. V. McKie, *Jour. S.M.P.T.E.* (July) 1950

NOTE—Omissions or errors in these listings will be corrected in the yearly index.

Correction:

Some errors have been discovered in the paper entitled "Some Characteristics of Diodes with Oxide-Coated Cathodes," by W. R. Ferris, which appeared in the March 1949 issue.

The second and sixth equations on page 145 should read:

$$\frac{d\xi_{\substack{\alpha \\ \beta}}}{d\eta} = \mp\, \varphi_{\substack{\alpha \\ \beta}}^{-\frac{1}{2}}.$$

Several expressions which appear on page 146, contain an incorrect sign; the following are the corrected expressions:

Second line

$$d\xi_\alpha = -\, d\eta_1 / \sqrt{\varphi_\alpha}$$

Fifth line

$$\frac{dI}{I} = \left(\frac{d\eta_2}{\sqrt{\varphi_\beta}} + \frac{d\eta_1}{\sqrt{\varphi_\alpha}} \right) \Bigg/ \tfrac{1}{2} (\xi_\beta - \xi_\alpha)$$

Sixth line

$$= \frac{\sqrt{\varphi_\alpha}\,(d\eta_2 - d\eta_1)}{\tfrac{1}{2}(\xi_\beta - \xi_\alpha)\,\sqrt{\varphi_\alpha\,\varphi_\beta}} - \frac{\sqrt{\varphi_\alpha} + \sqrt{\varphi_\beta}}{\tfrac{1}{2}(\xi_\beta - \xi_\alpha)\,\sqrt{\varphi_\alpha\,\varphi_\beta}} \left(\frac{dI}{I} \right)$$

Seventh line

$$\frac{dI}{I} = \frac{(d\eta_2 - d\eta_1)\,\sqrt{\varphi_\alpha}}{\sqrt{\varphi_\alpha} + \tfrac{1}{2}(\xi_\beta - \xi_\alpha)\,\sqrt{\varphi_\alpha\,\varphi_\beta} + \sqrt{\varphi_\beta}}$$

Ninth line

$$\frac{1}{I}\frac{dI}{dV} = \frac{e\sqrt{\varphi_\alpha}}{kT} \cdot \frac{1}{\sqrt{\varphi_\alpha} + \tfrac{1}{2}(\xi_\beta - \xi_\alpha)\,\sqrt{\varphi_\alpha\,\varphi_\beta} + \sqrt{\varphi_\beta}}$$

The errors in sign were not present in the expressions from which the curves of Figure 2, page 140, were calculated.

AUTHORS

ALBERT W. FRIEND — (See *RCA Review*, Volume XI, No. 1, March 1950, page 157.)

GEORGE W. GRAY attended Princeton University as a civilian and in the Navy V-12 Program until 1943 when he was assigned to active duty in the Navy. After release to inactive duty in 1946, he returned to Princeton University and received the B.A. degree in Physics. In March of 1947 he joined the technical staff of RCA Laboratories Division at Princeton, N. J. Mr. Gray is at present a member of the Electronic Research Laboratory engaged in television research.

GRANT E. HANSELL received the B.S. degree in Electrical Engineering from Purdue University in 1931. He joined the Research and Advanced Development group of RCA Communications, Inc. in 1931 and was transferred to the Communications Research Section of RCA Laboratories Division in 1942. Mr. Hansell is a Senior Member of the Institute of Radio Engineers.

ARTHUR S. JENSEN received the B.S. degree in 1938, the M.S. degree in 1939, and the Ph.D. degree in 1941 in Physics from the University of Pennsylvania where he was a research fellow from 1939 to 1941. After a short period as a research physicist at the Naval Research Laboratory, he reported for active duty with the U. S. Naval Reserve in August, 1941. From then until 1946 he served as an officer-instructor in physics and aviation physics at the U. S. Naval Academy with the rank of lieutenant commander. At the end of 1945, he joined RCA Laboratories Division. Dr. Jensen is a Member of the Institute of Radio Engineers, the American Physical Society, the American Association of Physics Teachers, the American Association for the Advancement of Science, Pi Mu Epsilon, and Sigma Xi.

CHARLES E. MOORE received the B.S. degree in Electrical Engineering from the University of Michigan in 1939. He completed some further graduate work while acting as Broadcast Engineer and Assistant to the Director of Broadcasting for the University of Michigan Extension Service. From 1941 to the Fall of 1945, he was engaged in the development of radar at the Radiation Laboratory, Massachusetts Institute of Technology, Cambridge, Massachusetts. Since that time, he has been with Radiomarine Corporation of America, New York, N. Y., in charge of the design and development radar and other microwave equipment. Mr. Moore is a Member of the Institute of Radio Engineers.

CHARLES C. SHUMARD received the B.S. degree in Electrical Engineering from the University of Missouri in 1921. After two years in power work with the Commonwealth-Edison Company in Chicago, he became Instructor (1923) and Assistant Professor (1924) in Electrical Engineering at the Georgia School of Technology where he received the M.S. degree in Electrical Engineering in 1927. Since 1927 he has been employed by RCA; first, in the Van Cortland Park Laboratories in New York City, subsequently in the Camden, N. J. and Harrison, N. J. plants and currently in the Laboratories Division in Princeton, N. J. Mr. Shumard has been engaged in various development and research projects including receiving tube applications, transmitter problems and network analysis.

BERNARD N. SLADE received the B.S. degree in Electrical Engineering from the University of Wisconsin in 1948. He joined the RCA Victor Division immediately after graduation. Mr. Slade is associated with the Advanced Development Group at Harrison where he is working on the development of crystal triodes. He is taking part-time graduate work in electrical engineering at Stevens Institute of Technology. Mr. Slade is an Associate Member of the American Institute of Electrical Engineers and a Member of the Institute of Radio Engineers.

LELAND E. THOMPSON received the B.S. degree in Electrical Engineering from the University of South Dakota in 1929. From 1929 to 1930 he was a member of the Test Department and later an engineer in the Commercial Receiver Design Group of the General Electric Company. In 1930 he joined the RCA Victor Division and engaged in the development of special radio receivers until 1943 when he began work on Microwave Relay systems and is now engaged in advanced development work in this section. Mr. Thompson is a Senior Member of the Institute of Radio Engineers.

RCA REVIEW

a technical journal

RADIO AND ELECTRONICS
RESEARCH · ENGINEERING

INDEX

VOLUME XI — 1950

TABLE OF CONTENTS

March

June

September

December

INDEX, VOLUME XI

Authors, Volume XI